



# **Investigation of 2-(2-Methylaminoethyl)pyridine as a Green Corrosion Inhibitor for Carbon Steel for Applications in The Oil and Gas Industry**

A thesis submitted to McGill University in partial fulfillment of  
the requirements of a degree of Masters of Engineering

By: Aqeel Alrebh

Department of Chemical Engineering, McGill University,  
Montréal, Québec, Canada H3A 0C5

© Aqeel Alrebh 2016

# Abstract

Carbon steel (CS) is extensively used in the oil and gas industry as a material of construction of equipment and piping facilities. Naturally, this metal undergoes electrochemical reactions (also called corrosion reactions) with the surroundings to form thermodynamically stable products—rusts. This phenomenon is a serious and of a major challenge in various industries. It has been shown that corrosion costs, directly and indirectly, an industrialized country as high as 5% of its GDP. In addition, corrosion of CS in acidic media is a more challenging problem since acids tend to accelerate corrosion processes. For applications where internal general corrosion is a concern, using corrosion inhibitors is one of the most effective options to control it. However, most of the currently-used inhibitors are toxic and not environment-friendly.

The objective of this work was to investigate the possibility of using 2-(2-methylaminoethyl)pyridine (MAEP) as an eco-friendly corrosion inhibitor for CS in acidic media, under various conditions, such as varying MAEP concentration, temperature, pH, acid concentration, long-term effectiveness, and in the presence of crude oil. Various electrochemical and surface/solution analysis techniques were used.

The results showed that MAEP is capable of mitigating corrosion of CS in 0.1 M HCl to more than 90% of corrosion inhibition efficiency at a concentration of 25 mM at room temperature. The inhibition mechanism was explained on the basis of MAEP adsorption and the subsequent minimization of diffusion of corrosive species to the CS surface. The adsorption of MAEP was found to be predominantly chemical and the adsorbed MAEP layer was stable over a long period of time (up to 30 days). The adsorption obeyed the Langmuir isotherm. Furthermore, the MAEP adsorption thermodynamics and kinetics were evaluated.

The presence of Wyoming sweet crude oil in various low volume ratios in the electrolyte was studied, too. The results showed that the presence of oil resulted in a decrease in CS corrosion rate, even in the absence of MAEP. However, the addition of MAEP further enhanced the protection, but only at low oil volume ratios.

# Résumé

L'acier carbone (CS) est largement utilisé dans l'industrie du pétrole et du gaz comme matériau de construction d'équipements et de tuyauteries. Ce métal subit de façon naturelle des réactions (également appelées réactions de corrosion) dans l'environnement pour former des produits thermodynamiquement stables – la rouille. Ce phénomène est un défi sérieux et important dans diverses industries qui génère un impact financier pour les pays industrialisés à hauteur de 5% de leur PIB. De plus, la corrosion du CS dans les milieux acides est problématique, les milieux acides contribuant à accélérer le phénomène de corrosion. Pour les applications où la corrosion générale interne est importante, l'utilisation d'inhibiteurs de corrosion est l'une des options les plus efficaces pour la contrôler. Cependant, la plupart des inhibiteurs actuellement utilisés sont toxiques et néfastes pour l'environnement.

L'objectif de ce travail était d'étudier la possibilité d'utiliser la 2-(2-méthylaminoéthyl)pyridine, (MAEP) comme inhibiteur de corrosion écologique pour l'acier carbone dans des milieux acides en fonction d'une gamme de paramètres comprenant la concentration en MAEP, la température, le pH, la concentration en acide, l'efficacité à long terme et en présence d'huile brute. Différentes techniques électrochimiques ont été utilisées comprenant: résistance à la polarisation, spectroscopie d'impédance électrochimique et polarisation Tafel.

Les résultats ont démontré une bonne cohérence entre les techniques utilisées. Ils ont également montré qu'une concentration de 25 mM MAEP à température ambiante pouvait diminuer le phénomène de corrosion de plus de 90% dans une solution de 0.1 M d'acide hydrochlorique. L'inhibition est expliquée par un phénomène d'adsorption qui s'est avérée être principalement chimique et stable sur une longue période de temps dépassant 15 jours. L'adsorption obéit à l'isotherme de Langmuir. Aussi, la thermodynamique et la cinétique de l'adsorption ont été évaluées à 10 mM de MAEP dans du 0.1 M acide hydrochlorique.

La présence de pétrole brut doux de Wyoming dans diverses ratios à faible volume dans l'électrolyte a également été étudiée. Les résultats ont montré que cet ajout contribuait à protéger le métal contre la corrosion. En outre, à une concentration de 10 mM apporte une protection supplémentaire contre la corrosion dans ce cas précis. Ce pendant, on constate que le MAEP était efficace uniquement à des rapports de volume d'huile faibles.

# Acknowledgement

I would like to express my gratitude to my supervisor, Prof. Sasha Omanovic, whose expertise, understanding, and patience, added considerably to my graduate experience at McGill University. I appreciate his vast knowledge and skills in many areas, and his tremendous assistance in writing this thesis. He provided me with direction, technical support and became more of a mentor and friend to me, than a professor.

I must also acknowledge Prof. Jean-Luc Meunier for reviewing my thesis and for his valuable input and recommendations as an external examiner.

I would like also to thank our department lab technicians Mr. Frank Caporuscio and Mr. Ranjan Roy for their help. Appreciations also go to the members of the Electrochemical Engineering and Corrosion Laboratory, especially, Dr. Nehar Ullah Khan, Mr. Mario Ascencio, Mr. Emmanuel Nwanebu, Mr. Abraham Gomez, Mrs. Saloumeh Ghasemian, and Mr. Deepak Sridhar for their support. Thanks go to my friend and officemate Mr. Simon Kwan for his very kind help when I started my work in the lab. Very special thanks to my colleague and closest friend Mr. Mahmoud Rammal for his great support, encouragement and continuous stimulation when discussing, debating, and interpreting the results of this work, and throughout my master's program and my stay in Montréal.

Very special thanks to Prof. Abdullah Shaikh, Prof. Hassan Al Muallem, and Prof. Basim Abussaud, faculty members at King Fahd University of Petroleum and Minerals, Dhahran, Saudi Arabia, for their support and encouragement to pursue graduate studies.

I recognize that this research would not have been possible without the financial assistance of the Ministry of Higher Education in Saudi Arabia and the Saudi Arabian Cultural Bureau through the King Abdullah Scholarships Program for Distinctive Students.

Finally and most importantly, I would also like to thank all of my family members for the full and tremendously kind support and love they provided me through my entire life and in particular, I must acknowledge my parents whom without their love, worry, encouragement, I would not have finished my master's program and my thesis. I would like to dedicate this work to them and to my younger loved brothers Mahdi and Jawad who untimely passed away while I was completing my program.

# Table of Contents

ABSTRACT .....	I
RÉSUMÉ .....	II
ACKNOWLEDGEMENT .....	III
LIST OF FIGURES .....	VI
<b>CHAPTER 1: INTRODUCTION .....</b>	<b>1</b>
<b>CHAPTER 2: BACKGROUND AND LITERATURE REVIEW .....</b>	<b>6</b>
2.1 Corrosion in The Oil and Gas Industry .....	8
2.1.1 Crude Oil and Corrosion.....	10
2.1.2 Acidizing Wells .....	11
2.1.3 Acid Pickling and Surface Cleaning.....	12
2.1.4 Oil Pipelines Pigging .....	13
2.1.5 Brackish Water .....	13
2.2 Corrosion Protection .....	14
2.2.1 Proper Material Selection .....	14
2.2.2 Monitoring and Inspection.....	15
2.2.3 Coating.....	16
2.2.4 Cathodic Protection .....	16
2.2.5 Corrosion Inhibitors.....	17
2.3 Corrosion Inhibitors .....	17
2.3.1 Anodic Inhibitors.....	18
2.3.2 Cathodic Inhibitors .....	18
2.3.3 Mixed Inhibitors .....	20
2.4 Green Corrosion Inhibitors.....	21
2.5 Adsorption of Corrosion Inhibitors .....	22
2.5.1 Physical Adsorption.....	23
2.5.2 Chemical Adsorption.....	23
2.5.3 Thermodynamics of Adsorption .....	24
2.6 Adsorption Isotherms .....	25
2.7 Kinetics of Corrosion Reactions .....	27
2.8 Selection of Corrosion Inhibitors for oil and gas applications .....	29
2.8.1 MAEP: Green Inhibitor .....	31
<b>CHAPTER 3: OBJECTIVES .....</b>	<b>32</b>
<b>CHAPTER 4: MATERIALS AND EXPERIMENTAL PROCEDURES.....</b>	<b>34</b>

4.1 Materials and Solutions .....	35
4.2 Electrochemical Cell .....	35
4.3 Experimental Equipment and Software.....	36
4.4 Experimental Methodology .....	37
4.5 Research Techniques .....	39
4.5.1 Open-Circuit Potential (OCP) .....	39
4.5.2 Electrochemical Impedance Spectroscopy (EIS) .....	39
4.5.3 Linear Polarization (LP) .....	39
4.5.4 Scanning Electron Microscopy (SEM).....	41
<b>CHAPTER 5: RESULTS AND DISCUSSIONS .....</b>	<b>42</b>
5.1 Effect of MAEP Concentration .....	45
5.1.1 Effect of MAEP Concentration on OCP.....	46
5.1.2 Effect of MAEP Concentration on Inhibition Efficiency – EIS measurements.....	48
5.1.3 Effect of MAEP Concentration on Corrosion Inhibition – PR Measurements .....	51
5.1.4 Effect of MAEP Concentration on Corrosion Inhibition – TP Measurements .....	53
5.2 Adsorption Isotherm for MAEP on a CS Surface .....	57
5.3 Kinetics of Adsorption and Desorption of MAEP .....	58
5.4 Effect of Temperature .....	61
5.5 Effect of pH.....	65
5.6 Effect of Hydrochloric Acid Concentration .....	67
5.7 Effect of Long-Term Immersion of CS in Electrolyte .....	70
5.8 Effect of Crude Oil.....	74
<b>CHAPTER 6: CONCLUSIONS.....</b>	<b>76</b>
6.1 Summary and Conclusions .....	77
6.2 Original Contribution .....	78
6.3 Future Opportunities .....	79
REFERENCES .....	80

# List of Figures

<b>Figure 2.1:</b> Chemical structure of MAEP.....	<b>31</b>
<b>Figure 4.1:</b> Schematic diagram of a three-electrode electrochemical cell.....	<b>36</b>
<b>Figure 5.1:</b> Pourbaix diagram for iron at 298 K .....	<b>43</b>
<b>Figure 5.2:</b> Open circuit potential variations (V) vs Time (s) of CS in 0.1 M HCl (pH 1.25) at T=298 K .....	<b>44</b>
<b>Figure 5.3:</b> An illustration of the metal/inhibitor/electrolyte interface showing the possible protection mechanism against corrosion.....	<b>45</b>
<b>Figure 5.4:</b> Open circuit potential (V) vs time (s) for selected MAEP concentrations in 0.1 M HCl (pH 1.25) at 295 K .....	<b>47</b>
<b>Figure 5.5:</b> $E_{oc}$ (V) for all the tested MAEP concentrations (mM) recorded after 1 hour of CS immersion in 0.1 M HCl (pH 1.25) at 295 K.....	<b>47</b>
<b>Figure 5.6:</b> Nyquist plot of CS taken at different MAEP concentrations in 0.1 M HCl at 295 K. (O) 0 mM, ( $\Delta$ ) 0.1 mM, ( $\times$ ) 0.5 mM, (+) 1 mM, ( $\square$ ) 5 mM, ( $\diamond$ ) 10 mM, (-) 20 mM MAEP. The solid curves represent data fitting .....	<b>49</b>
<b>Figure 5.7:</b> EEC models used to fit EIS data for (a) CS electrode in blank solution, and (b) on a CS electrode immersed in an electrolyte containing MAEP. $R_{e1}$ - electrolyte resistance; $CPE_{1}$ -double-layer and pseudo-capacitance; $R_{1}$ - charge transfer resistance, $CPE_{2}$ - SAM layer pseudo-capacitance, $R_{2}$ - adsorbed inhibitor layer resistance.....	<b>50</b>
<b>Figure 5.8:</b> Inhibition efficiency against blank solution calculated from EIS resistances for all the MAEP tested concentrations in 0.1 M HCl (pH 1.25) at 295 K. .	<b>51</b>
<b>Figure 5.9:</b> Current $i$ ( $\mu$ A) vs polarized potential (s) for blank and selected MAEP concentrations in 0.1 M HCl solution (pH 1.25) at 295 K.....	<b>52</b>
<b>Figure 5.10:</b> Inhibition efficiency for inhibitor-free solution calculated from PR resistances for all the MAEP tested concentrations in 0.1 M HCl (pH 1.25) at 295 K.....	<b>53</b>
<b>Figure 5.11:</b> Tafel Plot for CS in an inhibitor-free solution of 0.1 M HCl (pH 1.25) at 295 K. The method of determining the Tafel parameters graphically. ....	<b>54</b>

<b>Figure 5.12:</b> Tafel plots for CS immersed in 0.1 M HCl (pH 1.25) at 295 K for different MAEP concentrations. ....	<b>55</b>
<b>Figure 5.13:</b> Inhibition efficiency against blank solution calculated from $j_{\text{corr}}$ (and $R_T$ in the inset) for all the MAEP tested concentrations in 0.1 M HCl (pH 1.25) at 295 K. ....	<b>56</b>
<b>Figure 5.14:</b> Linearized form of Langmuir isotherm of MAEP adsorption on CS at 295 K where $\theta$ was calculated based on EIS results (inset: based on $R_T$ of Tafel results). The solid line represents the Langmuir model. ....	<b>58</b>
<b>Figure 5.15:</b> Polarization resistance, $R_p$ , against time of CS immersed in blank solution, and in 10 mM MAEP in 0.1 M HCl (pH 1.25) solution at 295 K. Solid line for visual aid only. Results obtained by the polarization resistance method. ....	<b>59</b>
<b>Figure 5.16:</b> Polarization resistance, $R_p$ Vs time for CS immersed in (o) blank electrolyte (■) 5mM, (▲) 7mM, and (●) 10 mM, and (×) 10 mM diluted to 7mM then to 5mM MAEP in 0.1 M HCl (pH 1.25) at 295 K. SD is $\pm 10 \Omega$ or less. Solid line for visual aid only. Results were obtained by the polarization resistance method. ....	<b>60</b>
<b>Figure 5.17:</b> Temperature dependence of polarization resistance of CS immersed in (o) 0 and in (●) 10mM MAEP in 0.1 M HCl (pH 1.25). Solid line for visual aid only. Resistances were obtained by the polarization resistance method. ....	<b>61</b>
<b>Figure 5.18:</b> Inhibition efficiency of CS in 10 mM MAEP in 0.1 M HCl (pH 1.25) at various temperatures. The efficiencies were calculated based on $R_p$ . ....	<b>63</b>
<b>Figure 5.19:</b> Arrhenius plots for CS immersed in (o) 0, and in (●) 10mM MAEP in 0.1 M HCl (pH 1.25) at various temperatures. Results were obtained from the polarization resistance method. ....	<b>64</b>
<b>Figure 5.20:</b> Tafel plots for CS in 0.1 M HCl solution at different pH values of 1.25, 2.0, 3.0, and $4.0 \pm 0.01$ at 295 K. ....	<b>65</b>
<b>Figure 5.21:</b> Tafel plots for CS in 10 mM MAEP in 0.1 M HCl solution at different pH values of 1.25, 2.0, 3.0, and $4.0 \pm 0.01$ at 295 K. ....	<b>66</b>
<b>Figure 5.22:</b> Corrosion inhibition efficiency for CS in 10 mM MAEP in 0.1 HCl at 295 K of different pH values (calculated from $R_p$ ). ....	<b>67</b>
<b>Figure 5.23:</b> Nyquist plots ( $-Z''$ vs $Z'$ ) for CS immersed in (o) the absence and (●) presence of inhibitor at 10 mM in 0.5 M HCl at 295 K. Symbols are	

experimental data and solid lines represent the simulated (modeled) spectra using the models in Fig. 5.7. ....	68
<b>Figure 5.24:</b> Nyquist plots ( $-Z''$ vs $Z'$ ) for CS immersed in (o) the absence and (●) presence of inhibitor at 10 mM in 1.5 M HCl at 295 K. Symbols are experimental data and solid lines represent the simulated (modeled) spectra using the models in Fig. 5.7. ....	69
<b>Figure 5.25:</b> Polarization resistances $R_p$ of CS in (o) the absence and (●) the presence of the inhibitor at 10 mM in various HCl concentrations at 295 K. Solid lines for visual aid only. Results were obtained from the polarization resistance method. ....	69
<b>Figure 5.26:</b> The inhibition efficiency of the inhibitor at 10 mM for different HCl concentrations at 295 K. Results were obtained based on the polarization method. ....	70
<b>Figure 5.27:</b> Scanning Electron Microscopy (SEM) image for CS freshly-polished with 600-grit paper. The corresponding length bar is 30 $\mu\text{m}$ . ....	71
<b>Figure 5.28:</b> Scanning Electron Microscopy (SEM) images for CS immersed in solutions in the absence of the inhibitor for a) 1 day, c) 7 days, and e) 30 days; and in the presence of the inhibitor at 10 mM for b) 1 day, d) 7 days, and f) 30 days where all at a temperature of 295 K during the immersion. The corresponding length bar is 30 $\mu\text{m}$ . ....	72
<b>Figure 5.29:</b> Sample of solutions sampled from the electrolytes where the CS samples (of total geometric area equal to ca. 9.34 $\text{cm}^2$ ) were immersed for a period of time shown in numbers (0 to 30 in days). ....	73
<b>Figure 5.30:</b> Iron concentration ( $\text{mg L}^{-1}$ per $\text{cm}^2$ CS exposed to electrolyte) in the liquid samples as a function of time. Results obtained by ICP-OES only for one run. ....	74
<b>Figure 5.31:</b> Inhibition Efficiency of MAEP in 0.1 M HCl in the presence of Wyoming crude oil at different volume ratios ( $\pm 0.1$ ) at 295 K ....	75
<b>Figure 5.32:</b> Polarization Resistance of CS in (○) 0.1 M HCl and oil, and in (●) 0.1 M HCl, 10 mM MAEP and oil. ....	75

# **CHAPTER 1: INTRODUCTION**

# 1. Introduction

Corrosion of metals is one of the most challenging problems in several industries. It is a spontaneous phenomenon that results in dissolution of metals when chemically and/or electrochemically interacting with corrosive surroundings, leading to weakening, failures or even collapse to the metals. Corrosive species could be in a liquid form such as water and aqueous (or in certain cases organic) electrolytes or in a gaseous form such as hydrogen sulfide (sour corrosion) and carbon dioxide (sweet corrosion) when dissolved in liquids [1].

In the oil and gas industry, the problem of corrosion is of a particular interest. With the trend of searching for new resources of hydrocarbons, upstream operations have become concentrated on deeper reservoirs where the environment is severer in terms of temperatures, pressures and the presence of higher levels of corrosive materials [2, 3]. In addition, the multi-phase transportation through underwater instalments and cross-country oil and gas lines causes the problem of corrosion to be more challenging [3]. Downstream operations, such as those in refinery facilities, suffer from the consequences of corrosion too, due to the presence of sulphur compounds, salty water, organic and inorganic chlorides, cyanides, and organic and inorganic acids. For example, the presence of hydrogen at elevated temperatures and pressure can cause hydrogen damage [4, 5]. Other examples include the presence of acidic species such as hydrochloric acid in the medium in applications like well acidizing.

There are several problems associated with corrosion. Economically, for example, it has been reported that it costs the United States around \$550 billion annually, which is almost 6% of the country's GDP [6]. From an operational point of view, corrosion has been a major complication for effective oil and gas production. Therefore, control and management of corrosion is essential for a cost-effective design of facilities and for ensuring safer, efficient and durable operations [3, 7]. The adverse obstacles associated with corrosion in the oil and gas industry may include shutdowns, loss and/or contamination of products, loss of efficiency, and facilities overdesign. Shutdowns, even for short periods, may cost \$50,000 or more per hour due to paused production. Moreover, replacement of a corroded piece of equipment such as a boiler may cost millions of dollars. Product losses can cause environmental pollution or even explosions in some cases, particularly for cases like natural

gas or flammable liquid leakages. In cases where corrosion results in contaminants, the efficiency of the operations may be disturbed (e.g., there will be a need for additional energy for transporting liquids if, for example, pipes are clogged by corrosion products), or the end-products can be contaminated [7]. Besides being a source of major economic losses and depletion of resources, corrosion is a potential cause of on-site fatalities, injuries, human health and environmental harms [8].

In general, there are seven main types of corrosion, which are classified with respect to manifestation of the damage they can cause—outward appearance or altered physical properties. These types are general (or uniform) corrosion, intergranular corrosion, galvanic corrosion, crevice corrosion, erosion-corrosion, pitting, and biological corrosion [7, 9]. The focus of this report will be on the first one: The general corrosion, which will be discussed in details later.

Various approaches and methods have been rigorously studied and implemented in order to mitigate corrosion. The commonly used methods include proper design of equipment where corrosion-resistant alloys are selected, painting, coating and lining, chrome treatment of steel surfaces, applying sacrificial zinc or magnesium layers to metallic structures, and using corrosion inhibitors. It can be said that almost all methods of corrosion protection fall into one of the following approaches. The first one is cathodic protection where a charge is transferred to the steel from another material (i.e., sacrificial material). The second one is anodic protection, where a charge is withdrawn from the steel. The last one which is achieved by sealing off metallic surfaces from the corrosive species present in the environment by a surface layer of another material (e.g. coating or corrosion inhibitors) [10, 11].

One of the most common and effective measures to mitigate internal corrosion in metals and protecting their surfaces is the use of corrosion inhibitors (internal corrosion, for example, might refer to corrosion of the inside of a pipe that is in contact with a corrosive electrolyte, while external corrosion then might refer to corrosion of the external surface of a pipe that is in contact with air or soil). In particular, some organic compounds have been found to be useful in inhibition of corrosion in alloys and metals like iron steel in acidic media [12-14]. Most of organic corrosion inhibitors are those containing heteroatoms (i.e., nitrogen, sulfur and/or oxygen), electronegative functional groups,  $\pi$ -electron in double or triple bonds, and/or aromatic rings [15-17]. These are deemed as

major centers of adsorption because they tend to form a chelate on the metal surface, which ultimately minimizes corrosion. This can happen by either ‘insulating’ the metal’s surface from the corrosive electrolyte by forming an adsorbed layer, or by influencing the mechanisms and kinetics of corrosion reactions. A chelate is formed when electrons are transferred from those centers (nucleophiles) to the metal (electrophile) establishing a coordinate covalent bond during a chemical adsorption process [18]. Physical adsorption may take place due to electrostatic Van der Waal’s interactions [19].

Concerns about the adverse environmental consequences of using and disposing corrosion inhibitors are increasingly being addressed. The concerns are related to toxicity, biodegradability, and bioaccumulation of these inhibitors when they are discharged into the environment. Some of the used conventional inhibitors may be found satisfactory and highly efficient in corrosion mitigation, but they pose hazards to the environment [20]. For example, chromium (IV)-based inhibitors are found good inhibitors for copper, yet, they are toxic [21]. Therefore, more research is required for designing/selecting organic molecules as green (i.e., environmentally friendly) inhibitors, and to increase their inhibition efficiency and stability once they are applied.

The main focus of the present thesis project was to investigate and evaluate an amino-pyridine derivate as a green corrosion inhibitor for carbon steel in acidic media, and in two-phase systems where a hydrocarbon (crude oil) is present in the acidic electrolyte. The potential use of the inhibitor is for oil and gas industry related applications where those conditions are frequently encountered. The justification of selecting that organic molecule is that it is of relatively low costs even when produced at high purity, it is environmentally friendly, it is relatively safe and non-toxic to humans, and finally it is easy to apply/add to electrolytes. The current work investigates some fundamental and applied aspects of the interaction of the selected amino-pyridine derivative on carbon steel surfaces under multiple experimental conditions involving the applied concentration of the inhibitor, the pH of the acidic electrolyte, the concentration of the acidic species in the electrolyte, and the temperature of the electrolyte. The work also investigates the kinetics of the adsorption of the molecule on the metal surface. Finally, the corrosion inhibition efficiency of the molecule was evaluated in the presence of crude oil in the electrolyte.

The rest of the thesis consists of the following chapters. Chapter 2: Background and Literature Review, where a discussion and review of the corrosion problem will be

presented in terms of its theoretical aspect as well as its industrial/practical aspect. The reader will be informed about the various methods of corrosion control and prevention with emphasis on corrosion inhibitors for carbon steel. The major and specific objectives of the research work will be presented in Chapter 3. Chapter 4 will highlight the experimental procedures, chemicals/materials and solutions, apparatus, and electrochemical and surface characterisation techniques used in this work. Chapter 5 will be devoted to presenting and discussing the results of the experimental work. Finally, the major conclusions will be summarized in Chapter 6.

# **CHAPTER 2: BACKGROUND AND LITERATURE REVIEW**

## 2. Background and Literature Review

Corrosion is the degradation of materials' physico-chemical and/or mechanical properties or the change of their mass (per unit volume) over time due to the surrounding corrosive effects. It also can be defined as metals deterioration as a result of chemical or electrochemical reactions with the surroundings [22]. Corrosion in metals is the tendency of their constituents to return to their most thermodynamically stable states i.e., forming oxides or sulphides found in their basic ores. Corrosion processes are governed by reactions on atomic levels, which implies that they can act on isolated regions, uniform surface areas, and can result in subsurface damage on microscopic level. It was mentioned earlier that there are several types of corrosion, however, the most common one encountered in the oil and gas industry is the uniform (general) corrosion where the degradation takes place in an even rate over the exposed area of the metal [9]. In general corrosion, scales originate at the surface and grow radially inwards as corrosive species (e.g. chloride ions) are small enough to diffuse in the highly porous layers of the deposits [23].

For uniform corrosion to occur in a system, three elements have to be present: an anode, a cathode, and an electrolyte. In a simulated corrosion process –which will be discussed in details later-, the anode is the site of the corroding metal, while the cathode is the electrical conductor to complete the circuit in the electrochemical cell but not consumed in the corrosion process. In a real corrosion process, a cathode could be just another site on the metal that is more 'noble'. The third element is the electrolyte. It contains the corrosive species, and it is the vicinity where dissolving metal ions are present. The electrolyte also contains negatively-charged ions (e.g.  $\text{OH}^-$ ) that reacts with the dissolved metal ions to form rusts [24].

When a metal (e.g. carbon steel) is exposed to a corrosive electrolyte (such as HCl solutions), atoms of the metal in the anodic sites dissolve resulting in positively-charged metal ions and electrons. This process is termed as the anodic reaction [25]. The electrons move to other metal atoms at the cathode sites where they are consumed in cathodic reactions. The positively charged ions either dissolve in the electrolyte, or bind with negatively charged ions (like  $\text{OH}^-$ ) to form rusts on the surface of the metal or precipitate in the electrolyte (when present at high concentrations). Such scenarios are frequently found in the oil and gas industry related applications where iron steel is commonly used as a material of construction of equipment.

## 2.1 Corrosion in The Oil and Gas Industry

In the oil and gas industry, the most common form of corrosion is the general (i.e. uniform) corrosion which occurs when a metal (mostly stainless steel and carbon steel) comes in contact with an aqueous environment, with the atmosphere, with a gaseous environment where corrosive gases are present. In addition, the types of general corrosion frequently encountered are the atmospheric corrosion, the sweet corrosion (caused by the presence of carbon dioxide CO<sub>2</sub>), and the sour corrosion (caused by the presence of hydrogen sulphide H<sub>2</sub>S). There are also other types, for example, corrosion induced by the presence of mercaptans derivatives (R-SH), oxygen O<sub>2</sub> and naphthenic acids (which are a range of aliphatic cyclic mono- and poly-carboxylic acids found in crude oil such as cyclohexane carboxylic acid) [24, 26-28].

Beside those corrosive constituents that are naturally present in crude oil and/or gas, hydrochloric acid HCl, and sulfuric acid H<sub>2</sub>SO<sub>4</sub> [15], and mixtures of nitric acid HNO<sub>3</sub> and Hydrofluoric acid HF [29, 30] are inherently corrosive too and frequently used for cleaning purposes (e.g. acid pickling) in refinery facilities and pipeline systems.

For stainless steel and carbon steel, the anodic corrosion reaction is as follows [31]:



where n is the number of transferred electrons (n could be 1, 2 or 3 depending on the oxidation state that could be induced, and its stability [32]). Other metals present in stainless steel like chromium also dissolve in a similar manner. Then, associated with that oxidation reaction is the reduction reaction where all the electrons released in the anodic reaction(s) are consumed. There are four common reactions at the cathode (i.e., reduction reactions) [24]:



which is the oxygen reduction reaction in an acidic solution (i.e., low pH),



which is the oxygen reduction reaction in a neutral or basic solution (i.e., mid to high pH),



which is the hydrogen evolution reaction from neutral water, and reaction (2.5) is the hydrogen evolution reaction from acidic solutions.



Oxygen reduction and hydrogen evolution reactions are competitive reactions occurring at the cathode. In the absence (or at low concentrations) of dissolved oxygen gas, hydrogen evolution reaction becomes dominant. For the iron ions, rust (oxides or hydroxides) will be formed upon reacting with oxygen or hydroxide ions in atmospheric corrosion. A simplified corrosion mechanism of mild/carbon steel is given by the following anodic reaction:

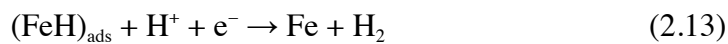


In atmospheric corrosion, other products could be formed and found in rust layers such as  $\text{Fe}(\text{OH})_3$ ,  $\alpha$ -,  $\beta$ -,  $\gamma$ -, and  $\delta$ - $\text{FeOOH}$ ,  $\gamma$ - $\text{Fe}\cdot\text{OH}\cdot\text{OH}$ ,  $\text{Fe}_3\text{O}_4$ , and  $\text{Fe}_2\text{O}_3$  [33, 34].

The anodic reaction of iron dissolution in acidic media where, for example, high concentrations of HCl are present is thought to follow this mechanism [35]:



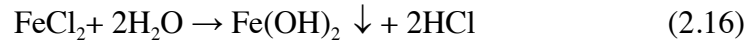
The cathodic reaction (i.e. hydrogen evolution), on the other hand, is thought to follow this mechanism [35]:



According to Z. Ahmad, an overall resulting reaction could be [8]:



Moreover, Talbot and Talbot [36] emphasise that iron(II) chloride doesn't occur in its molecular entity. Just like HCl, it is present in its ionic form when present in solutions. This implies that an overall redox reaction could be:



Balsaraf [37] demonstrates that iron(II) chloride undergoes hydrolysis producing precipitates of iron (II) hydroxide and HCl, according to reaction (2.16), triggering further corrosion reactions. Moreover, the solid products resulting from corrosion of carbon steel in acidic media are far from being only one product. In X-ray diffraction studies that Satapathy *et. al.* reported in [38], intermediates such as FeOH and  $(\text{FeClOH})^-$  are formed. After their formation, they convert to  $\gamma\text{-Fe}_2\text{O}_3$  and  $\gamma\text{-FeOOH}$  and form oxide layers on the metal's surface. The readers are recommended to refer to [39] read more about other iron oxide products that are reported using X-ray photoelectron spectroscopy (XPS)—a quantitative surface characterization technique.

In the following subsections, some applications will be presented where the problem of corrosion in acidic media -where HCl is present- is mostly encountered in the oil and gas industry (and in some other industries too). Additionally, it would be helpful for a reader to be informed about some chemical and physical properties of crude oil, and its relation to corrosion, which is the subject of the next subsection.

### 2.1.1 Crude Oil and Corrosion

Corrosion of steel has been known to happen in media where crude oil is present. It may be severe if some dissolved gases in the crude are present such as  $\text{CO}_2$  and  $\text{H}_2\text{S}$ , especially when a crude contains aqueous electrolytes [40]. Nevertheless, the presence of oil in corrosive media has shown to have a considerable effect on the corrosion process of mild steel. In some cases, it lowers the corrosion rate of the metal. It has been shown that different crude oils have appreciably distinctive effects on corrosion of steel. Essentially, the effectiveness of the corroded layer in protecting the metal from further dissolution is thought to be influenced by the oil type. A major effect originates from the content of the organic nitrogen and the acid content in an oil type [41]. So, corrosion or corrosion inhibition is highly dependent on the physical and chemical properties of the crude.

Crude oils have very complex compositions and differ broadly in their physical properties (such as solubility in water, boiling point, vapor pressure, and partition coefficient) and chemical properties (such as paraffinic, naphthenic, and aromatic crudes). Crude oils can vary depending on the oil producing regions as well as within locations and depths of a specific field [40]. Based on viscosity, volatility, and density (measured in API Gravity with respect to water) and other properties, there are four main types of crudes: very light oils, light oils, medium oils, and heavy oils. Having less amounts of sulfur and carbon dioxide makes a blend sweet [42]. An example of light sweet oil (also used in this work) is Wyoming API 32-36. It is extracted from Denver-Julesburg Basin, Laramie, Wyoming, USA.

As a final point, experimental corrosion studies (like corrosion in two-phase systems) simulating crude oil must include a specific produced oil in the test environment (rather than using a distillate like gasoline, kerosene, or blends). This is recommended to avoid errors associated with the differences in the chemical and physical properties [43].

### **2.1.2 Acidizing Wells**

Acidizing oil and gas wells (also referred to as chemical or acid stimulation) is a technique developed a century ago to enhance the recovery of oil and gas in existing wells aiming at bringing up the production levels to commercial rates. Acids, such as acetic acid, hydrofluoric acid, and hydrochloric acid have been injected into wells to dissolve materials within rock formations, or removing deposits at the wellbore face to enable higher natural flow rates of the hydrocarbons. Acidizing wells can be conducted by matrix acidizing or fracture acidizing where in the first, acids are involved in reactions at relatively low pressures and flow rates inside existing pores and natural fractures. While, in the latter one, acids are pumped at high concentrations, higher flow rates and pressures to create pores and fractures in the rock formations. Although other techniques are employed for the same purpose, acid treatment has been found very effective and economically viable [44, 45].

To increase the permeability in pores and fractures, strong acids have been used. Depending on the characteristics and conditions of a hydrocarbon reservoir, different acids and concentrations are applied. Hydrochloric acid is extensively used in carbonate-based wells where the concentrations could range from 3% to 28% w/w (ca. 9 M) and the exposure time can range from 2 to 24 hours [45, 46]. In such conditions, the acid injecting

equipment (like pumps), and the well equipment, tubing, piping, and casing are all subjected to severe corrosion attack.

Acid washing is another process that includes acid treatment. In this process, an acid like HCl, is used to clean up the wellbore and the tubular assembly of a well. This results in cleaning out scales such as calcium carbonates, rusts, and other debris that hinder the oil smooth flow out of the well. Depending on the type and the thickness of the carbonate formations, various types, amounts and concentrations of acids can be applied [47, 48].

After well-acidizing operations are completed, separate tanks are used to isolate and collect the spent acids (and water) from the oil. The isolates which have a low pH (typically around 2), are normally in large quantities. For example, the Naval Petroleum Reserve No. 1 (known as NPR-1: the fifth-largest oil field in California, USA) alone generates around 9,500 barrel/year of acidic wastes [47, 49]. The containers used for the waste, and the facilities used to recover, treat, and neutralize the acid -if required- are all prone to serious corrosion occurrence.

### **2.1.3 Acid Pickling and Surface Cleaning**

Acid pickling is one of the industrial processes used for removal of scales resulting from corrosion by exposing the metal to an acid for a period of time. It is applied in the steel production industry where scales such as iron oxides (e.g. FeO, Fe<sub>2</sub>O<sub>2</sub>, Fe<sub>2</sub>O<sub>3</sub>, Fe<sub>3</sub>O<sub>4</sub>, ...etc.) occur as a consequence of exposing the metal to high temperatures like 800 °C [50]. It has been used also in the oil and gas industry where iron hydroxides (e.g. Fe(OH)<sub>2</sub>, Fe(OH)<sub>3</sub>, ...etc.) can result from atmospheric corrosion. Actually, acid pickling is part of pre-commissioning of new plants where equipment such as reactors, heat exchangers, ...etc. are cleaned up before they are placed in service, to remove corrosion complexes resulted from operations such as welding [51].

Acid pickling is also applied in heat exchangers, boilers, and condensers. After sometime of operation, rust and/or fouling resulting from carbonates may build up, reducing the heat transfer efficiency and increasing the pressure drop (resulting in an increase in the operational costs). For example, it is estimated that for a 300,000 barrel/day refinery, solid particles accumulated in only preheaters (i.e. heat exchangers to preheat oil

before it enters to a distillation column) amount for about 15 tonne/year [43]. So, chemical treatment is implemented periodically in some situations making the equipment less prone to corrosion [52].

The main acids abundantly applied in industries are HCl and H<sub>2</sub>SO<sub>4</sub> in acid pickling for surface cleaning. The choice can include some organic acids, too. Depending on the type of metal, and the chemistry and the thickness of the rusts, the choice of the acid and the concentration can differ. For mild steel, however, HCl is preferred since the rate of dissolution of the iron oxides (and hydroxides) is higher [50].

As motioned previously, in such conditions, mild steel is susceptible to corrosion.

#### **2.1.4 Oil Pipelines Pigging**

Onshore and offshore oil pipelines are subjected to internal corrosion, fouling, and/or deposits that obstruct inefficient fluid flow and might cause pipe failures. So, technologies have been developed to overcome this issue. One of them is applying internal in-situ coating and lining using epoxy to the pipe internal walls. However, before applying it, mechanical and chemical cleanup are required. The mechanical cleanup is usually done by abrasive pigging (where a pigging bullet sweeps through the pipe). This followed by HCl injection to dissolve and remove the scales [53].

Involving the metal acid in the chemical treatment makes the pipe walls suffer from corrosion.

#### **2.1.5 Brackish Water**

When the total dissolved solids (TDS) in water is between 1,500 and 5,000 ppm, the water is said to be brackish (above that is saline water) [54]. In the case where water is recovered from oil wells, salts such as MgCl<sub>2</sub>, and CaCl<sub>2</sub> are present with varying concentrations depending on the oil well location and depth, and the type of oil (e.g. light, medium or heavy). During preheating of the oil at temperatures above 120 °C, the chloride ions dissociated from those salts form gaseous HCl according to the hydrolysis reaction (2.17). Upon its condensation, HCl becomes corrosive to metals [55].



In addition to what has been already mentioned in the above subsections, other causes of corrosion can occur. For example, the presence of phantom chlorides (also known as organic chlorides) in crude oil can result in decomposing them and forming HCl which is harmful to downstream equipment. This usually happens when these salts are not separated very efficiently from the oil to below  $1 \text{ mg L}^{-1}$  levels [55].

Due to the significance of the above applications in the oil industry, solutions for corrosion protection and control are continually sought and researched. Additionally, it is known that the presence of crude oil (along with aqueous solutions and spent acids when flowing out of an oil well) on the surface of a metal like steel can diminish corrosion. Nevertheless, more studies on two-phase systems are required to address enhanced protection [56]. In the following section, some methods of corrosion protection are presented and discussed.

## **2.2 Corrosion Protection**

As briefly mentioned earlier, there have been attempts to mitigate corrosion of metals. The attempts include, for example, applying better practices for proper material selection during the design phase or replacement of a piece of equipment, adequate corrosion monitoring and inspection of equipment, applying internal and/or external coatings with polymers or noble metals, applying painting and/or lining, applying anodic and/or cathodic protection, and using corrosion inhibitors [7, 24]. Each of the following subsections briefly discusses one of those methods.

### **2.2.1 Proper Material Selection**

There is an ever-increasing variety of metals and alloys with each having its own characteristics, applications, advantages, and limitations. For material specialists, it is important, when it comes to selecting a metal for an application, to understand the functional requirements including corrosion considerations. Several methodologies incorporating knowledge-based and intelligent database systems have been developed in the past to help address the issue of material selection. In addition, some researchers presented design models such as the graph theory and the matrix approach that involve calculations taking into consideration, among other factors, corrosion resistance [57].

**Table 2.1:** Chemical composition of G1117 low carbon steel [58].

Element	C	Mn	P	S	Fe
Composition (wt. %)	0.14 – 0.20	1.00 – 1.30	0.04	0.08 – 0.13	balance

There are many types (and grades) of iron steel. Amongst them are API 5CT grade L80 and 13Cr steel, API 5L X52 steel (corrosion resistant to some extent [59]), N-80 Steel (for two-phase high velocity flow [60]), X65, 0.5% Cr and St52 (typically used for pipelines [61]). In general, low carbon steel are commonly used in the oil and gas sector as material of construction of equipment [62]. A typical composition of which is given in Table 2.1 [58]. It is for grade 1117 (which is the one used in this research). This carbon steel alloy has a density of  $7.85 \text{ g cm}^{-3}$  and an equivalent weight of  $27.85 \text{ g mol}^{-1}$ . Although steels vary in their chemical compositions and their physical properties, they all share a common reality: they corrode in aggressive environments. The selection of the appropriate iron-based alloys depends on multiple factors, like the economic feasibility, the mechanical and thermal properties of the metal. Another very critical consideration is the metal corrosion resistivity. From corrosion point of view, the selection of the right (carbon) steel alloy may depend on the conditions of the electrolyte which the metal to be used in/at (i.e., temperature, pressure, pH, types and concentration of corrosive materials, and flow) [29, 63, 64].

### 2.2.2 Monitoring and Inspection

To keep facilities fit-for-service and sustainable, the conditions of the equipment must be known at all times using inspection techniques. These techniques involve corrosion coupon exposure (i.e. weight loss measurements), wall thicknesses measurements and identifying defects such as cracks, pits or bulges [65]. In addition to these traditional methods, modern electrochemical techniques were developed for on-line and non-destructive inspection. For example, Linear Polarisation Resistance (LPR), Electrochemical Impedance spectroscopy (EIS), Electrochemical Harmonic Analysis (EHA), and Electrochemical Noise Monitoring (ENM). The techniques usually give either engineering data, which is related to changes in physical dimensions and properties of material, or operational data, which is information collected from inserted probes and chemical analyses of process streams to monitor changes in the corrosivity of the process

environment [66]. Based on the results of these tests, proper action is taken to preserve the metal of concern from corrosion to avoid equipment failures.

### **2.2.3 Coating**

Coating a metal with a polymer (or with electrically conductive polymers [67]) has been found to provide a form of anodic protection that is significantly capable of reducing corrosion rates in acidic media [68]. Examples of coating materials include epoxy, emeraldine salt, polyaniline, polyaniline/epoxy blends, polyvinyl chloride, and polypyrrole [69].

Metals could be also coated with other corrosion resistive metals for galvanic functions and corrosion protection. For example, metals like chromium, cadmium, zinc and nickel could be used for that purpose [70].

### **2.2.4 Cathodic Protection**

Cathodic protection is one of the most important approaches to control corrosion. In essence, when a metal surface is cathodically protected, it can withstand corrosive environments without deterioration. Cathodic protection can be either impressed current cathodic protection, or sacrificial anode cathodic protection. In cathodic protection, an external current polarizes the entire surface of the metal to the thermodynamic potential of the anode; hence, the surface becomes equipotential. In other words, a net positive current enters the metal at all regions of the metal surface that inhibits the tendency of metal ions from entering the solution [7].

Cathodic protection can be applied to metals in all soils and aqueous media. It has been found effective in protecting metals against general corrosion, pitting corrosion, corrosion cracking, corrosion fatigue and intergranular corrosion but not hydrogen cracking [7].

However, the literature reveals some disadvantages of cathodic protection. For example, under certain conditions, alternating currents have been found to cause corrosion even at a lower rate causing the metals to dissolve [71].

### **2.2.5 Corrosion Inhibitors**

Another way to mitigate corrosion is by adding corrosion inhibitors to corrosive media. Corrosion inhibitors are organic or inorganic substances that when added in small quantities to corrosive media can –to some extent- protect the surface of metals. They are commonly used in the oil and gas industry. The most probable mechanism of inhibition is by the adsorption of ions or molecules of the inhibitor onto the surface of metals (forming a layer that reduces the diffusion of the corrosive species into the surface), or by decreasing the rate of anodic and/or cathodic reactions by interfering in the redox reactions mechanisms. Also, they may increase the potential of a metal so that it enters the passivation region where a natural oxide film forms [72, 73]. Corrosion inhibition and examples of inhibitors are discussed in detailed in the next section.

## **2.3 Corrosion Inhibitors**

Generally, any process of corrosion control or mitigation is considered corrosion inhibition. However, it is mostly referred to the addition of a particular chemical that inhibits the oxidation reactions of the metal (i.e. metal corrosion). A chemical inhibitor could be in the form of a liquid or vapor or both. There are two main steps involved in the process of inhibition: the transport of the inhibitor to the metal surface and the interaction of the inhibitor with the metal surface. Nevertheless, the inhibition is a complex phenomenon that depends primarily on the formation of shielding layers on the metal surface [20].

Corrosion inhibitors can be classified into different categories: based on their physical nature, they could be either organic or inorganic [74]; and based on their phase, they could be liquid or vapour [75] (e.g., volatile solid particles which have the ability to vaporise and condense on a metallic surfaces to make them less vulnerable to corrosion [76]). Dominantly, however, they are classified based on their inhibition action: 1) anodic inhibitors, which inhibit the anodic reactions; 2) cathodic inhibitors, which hinder the cathodic reactions; and 3) mixed inhibitors, which control both the cathodic and the anodic reactions [20].

### 2.3.1 Anodic Inhibitors

Anodic inhibitors (also called passivators) are usually inorganic chemicals that, when added to a corrosive environment, suppress anodic reactions (see reaction 2.1). Usually, in an anodic treatment for general corrosion, the inhibition action takes place rapidly. Anodic inhibitors are effective since they cause a large anodic shift of the corrosion potential (usually several tenths of a volt), driving the potential of the metal surface to the positive direction in the passivation range. Hence, they are named passivators [77, 78]. Examples of anodic inhibitors include chromate, nitrite, benzoate, silicate, phosphate, and borate, and anions of weak acids [8, 20].

In general, there are two types of passivating inhibitors. The first one is the oxidizing anions that can passivate metals in the absence of oxygen. Examples of this group include chromate, nitrite, and nitrate. The second type is the nonoxidizing ions, which involve oxygen to passivate metals. Examples of this type include phosphate, tungstate, and molybdate [78].

Anodic inhibitors are very effective and widely used, however, appropriate dosage of them (i.e., not below a critical concentration) is required. Sodium nitrite ( $\text{NaNO}_2$ ), for example, is an anodic inhibitor used for carbon steel protection. It requires being above a critical concentration, otherwise, nitrite may cause localized pitting attack to the metal [8, 77]. In addition, anodic inhibitors work in alkaline media (i.e., pH values above 8). For example, sodium phosphate ( $\text{Na}_3\text{PO}_4$ ) is an effective anodic inhibitor in the presence of oxygen, however, its protective property toward steel is a function of the alkalinity of the electrolyte [77].

### 2.3.2 Cathodic Inhibitors

Cathodic inhibitors, also known as non-passivating inhibitors [20], either slow the cathodic reactions or selectively precipitate on cathodic areas, thus, increasing the surface impedance and limit the diffusion of reducible species into these areas [77, 78] (reactions 2.2 and 2.5). The possible reduction reactions (i.e., cathodic reactions) that can take place in an acidic medium at a cathode are the reduction of oxygen, and hydrogen evolution (the dominant reaction). These reactions take place when the respective species adsorb on the cathode [8].



In reaction 2.2, oxygen molecules diffuse to the surface where their bonds break down forming adsorbed atoms on the surface. The adsorbed atoms then react with other hydrogen atoms already adsorbed on the metal to form hydroxyl ions. Upon using a cathodic inhibitor like zinc, it reacts with the hydroxyl ion to form an insoluble compound that precipitates on the metal surface sealing the cathodic sites off and preventing further reactions. Hence, they are called cathodic inhibitors [8]. Cathodic inhibitors that act in that way are sometimes called cathodic precipitates. Ions such as calcium, zinc and magnesium, azoles and calcium bicarbonate  $\text{Ca}(\text{HCO}_3)$ , amines, phosphates, zincates, aniline and its chloroalkyl nitro-substituted form, and amino-ethanol groups are good examples of this class of inhibitors [8, 77, 78].

The factors controlling the degree of the cathodic reactions rate (as in reduction of oxygen) include the conditions of the electrolyte such as the flow (i.e., stagnant or flowing media), temperature, pressure, and the salts content since they all affect the concentration, mass transfer, the solubility and the adsorption rate of oxygen [8].

Other cathodic inhibition mechanisms include suppressing hydrogen evolution at the cathodic sites. The inhibitors that act this way are known as cathodic poisons. Alternatively, cathodic inhibition can be achieved by adding inhibitors that react with oxygen ions (also known as oxygen scavengers e.g., sodium sulphite  $\text{Na}_2\text{SO}_3$ ) thus inhibiting oxygen from depolarizing the cathode [78].

There are some differences between the cathodic inhibitors and the anodic ones. Unlike anodic inhibitors, cathodic inhibitors do not activate pitting attack, however, they are not as effective as the anodic ones in reducing the corrosion processes [77]. In addition, cathodic inhibitors have only a minor effect on the corrosion potential of the metal, changing it either in the noble or active direction usually by no more than a few millivolts [20]. For these reason, mixed inhibitors attained a particular attention in the research of corrosion inhibition in the recent years. This class of inhibitors are discussed in the next subsection.

### 2.3.3 Mixed Inhibitors

Organic inhibitors used for corrosion inhibition are mixed inhibitors. When added to a corrosive media, they have the ability to hinder both the anodic and the cathodic reactions of a metal [20, 77]. Organic inhibitors are usually designated as ‘film-forming’ chemicals since they have the ability to protect a metal by forming a hydrophobic film on its surface [20, 77].

Polarization curves and Tafel plots (will be explained later) to some extent point out the nature of inhibition. A change in corrosion potential upon adding an inhibitor indicates that the corrosion processes are being suppressed. In general, anodic inhibitors cause a change in potential in the positive direction, while, a change in potential in the negative direction designates inhibition of the cathodic processes. However, in the case of mixed inhibitors, no recognizable changes in the corrosion potential are observed. This suggests that both anodic and cathodic processes are inhibited. The reason for this is that mixed inhibitors influence the whole surface of a metal when added in sufficient concentrations. It has been shown that corrosion inhibition is more effective when both the anodic and cathodic reactions are inhibited compared to when one of them alone is controlled. Normally, when a mixed inhibitor covers less areas, it mostly covers the anodic sites, while, at a high coverage area both anodic and cathodic sites are covered. Therefore, both anodic and cathodic corrosion reactions are inhibited [20, 78]. In addition, a shift of the polarization curve with no alterations in Tafel slopes when adding an inhibitor, indicates that the adsorbed inhibitor is blocking active sites and inhibiting the reaction but without affecting the mechanism of the corrosion process. On the other hand, a change in the Tafel slopes when an inhibitor is used shows that the effect of the inhibitor is on the corrosion reaction mechanism [20].

The vacant orbitals in a metal under study has its effects on the inhibition properties. For example, Vračar and Dražić [79] investigated some organic molecules as corrosion inhibitors for iron and found that the molecular orbital interactions correlate with the inhibition properties. They compared the corrosion inhibition in iron using thiophenol, phenol, and aniline as inhibitors and found that the best efficiency for thiophenol came from the interaction between the sulphur lone pairs and the vacant orbitals in iron atoms.

The effectiveness of mixed inhibitors depends on several factors such as the chemical composition and structure of the molecule used as an inhibitor, and its affinity

(thus, spontaneity) to adsorb on the metal surface. In addition, the temperature and pressure of the system play a vital role because the film formation is an adsorption process which is greatly affected by the system conditions. Another factor that influences the effectiveness of the film-forming inhibitors is their ionic charge (if applicable) and the charge of the surface of the metal. Positively charged ions of inhibitors such as amines will adsorb on negatively charged metals. While, the opposite is true for the sulfonates, as an example, which are negatively charged ions of inhibitors that tend to adsorb on the positively charged metals. Another critical factor that influences the effectiveness of an organic inhibitor is its concentration. For any specific inhibitor in any given corrosive medium there is an optimum concentration that leads to a maximum area coverage [78].

## 2.4 Green Corrosion Inhibitors

With the extensive use of different inhibitors in different sectors, concerns have been raised regarding health, safety and environment due to handling, using and disposing these chemicals. As a consequence, the field of development and design of corrosion inhibitors have constantly been influenced by new regulations. These regulations are meant to control the adverse environmental consequences of inhibitors, which are increasingly being addressed. The concerns are related to the toxicity, biodegradability, and bioaccumulation of these inhibitors when discharged into the environment. Some of the used conventional inhibitors may be found satisfactory and highly efficient in corrosion mitigation, but they pose hazards to the environment that are not yet fully understood. For example, chromium (IV)-based inhibitors are found good inhibitors for copper, yet, they are toxic [21]. Another example is those inhibitors that contain hexavalent chromium,  $\text{Cr}^{6+}$  which are now deemed carcinogens [20]. Therefore, more research is required for developing green (i.e., environmentally friendly) inhibitors, and to increase their inhibition efficiency and stability once they are applied. The term ‘green’ inhibitors refers to being non-toxic, naturally-occurring, biological, and/or biocompatible molecules such as plant extracts and food dyes [80, 81].

For aqueous electrolytes, many molecules have been designed and studied as potential green inhibitors -either organic or inorganic- against corrosion of metals like carbon steel. Examples of green inhibitors include plant extracts, essential oils, purified compounds such as amino acids [80], cellulose derivatives [82], some alkaloid derivatives

[81], guanidine derivatives [83], tryptophan derivatives [84], 4-phenylthiazole derivatives [85], triazole derivatives [86], oxo-triazole derivatives [87], imidazoline derivatives [88] L-Cysteine derivatives [89], flavone derivatives [82], and methionine derivatives [90]. In addition to those naturally-occurring molecules, medical drugs have been considered and studied as ideal green corrosion inhibitors. Examples include antibiotics, natural penicillins, aminopenicillins, macrolides and cephalosporins [91].

However, it is not expected that all 'green' chemicals be ideal candidates as corrosion inhibitors and this is due to several reasons, as it will be shown in the next sections.

## 2.5 Adsorption of Corrosion Inhibitors

Adsorption of organic inhibitors on the metal surface can, to a large extent, change the corrosion resisting properties of metals. Because the degree of corrosion inhibition is a function of adsorption (i.e., the surface coverage by the inhibitor), understanding the organic compounds adsorption is vital [92]. Organic corrosion inhibitors are said to be effective in corrosion inhibition based on the chemical properties and of the molecule used, its affinity (and spontaneity) to adsorb on the metal surface, and its ionic charge (when applicable). The adsorption (i.e., film-formation process) is affected by the temperature and pressure of the system too [78]. The adsorbed molecules form a film on the metal surface which minimize diffusion of corrosive ions to the metal surface, therefore, retarding both the anodic and the cathodic reactions. It can also be said that the adsorbed inhibitor minimizes metal atoms from participation in corrosion reactions [20].

Several elements influence the adsorption of inhibitors on metals. They stem from surface measurements, inhibitive efficiency measurements, and knowledge of adsorption isotherms. These elements are related to 1) the surface charge on the metal, 2) the nature of the functional groups and the structure that makeup the inhibitor, 3) the interaction of the inhibitor with water molecules, 4) the interaction of adsorbed inhibitor species with each other 5) the interaction of the molecules with the atoms of the metal, and 6) the type of adsorption of inhibitors (i.e. physical, chemical, or mixed-type adsorption) [78]. Theoretically, in addition, it is thought that the inhibition progression is a simple substitution of the solvent molecules (water in this case) adsorbed on the metal surface by the inhibitor molecules as shown in the reaction (2.18) [93], where "I" refers to an inhibitor

molecule, and  $n$  to the relative size (or size ratio) of the inhibitor molecule to a water molecule. Hence, the size of the inhibitor molecule has an effect on the inhibition efficiency.



Organic inhibitor molecules can adsorb on metals either by physical adsorption processes, chemical adsorption ones, or both.

### 2.5.1 Physical Adsorption

Van der Waal's electrostatic forces that exist between the inhibitor (present in an electrolyte) and the metal surface cause this type of adsorption. It is commonly thought to be through donation of an excess negative (or positive) charge to the metal surface [94]. Sometimes, physical adsorption is referred to as physisorption. During metal cathodic polarization, the metal surface becomes positively charged. In this case, negatively charged anionic inhibitor will adsorb on the metal surface. Similarly, positively charged cationic inhibitor will adsorb on the metal surface when it is negatively charged (i.e., during anodic polarization). Nuñez [95] summarizes the factors by which this phenomenon can occur. It can occur through 1) the electrostatic attraction between the charge on both the inhibitor and the metal, 2) the dipole interactions between the two materials when they are uncharged, 3) the  $\pi$ -electrons in the molecule and the orbitals in atoms of the metal, or 4) a combination of those interactions. Physisorbed inhibitor molecules have relatively weak electrostatic forces and can be detached from the surface by physical means such as increasing the temperature and/or velocity of the media (i.e., shear stress) [8].

### 2.5.2 Chemical Adsorption

Chemical adsorption, also called chemisorption is an adsorption process that results in a strong binding of the inhibitor with the metal surface [8]. Actually, in chemisorption a charge transfer or charge sharing takes place between the inhibitor molecule and the surface of metal. An inhibitor that is chemisorbed usually interferes with the dissolving metal atoms through interacting with them, thus, blocking active surface sites. However, it has been noticed that chemisorbed molecules have a certain residence time. That is, they

are in dynamic processes of adsorption/desorption steps. Chemisorption is known for its high heat of adsorption, persistence and irreversibility. Inhibitors that have a functional group containing a heteroatom like N, S, or O normally adsorb chemically. Also, the presence of electrons that are loosely bonded, such as  $\pi$ -electrons in aromatic rings, double/triple bonds, unpaired electrons in a functional group can result in chemical bonding [38]. These electrons, upon adsorption, are transferred to (or shared with) vacant d-orbitals of the transition metals. What is thought to happen in this type of adsorption is that an overlap of occupied orbitals in the inhibitor with the partially empty  $d$ - or  $f$ -orbital in the atoms of the metal [93]. This is supported by quantum chemical calculations performed for organic inhibitors on carbon steel where it was found that a fraction of electrons were transferred from the inhibitor to the metal [12]. In the same study, it was also found that as the difference between the energies of the highest occupied molecular orbital (HOMO) in the binding centre of an inhibitor and the lowest unoccupied molecular orbital (LUMO) in the metal atoms increases, the inhibition efficiency of the inhibitor increases.

Electronegativity of the heteroatom in an inhibitor molecule plays a major role in the adsorption process (hence, the inhibition efficacy): The higher the electronegativity, the lower the adsorption (i.e., lower corrosion protection). Sulfur-containing compounds, for example, are usually better corrosion inhibitors than the nitrogen-containing ones because sulfur has lower electronegativity compared to nitrogen [96, 97].

### 2.5.3 Thermodynamics of Adsorption

From thermodynamics standpoint, the standard free energy of adsorption  $\Delta G_{\text{ads}}^{\circ}$ , the standard heat of adsorption  $\Delta H_{\text{ads}}^{\circ}$ , and the standard entropy of adsorption  $\Delta S_{\text{ads}}^{\circ}$  can provide some insight on the adsorption nature of an organic molecule.  $\Delta G_{\text{ads}}^{\circ}$  can provide information on the overall spontaneity of the molecule to adsorb and form a film, and also the stability of the film [98]. Negative values of  $\Delta G_{\text{ads}}^{\circ}$  suggest a spontaneous adsorption process and the more negative values imply higher spontaneity. Positive values, however, suggest that adsorption is not favoured (i.e. no or extremely low adsorption) implying that desorption is the favoured process at the standard conditions [99].

Standard entropy of adsorption,  $\Delta S_{\text{ads}}^{\circ}$  may infer the degree of orderness (or disorderness also called the degree of freedom of adsorbate) of that molecules at a liquid/metal interface. It has been seen across multiple sources in the literature that there is an agreement

over the connotation associated with negative values of entropy of adsorption. They indicate that the molecules of the inhibitor became more ordered (or less dis-ordered) as adsorption progresses, and may infer the presence of associative processes on the surface [98-102]. Others add, for exothermic heat of adsorption (i.e. negative  $\Delta H_{\text{ads}}^{\circ}$ ), negative change in entropy must result (i.e. negative  $\Delta S_{\text{ads}}^{\circ}$ ) [103]. However, positive entropy changes have been interpreted as a consequence of desorption of water molecules from the metal surface [104, 105]. Others suggest that positive entropy changes may refer to dissociation processes of the adsorbate molecules [99], or its decomposition on the surface of the metal [94]. In addition, others suggest that a positive change in entropy is due to an increasing in the disorderness that happens to the reactant while becoming metal-adsorbed complexes [106].

Standard heat of adsorption,  $\Delta H_{\text{ads}}^{\circ}$ , can offer information on the type of adsorption. For an endothermic adsorption process ( $\Delta H_{\text{ads}}^{\circ} > 0$ ), the type of adsorption is of chemical nature. However, an exothermic adsorption process ( $\Delta H_{\text{ads}}^{\circ} < 0$ ) could refer to physisorption, chemisorption or both together. A value of  $\Delta H_{\text{ads}}^{\circ}$  less negative than  $-40 \text{ kJ mol}^{-1}$  is attributed to physisorption, while, values more negative than  $-100 \text{ kJ mol}^{-1}$  can characterize chemisorption [94].

Although the type of adsorption is seen to be determined by  $\Delta H_{\text{ads}}^{\circ}$ , it can be qualitatively determined by studying the kinetics of desorption of the inhibitor. This is discussed in details in section 5.2.

## 2.6 Adsorption Isotherms

Adsorption of organic compounds on metals is a function of several factors that include the polarization and the chemistry of the metal surface, the electronic characteristics of the adsorbed species, the temperature of the system, types of corrosion reaction occurring, and the electrochemical potential of metal-electrolyte interface. Upon these factors, either physical adsorption, chemical adsorption or comprehensive adsorption can take place on a metal surface [107]. Adsorption of an inhibitor on a metal surface is commonly explained by adsorption isotherms. They provide useful information as to how the corrosion inhibition process can be attained and provide insights on the nature of interactions between the metal and the inhibitor as a function of its concentration [20].

Under isothermal conditions, adsorption processes of inhibitors on carbon steel seem to mostly obey the Langmuir, Temkin, or Frumkin isotherms. Some other cases found to obey other isotherms like Flory-Huggins, Dhar-Flory-Huggins, Viral Parsons, Bockris-Swinkels, and the thermodynamic-kinetic model of El-Awady [93]. All those isotherms are explained in details elsewhere [14, 16, 79, 107, 108].

The Langmuir isotherm represents adsorption of molecules to form only a monolayer on the surface of the metal, thus excluding multilayered adsorbate films. The model assumes a reversible process, no lateral interactions between the adsorbed molecules, and the uniformity of the metal surface in terms of its energy. The model is shown in the following equation:

$$\frac{C}{\theta} = \frac{1}{\beta_{\text{ads}}} + C \quad (2.20)$$

which can be verified by a plot of  $C/\theta$  versus  $C$ . The parameter  $\theta$  is the fractional surface coverage at a specific concentration of an adsorbate (which is the inhibitor in this thesis). This parameter is unitless, and it is defined as the ratio of the covered area relative to the maximum coverage that can be attained ( $\Gamma/\Gamma_{\text{max}}$ ) and  $\Gamma$  is usually represented in units of quantity of the adsorbate (e.g. mol or g) per the surface area ( $\text{m}^2$ ) in the case of corrosion studies.  $C$  is the concentration of the inhibitor in an electrolyte in  $\text{mol dm}^{-3}$ , and  $\beta_{\text{ads}}$  is the affinity of the inhibitor molecules toward adsorption sites, in  $\text{dm}^3 \text{mol}^{-1}$ . At a constant temperature,  $\beta_{\text{ads}}$  is related to the Gibbs-free energy of adsorption by this relation [107]:

$$\beta_{\text{ads}} = \frac{1}{C_{\text{sol}}} \exp\left(\frac{-\Delta G_{\text{ads}}}{RT}\right) \quad (2.21)$$

where  $\Delta G_{\text{ads}}$  is the Gibbs free energy of adsorption,  $R$  is the gas constant,  $T$  is the temperature of the system in Kelvins, and  $C_{\text{sol}}$  is the molar concentration of the solvent used (it is  $55.5 \text{ mol dm}^{-3}$  for water). When Gibbs free energy of adsorption is evaluated at various temperatures, the enthalpy of adsorption,  $\Delta H_{\text{ads}}$ , and entropy of adsorption,  $\Delta S_{\text{ads}}$ , can be estimated by utilizing equation (2.19):

$$\Delta G_{\text{ads}} = \Delta H_{\text{ads}} + T\Delta S_{\text{ads}} \quad (2.19)$$

The significance of estimating those parameters, as mentioned earlier, stems from their ability to define the thermodynamic nature of an adsorption process at equilibrium.

Finally, some factors have strong evidence in affecting adsorption. For example, adsorption of organic compounds found to increase with inhibitor molecular weight and its dipole moment. For alkyl-chained and fatty acids organic inhibitors, it was perceived that protective efficiency against corrosion improves with increasing the length of alkyl chains. The concentration, furthermore, when increased gives better results [79].

## 2.7 Kinetics of Corrosion Reactions

The exact mechanism as to how inhibitors actually work is not yet fully understood. Nevertheless, in most cases empirical analysis has provided information on the effectiveness of a particular inhibitor for a particular substrate in a particular medium. Furthermore, understanding the chemistry of the surface of the metal and the adsorbed molecules is important for revealing information about the inhibition action, so, surface analytical techniques are required [109]. Unexpectedly, in some cases, at low surface coverage some inhibitors have high efficiency. In contrast, some inhibitors, such as thiourea and amines in diluted solutions may stimulate corrosion [78].

Apparent activation energy of corrosion reactions  $E_a$  (in  $\text{J mol}^{-1}$ ) can be related to the rate of corrosion reactions, also referred to as the kinetics of the reactions. It is simply an indicator of how fast a reaction proceeds, regardless of its spontaneity (i.e.  $\Delta G_{\text{ads}}$ ). Since a corrosion reaction comprises probably more than one step (i.e. it involves a mechanism of series of reactions involving the formation of complexes between the reactants and the final products), so, we are here talking about the activation energy of the rate determining step of a corrosion reaction. It is thought that corrosion rate (CR), which is an equivalent to an overall reaction rate constant in a chemical reaction  $k$ , is related to  $E_a$  through an Arrhenius-type equation (2.21) [110]. CR can be represented by the corrosion current  $i_{\text{corr}}$  (i.e. the charge transfer per a unit time in an electrochemical reaction, also measured in Amperes), or the inverse of the charge transfer resistance  $R^{-1}$  measured in  $\Omega^{-1}$ . So, the activation energy can be found by either of the Arrhenius equations (2.22 or 2.23) [15].

$$j_{\text{corr}} = A \cdot \exp\left(\frac{E_a}{RT}\right) \quad (2.21)$$

$$\ln j_{\text{corr}} = \ln A - \frac{E_a}{RT} \quad (2.22)$$

$$\ln R_P^{-1} = \ln A - \frac{E_a}{RT} \quad (2.23)$$

where  $A$  is the frequency factor of the reaction ( $A \text{ cm}^{-2}$ ),  $R$  is the gas constant and  $T$  is the temperature in K. So, plotting  $\ln j_{\text{corr}}$  (or  $\ln R^{-1}$ ) as a function of  $1/T$  will result in a straight line where the slope of it is the activation energy of the reaction (assuming the reaction mechanism is constant) –on should note that this activation energy value is an *apparent* value as the corrosion reaction rate might be also limited by mass transport, adsorption/desorption of reactants/products, to name a few. Doing so, when an inhibitor is present on the corroding surface, may result in the same value of the activation energy measured in its absence or can result in a different value. Ideally, the presence of an inhibitor inhibits corrosion by increasing the activation energy (or just blocking active sites on the corroding surface –no change in the activation energy). However, there are organic inhibitors that decrease the activation energy [111]. It is thought, in general, that if there is no change in activation energy upon adsorption of inhibitor, this may imply that the inhibitor has no influence on the mechanism of the corrosion reactions: Its presence on the surface is just as a physical barrier blocking the surface from interacting with the corrosive species [112]. According to some authors [110, 113], however, if the difference ( $E_{a,\text{blank}} - E_{a,\text{inhibitor}}$ ) is positive (or unchanged, according to some authors like [112]), then this may indicate that the inhibitor is involved in reacting with the surface (chemisorption) obstructing it from further reaction with the corrosive species.

Although the interpretation of the rise/drop of  $E_a$  sounds paradoxical, lower values of the frequency factor  $A$  strongly suggest that there is less collisions of the corrosive species with atoms of the metallic surface which is a natural premise of corrosion inhibition [110]. However, it is found in quite frequent situations that the presence of an inhibitor (of good inhibition efficiency) can increase the value of  $A$  [103]. Tang *et al.* [101] suggest that both the change of activation energy and the pre-exponential factor should be studied together in order to come to a decisive and reasonable conclusion, since they may change as the concentration of an inhibitor changes. For example, at a particular concentration,  $E_a$  may drop (virtually accelerating the corrosion rate) but associated with a drop in  $A$ . This implies a definite reduction of corrosion rate since the collisions become less. Conversely, at some other concentration,  $A$  may increase but  $E_a$  increases with it too. This also means a definitive reduction in corrosion rate, since there is a larger energy barrier for corrosion reactions to happen.

To conclude, the kinetics of corrosion reactions are determined by the activation energies and the pre-exponential factors in the presence and the absence of an inhibitor (excluding a possible influence mass-transport).

## 2.8 Selection of Corrosion Inhibitors for oil and gas applications

Corrosion in the oil and gas industry occurs in a wide range of conditions and due to a wide range of reasons. However, when it comes to selecting an inhibitor, it was found from the literature that the selection is mostly based on two main aspects. The first one is associated with the system itself (i.e., the electrolyte and the metal applied), and the second one is associated with the nature of the inhibitor. With regards to the system, it was found, for example, that the type of corrosion taking place, the temperature and the pressure of the system, the pH of the solution, the types of corrosive species present in the media and their concentrations, the phase(s) of the media in which corrosion occurs, the electro/chemical properties of metals used, and the morphology of these metals all play major role in the process of selecting an appropriate inhibitor [6, 17, 94, 97, 114-116].

Selection of a corrosion inhibitor that is to be used in the oil and gas industry should be based on several factors. It should be made of readily available materials taking into account its cost effectiveness. Also, it should be non-toxic and environment-friendly. In addition, it should contain a functional group that has a heteroatom like N, S, or O that can readily adsorb on the metal. The presence of electrons that are loosely bonded, such as  $\pi$ -electrons in aromatic rings, double/triple bonds, unpaired electrons in a functional group is important too since they are capable of inducing chemical adsorption. In addition, an inhibitor molecule should contain a fatty part (like a long alkyl group) to encourage hydrophobicity near the metal surface which in turn helps preventing corrosive species present in the aqueous phase from diffusing to the surface [20, 96, 97].

The remaining part of this section will be devoted for presenting several examples of inhibitors that have been studied very recently for general corrosion of carbon steel in different system conditions. This will be followed by a subsection presenting the molecule that has been selected as a green corrosion inhibitor for the present work.

Behpour *et al.* [17] studied three Schiff bases 2-(((2-sulfanylphenyl)imino)methyl))phenol (A), 2-(((2)-1-(4-methylphenyl)methylidene]amino)-1-benznethiol (B), and 2-

((2-sulfanylphen-yl)ethanimidoyl))phenol (C) on corrosion inhibition of mild steel in 15% HCl solution. They utilized weight loss measurements, polarization, and electrochemical impedance spectroscopy (EIS) methods. The results of the show that A and B have efficiency of 99% at 200 mg L<sup>-1</sup>, individually or mixed. C, showed efficiency of more than 80%. The inhibition efficiencies increased with concentration, which reveals that inhibition was mainly due to adsorption.

Aljourani *et al.* [94] investigated benzimidazole, 2-methylbenzimidazole, and 2-mercaptobenzimidazole as corrosion inhibitors for mild steel in 1M HCl solution. They also evaluated their adsorption and the inhibition efficiency as functions of the inhibitors concentrations and the temperature of the electrolyte. Tafel polarization, and EIS were used in this research. They found that the inhibitors are suitable for mild steel in 1M HCl solutions and their efficiencies increased with concentration. Also, it was found that the corrosion current density increased with temperature, but, the rate is lower in the presence of the inhibitors.

Gao *et al.* [117] synthesized and investigated two tertiary amines: 1,3-dimorpholin-4-yl-propan-2-ol, and 1,3-bis-diethylamino-propan-2-ol, as corrosion inhibitors for carbon steel. The electrochemical potentiodynamic polarization and EIS measurements were carried out to evaluate their inhibitive performance. Corrosion inhibition was found to increase as a function of concentration of these products with a maximum inhibition of 95% at  $2.5 \times 10^{-2}$  M. It was found that the adsorption of these inhibitors followed the Langmuir isotherm.

Granese *et al.* [118] did electrochemical and surface analysis investigating heterocyclic nitrogen compounds n-hexadecyl derivatives of pyridine (P), quinoline (Q) and acridine (A) as inhibitors for steel. They incorporated Tafel curves, EIS and ellipsometric measurements in their study. It was found that the inhibition efficiency increases with the number of aromatic rings on the molecules. The highest inhibition was found with the A derivatives, while P derivatives showed the lowest. It was also found that the n-hexadecyl derivatives of the N heterocyclic compounds inhibit better than the respective non-substituted ones, which, according to the investigators, could be due to a greater blocking effect by hydrophobic long chains.

For this work an amino-pyridine derivative (MAEP) was used as a corrosion inhibitor.

### 2.8.1 MAEP: Green Inhibitor

After investigating some work in the literature comparing multiple organic molecules in terms of the chemical structure versus the inhibition efficiency and how they behave in different media, several commercially-available derivatives were nominated as potential green inhibitors in this project. Among these options, it was rationalized that a potential candidate would be a molecule with an aromatic ring with nitrogen atom in it (i.e. pyridine) and another nitrogen in the side chain (i.e. an amino group) as well as a fatty group (i.e. an alkyl group). Several molecules were found available on the market. Narrowing down the choices based on cost, availability, purity, and toxicity record, it was concluded that 2-(2-Methylaminoethyl)pyridine (MAEP) would be a reasonable choice. The chemical structure along with a 3D model<sup>†</sup> of the molecule are shown in Fig.2.1.

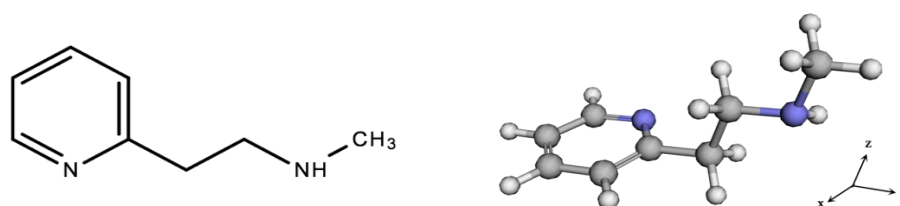


**Figure 2.1:** Chemical structure of MAEP (<sup>†</sup>3D model was generated by drugbank.ca)

According to the supplier data sheet [119], the molecular weight of this molecule is 136.19 g mol<sup>-1</sup>, and at room temperature and atmospheric pressure, it exists in a liquid form with a density of 0.984 g mL<sup>-1</sup> and a boiling point of 114 °C. Being in a liquid form with high solubility in water (miscible) makes it easy to be applied to electrolytes. The structure of the molecule suggests that one end is hydrophilic (i.e. the aromatic ring) and the other end is relatively hydrophobic (i.e. the methyl group). This may result in expelling away hydrated ions from the surface of a metal once the hydrophilic part of the molecule adsorbed on it. In addition, the product has relatively low toxicity level and high chemical stability. It is worth to mention that this chemical is among pyridine derivatives that have been used as a medical treatment for some illnesses for their antiviral, antifungal, antioxidant, and anti-thyroidal actions [120].

## **CHAPTER 3: OBJECTIVES**

### 3. Objectives

The main objective of the present research was to study the possibility of applying a selected amino-pyridine derivative, MAEP, as a non-toxic green inhibitor for general corrosion of carbon steel (CS) surfaces in acidic media for oil and gas industry related applications.

Corrosion inhibitors have been widely investigated for industrial application in the oil and gas industry. However, a major part of the research focused mainly on the action of inhibitors in the aqueous phase. Therefore, there is a need for investigating the effect of the corrosion inhibition in the oil phase, too. The reason is that the oil phase can enhance the performance of an inhibitor, and strengthen the corrosion inhibition by oil wetting, water entrainment, and by rendering the metal surface hydrophobic [121]. So, a secondary objective of this work was to test the efficacy of the selected molecule in two-phase systems contain light crude oil.

In order to meet the main and the secondary objectives, specific objectives were to be achieved:

- To investigate the adsorptive-type interactions of MAEP with the CS surface in acidic solutions (adsorption thermodynamics and kinetics).
- To investigate the influence of varying the environment conditions like temperature, pH, the acid concentration, time of immersion, and the volume % of the oil present in the solution on the inhibition efficiency.
- To study the topography of the CS samples in presence and in the absence of the organic molecule.

# **CHAPTER 4: MATERIALS AND EXPERIMENTAL PROCEDURES**

## 4. Materials and Experimental Procedures

The materials, solutions, electrochemical cell, experimental procedures, and the electrochemical techniques used in this work will be introduced in this chapter.

### 4.1 Materials and Solutions

The molecule that was investigated as a corrosion inhibitor is 2-(2-Methylaminoethyl)pyridine (MAEP), 97% pure (refer to section 2.8.1 for more details). It was purchased from Sigma-Aldrich Canada Ltd. (Product No. M28804) and was used as it is without further purification. The chemicals used in the electrolytes preparation were purchased from Thermo Fisher Scientific Inc.: hydrochloric acid, HCl, 38w/w% in concentration (product No. 351280-500); and 0.5 M sodium hydroxide solution that was prepared using NaOH that is 97% in purity (Product No. 1310-73-2). The hydrocarbon used in the two-phase system was Wyoming Crude Oil (refer to section 2.1.1). It was purchased from ONTA Inc. (Product name *Light, Sweet Wyoming Crude Oil, February 2016*). It was used as received without any treatment.

The electrolytes were prepared by diluting HCl in nano-pure water of 18.2 MΩ cm in resistivity to make 0.1 M HCl solution (called electrolyte onward, unless otherwise mentioned). 0.5 M NaOH was used to adjust the pH of the solutions. In the two-phase system experiments, oil was added in vol%.

### 4.2 Electrochemical Cell

A three-electrode electrochemical cell was used in all the corrosion experiments. The reference electrode used was a saturated calomel electrode (SCE) and all potentials reported in this work are quoted with reference to it. The counter electrode was a graphite rod. The working electrode was prepared from a low carbon steel rod. It was purchased from McMaster-Carr Company (part No. 8290T14). Its diameter was 5/8" (~1.59 cm). The chemical composition of this steel is given in Table 2.1. The rod was cut into button-like shaped samples of 3 mm in thickness. A Teflon holder was used to hold a working electrode sample when it is immersed in the electrolyte, allowing 1.039 cm<sup>2</sup> of its geometric surface

area (of one face) to be exposed to the electrolyte. A schematic diagram of the three electrode cell is shown in Fig. 4.1.

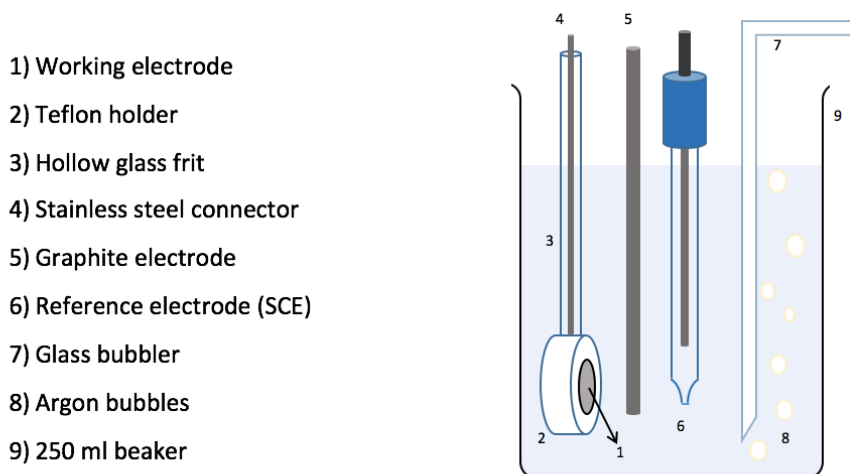


**Figure 4.2:** Schematic diagram of a three-electrode electrochemical cell

For the temperature-dependent experiments, the same cell was used but was placed in a water bath of a controllable temperature. A thermometer was added to the cell to measure the temperature.

In the two-phase experiments, a magnetic stirrer was used to get some degree of homogeneity between the oil and water.

### 4.3 Experimental Equipment and Software

An AUTOLAB potentiostat/galvanostat/FRA PGSTAT 30 that is controlled by FRA2 (for EIS) and GPES v.4.9 (for other measurements) software was used to perform all the electrochemical measurements. Using this software, open circuit (OCP), electrochemical impedance spectroscopy (EIS), and Linear Polarization tests for both polarization resistance and Tafel plots were made. For OCP, the potential of the cell was recorded under zero current conditions for 1 hour. For better characterization of the interface and the surface processes, EIS measurements were made over a series of frequencies ranging from 50 kHz to 50 mHz with an alternating current (AC) at a root-

mean-square voltage amplitude of  $\pm 10$  mV with respect to the open circuit potential,  $E_{OC}$ . After that, polarization resistance measurements were made in a window of  $\pm 10$  mV with respect to the open circuit potential, with a step potential and a scan rate of 0.45 mV, and 1.5 mV s<sup>-1</sup>, respectively. After that, Tafel plots were recorded: the polarization of working electrode was done from -200 mV to +200 mV vs.  $E_{OC}$  with a step potential and scan rate equal to 0.45 mV and 1.5 mV s<sup>-1</sup>, respectively.

To evaluate the samples surface morphology, a scanning electron microscopy (FEI Quanta Environmental Scanning Electron Microscope (ESEM<sup>TM</sup>)) was employed. The beam accelerating voltage was set at high voltage (HV) of 3 kV for the imaging and the resolution was set at 1024x800.

Inductively-coupled plasma optical emission spectroscopy (ICP-OES) was used to analyze the iron content in electrolyte samples for the long-term sample immersion experiments.

#### **4.4 Experimental Methodology**

The working electrode surface (the side that was exposed to the electrolyte) was treated prior to each experiment. The treatment started with water-wet polishing using 120-grit paper then followed by ethanol-wet polishing with 600-grit. Between the two polishing steps, the sample was rinsed thoroughly with deionized water. After the second polishing, the sample was rinsed with ethanol and then it was degreased with ethanol again in an ultrasonic bath for about 5 minutes. It was subsequently rinsed with ethanol and dried with argon. This was done to avoid corroding the sample by water or air as much as possible. After that, the sample was assembled in the Teflon holder which was then immersed in a 200ml of electrolyte for an hour at open-circuit potential (OCP) in order for the redox reactions to reach a steady state, indicated by a relatively constant electrode potential. After this step, three other measurements were conducted in the following order: EIS, polarization resistance (PR), and Tafel measurements.

The electrolytic solution was deoxygenated by argon gas of 99.998% purity at a rate of 3-5 bubbles per second for 30 minutes prior to the sample immersion and throughout the electrochemical measurements. The measurements were done in a temperature range of 295 K to 333 K.

For the inhibitor concentration-dependent experiments, after immersing the electrode, a specific amount of the inhibitor was added immediately to the electrolyte to achieve a specific concentration (the injection of the inhibitor was done far from the working electrode). Then the measurements were conducted.

For the pH-dependent experiments, the pH of the electrolyte was adjusted by 0.5 M NaOH prior to the deoxygenation step.

In the two-phase system experiments, the crude oil was mixed with the electrolyte at a specific volume percent. The addition of oil was prior to argon-purging.

For the inhibitor adsorption kinetic measurements, the sample was immersed in the inhibitor-free electrolyte, then the inhibitor was injected right away. The first PR measurement was started immediately. Then, the same was repeated chronologically after that in this order: 5, 10, 15, 20, 30, 40, 60, 90, 120, 150, 180, 240 minutes. The same measurements were done in the absence of the inhibitor –control measurement.

The kinetics of desorption was studied to qualitatively assess the type of adsorption. PR measurements were conducted every 30 minutes for 6 hours. The procedure was as follows: an electrolyte of 10mM inhibitor was prepared and the PR test were carried out for CS sample every 30 min for 2 hrs (adsorption of the inhibitor). Then, a specific amount of inhibitor-free electrolyte (that was pre-purged with argon) was added after two hours to first dilute the initial 10 mM concentration to 7mM and then again after two hours to further lower the inhibitor concentration to 5mM. PR test were carried out immediately after each dilution and every 30 min.

For the long-term immersion experiments, the samples were immersed in the electrolyte (in the presence of 10mM of inhibitor and in the absence of it) for 1, 7, 30 days, separately. Samples (aliquots) of the solutions were collected after different durations of time for ICP-OES measurements. At the end of each immersion period, the carbon steel specimens were then rinsed with deionized water and dried with argon for SEM imaging.

All the values reported in this work are average values of at least three replicates where their standard deviations were reported along with them (where applicable).

## 4.5 Research Techniques

In this section, the techniques that were used in this study are briefly discussed.

### 4.5.1 Open-Circuit Potential (OCP)

The open-circuit-potential (OCP) measurement was used here to monitor the change in the working (corroding) electrode potential with time. In OCP measurements, the net current flow is zero [122]. OCP measurements can give indication on the initial kinetics of corrosion processes, passivation, and on the time needed to reach a steady state (or equilibrium state, in certain instances).

### 4.5.2 Electrochemical Impedance Spectroscopy (EIS)

Electrochemical Impedance Spectroscopy (EIS) is an accurate method used in corrosion research that is not influenced by the low conductivity of an electrolyte. The technique can provide information on the structure of electrode/electrolyte interface and on the kinetics of (corrosion) reactions, including electron-transfer and mass transport. In this research, EIS was used to determine the resistance of the system to corrosion, by comparing the polarization resistance in the presence ( $R_i$ ) and absence ( $R_o$ ) of inhibitor in the electrolyte [117, 123]. The comparison was in terms of the efficiency  $\eta$  of inhibition using to the following relation:

$$\eta = \left(1 - \frac{R_o}{R_i}\right) \times 100\% \quad (4.1)$$

where the resistance values were obtained by modelling an EIS spectrum.

### 4.5.3 Linear Polarization (LP)

In this work, two Linear Polarization (LP) techniques were used: polarization resistance (PR), and Tafel polarization. In both techniques, the working electrode is polarized at a slow scan rate around the corrosion potential (OCP) and current is measured. According to the Butler-Volmer equation [124], if the polarization is done up to 30 mV around OCP (refer to Fig. 5.9), the dependence of current on potential can be considered

linear. Thus, the Ohm law can be applied to calculate the corresponding resistance of the electrode to corrosion, and the inhibition efficiency can then be calculated using Eq. (4.1).

In Tafel polarization, the electrode is polarized within a potential region of ca.  $\pm 200$  mV vs  $E_{OC}$  at a slow scan rate and current is measured (refer to Fig. 5.11). From the corresponding plot, corrosion current  $i_{corr}$  (or corrosion current density  $j_{corr}$ ) can be determined along with the anodic and cathodic Tafel slopes,  $\beta_a$  and  $\beta_c$ , respectively. In addition to enabling the direct determination of corrosion current, the Tafel polarization plot allows for calculation of corrosion current from also PR and EIS measurements, according to [126]:

$$i_{corr} = \frac{\beta_a \beta_c}{2.3(\beta_a + \beta_c)R_p} \quad (4.2)$$

where  $\beta_a$  and  $\beta_c$  are the anodic and cathodic Tafel slopes ( $V \text{ decade}^{-1}$  of current) of the anodic and the cathodic branches in the Tafel plots, and  $R_p$  is the polarization resistance determined from PR or EIS measurements.

Both the resistance and the current (or current density) can be then utilized in calculating the efficiency of the inhibitor by equations 4.1 and 4.3, respectively, where  $j_{corr,i}$  is the current density in the presence of the inhibitor and  $j_{corr,o}$  is in its absence [123].

$$\eta_i = \left( 1 - \frac{j_{corr,i}}{j_{corr,o}} \right) \times 100 \% \quad (4.3)$$

Corrosion rate ( $\text{mm year}^{-1}$ ) can be calculated using the corrosion current density  $j_{corr}$  ( $\mu\text{A cm}^{-2}$ ) utilizing the following equation:

$$\text{C.R.} = \frac{0.00327 j_{corr} (\text{E.W.})}{\rho} \quad (4.4)$$

where  $\rho$  it the density of the alloy in ( $\text{g cm}^{-3}$ ), and (E.W.) is the equivalent weight of the alloy in ( $\text{g}\cdot\text{mol}^{-1}\cdot\text{C}^{-1}$ ) which can be calculated using equation (4.5).

$$\text{E.W.} = \frac{100}{\sum_{i=1}^n \frac{x_i z_i}{M_{w,i}}} \quad (4.5)$$

where  $x_i$  is the amount of materials present in the alloy in %,  $z_i$  is the oxidation number of the respective material, and  $M_w$  is its molecular weight in ( $\text{g mol}^{-1}$ ). 0.00327 has a unit of ( $\text{s}\cdot\text{mol}\cdot\text{mm}\cdot\text{year}^{-1}\cdot\text{cm}^{-1}$ ).

#### **4.5.4 Scanning Electron Microscopy (SEM)**

Scanning Electron Microscopy (SEM) was used to visualize the topography of the CS samples. The output of this technique are micrographs for the surface of the samples in which the topographical difference between the samples -where the inhibitor was used and the control samples at different immersion times- will be evident [127].

# **CHAPTER 5: RESULTS AND DISCUSSIONS**

## 5. Results and Discussion

Steel alloys (like low carbon steel) is prone to general corrosion in acidic media as can be seen in the Pourbaix diagram in Fig. 5.1 [97]. For example, at low pH (e.g. 1), it can be seen that the iron atoms start to dissolve at potentials starting from approximately -0.6 V and above (vs hydrogen standard electrode SHE) that is equivalent to -0.844 V and above (vs standard calomel electrode SCE). It forms  $\text{Fe}^{2+}$ , but it can also form  $\text{Fe}^{3+}$  once the potential exceeds ca. 0.8 V (vs SHE or 0.556 V vs SCE). In conditions where 0.1 M HCl (pH of 1.25) being the electrolyte at 298 K and the G 1117 low carbon steel being the working electrode immersed in it, the open circuit potential of the sample starts at around -0.595 V (i.e. -0.351 V vs SHE) and levels off at -0.576 V (i.e. -0.332 V vs SHE) reaching a steady state, as shown in Fig. 5.2.

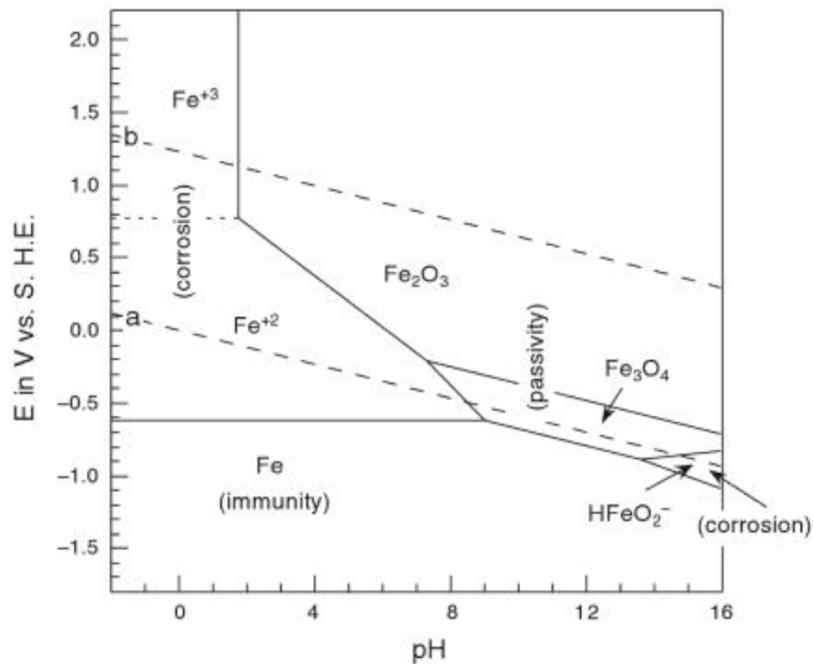


**Figure 5.1:** Pourbaix diagram for iron at 298 K [97]

It is evident that corrosion is still taking place since OCP values fall within the corrosion zone in the Pourbaix diagram i.e. the sample is not in the immunity or the passivation zones. In the absence of oxygen, corrosion is accompanied by hydrogen evolution reaction since the mentioned potentials at the mentioned pH value fall in the area below the a-dashed line in the diagram. Based on that, it is found that iron in low CS alloys

is found to dissolve in 0.1 M HCl and, hence, protection against corrosion in such conditions is required.

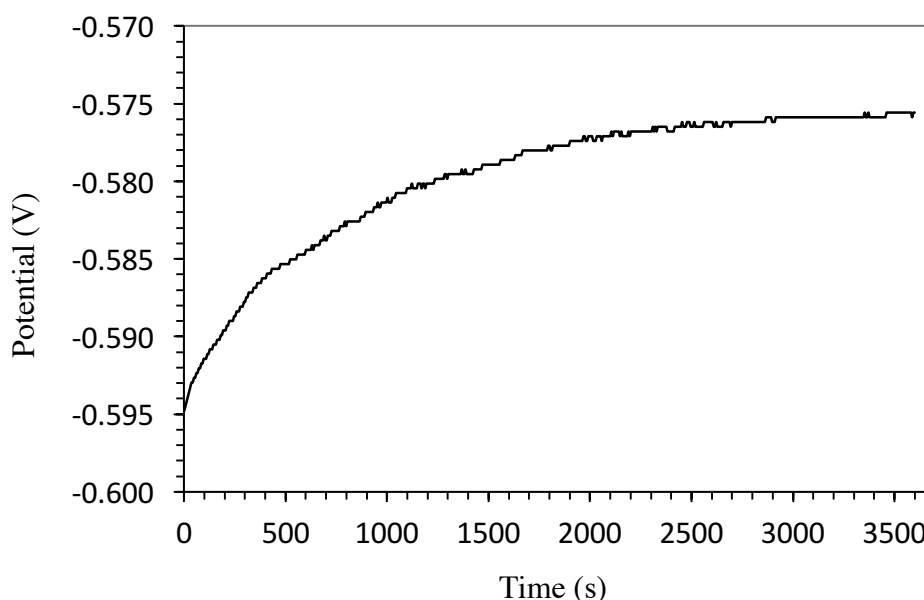


**Figure 5.2:** Open circuit potential variations (V) vs Time (s) of CS in 0.1 M HCl (pH 1.25) at T=298 K

In an attempt to lower down the corrosion rate of CS in such conditions, an aminopyridine molecule, namely 2-(2-methylaminoethyl)pyridine (MAEP), was chosen and applied as a potential ‘green’ corrosion inhibitor and its performance was monitored under various conditions.

The rest of the thesis will be devoted to present and discuss the results of 1) applying MAEP at different concentrations in 0.1 M HCl while keeping other parameters constant; 2) studying the kinetics of its adsorption, which could be done by applying it at an optimum concentration and measuring the change in the charge transfer resistance of the WE at different time intervals; 3) studying the type of adsorption of the molecule; 4) applying MAEP at the optimum concentration to the electrolyte and varying the temperature; 5) applying it to the electrolyte of varying pH values; 6) injecting it to media of varying HCl concentration; 7) applying it in two-phase electrolytes where crude was present in varying volume percentages along with 0.1 M HCl solution; and finally 8) studying the topography of CS samples in SEM after immersing them in 0.1 M HCl for different time intervals.

## 5.1 Effect of MAEP Concentration

The selected organic molecule as a corrosion inhibitor, MAEP, has distinctive structural features (see Fig. 2.1). It is suggested here that the pyridine group, having  $\pi$ -electrons and lone pair electrons in the N atom, functions as the binding part with the  $d$ -orbital in the metal atoms building a self-assembling monolayer (SAM) on the surface. The other end of the molecule, i.e. the methyl group, is hydrophobic and serves as a barrier between the surface of the metal and the hydrated corrosive ions such as  $\text{Cl}^-$  present in the electrolyte. Fig. 5.2 shows an illustration of a possible mechanism of corrosion inhibition by a MAEP SAM. However, the concentration of the inhibitor plays -to some extent- a crucial role in protecting the metal. Based on the schematics, it is hypothesized that as the concentration increases, the degree of protection should increase and reach a maximum (constant) value.

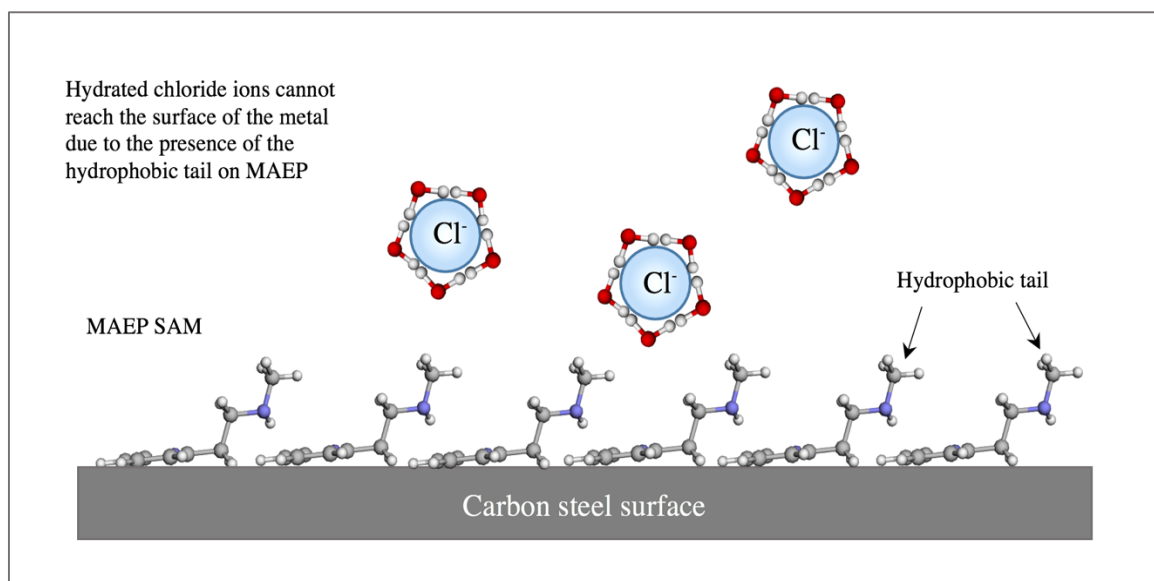


**Figure 5.3:** An illustration of the metal/inhibitor/electrolyte interface showing the possible protection mechanism against corrosion

This hypothesis was tested by introducing the organic molecule at different amounts to 0.1 M HCl making various concentrations of MAEP (i.e. 0.05, 0.1, 0.2, 0.5, 0.7, 1, 3, 5, 7, 10, 13, 15, 17, 20, 25 mM) against a control experiment where the electrolyte was blank (i.e. inhibitor-free). In each experiment, after the working electrode was

introduced to the cell, it was left to stabilize for 1 hour at open circuit potential. Then, it was subjected to EIS (refer to section 4.3 for more details) to measure the charge transfer resistance. After that, polarization resistance, PR, measurement was conducted followed by Tafel polarization, TP.

It was important that the set of measurements to be done in that order since EIS and PR are non-destructive tests while TP is destructive. The reason for that is in EIS and PR, the potential was polarized in a very small window with respect to the open circuit potential  $E_{OC}$  i.e.  $\pm 10$  mV for EIS and  $\pm 20$  mV for PR, while  $\pm 200$  mV vs  $E_{OC}$  was used for TP.

The results of those measurements are presented in the following subsections. It is important to mention that all the experiments were replicated at least three times.

### **5.1.1 Effect of MAEP Concentration on OCP**

Although the experiments in this sections were carried out at 295 K, it is expected that Pourbaix diagram would still be a good source to begin with for comparison. The diagram shows that iron starts to dissolve at potentials approximately above -0.844 V (vs SCE) at 298 K and pH of 1.25. Fig. 5.4 shows OCP in the absence and the presence of the inhibitor at selected concentrations. In the absence of the inhibitor,  $E_{OC}$  was shown to fluctuates between -0.576 V and -0.561 V which implies that iron ions are being produced. However, when the inhibitor was introduced, the potential increased indicating a level of protection. Also, it can be seen that in the absence of the inhibitor, the potential increase gradually with time reaching a quazi-constant value. The increase in the potential is most likely related to the buildup of corroded surface a layer that partially blocks the surface and slows down corrosion, until a steady-state is reached. It can also be seen that in the presence of the inhibitor, the general trend is relatively similar to the one in the control experiment which might be explained in the same manner. However, as the concentration of MAEP increases, the potential was seen to also increase. This increase can be related to an increase in the surface coverage by the inhibitor. It was found that at higher concentrations (above 10 mM MAEP), the  $E_{OC}$  did not increase much relative to the starting point. In fact, at higher concentrations, the plateau  $E_{OC}$  does not vary with MAEP concentration, as seen in Fig. 5.5. In conclusion, the results in Fig. 5.4 indicate MAEP works as a corrosion inhibitor. Other measurements were performed to further verify this assumption.

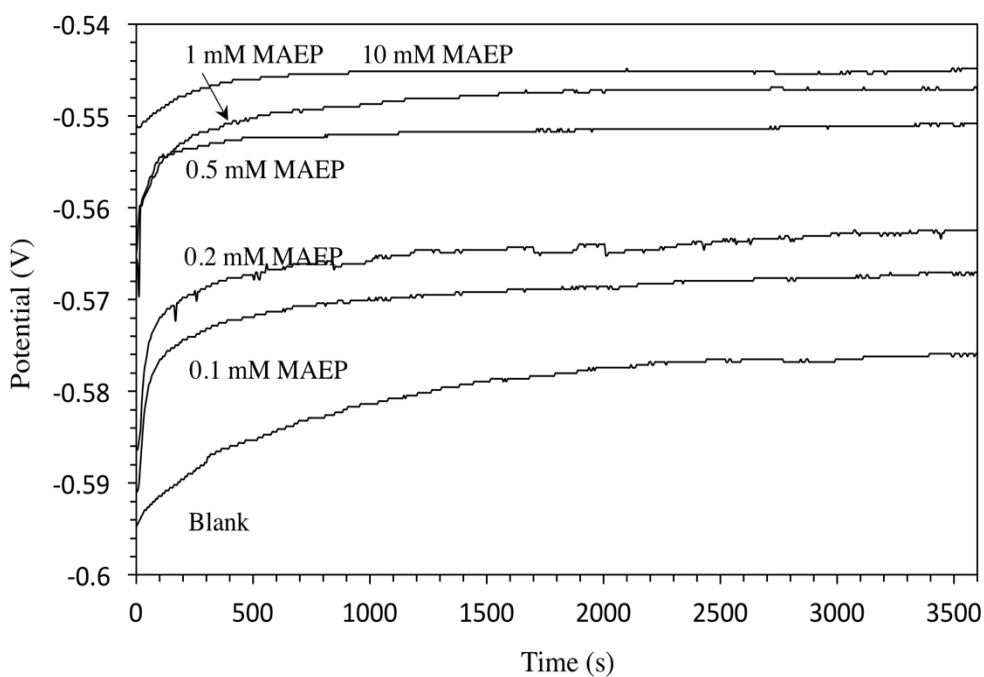


**Figure 5. 4:** Open circuit potential (V) vs time (s) for selected MAEP concentrations in 0.1 M HCl (pH 1.25) at 295 K

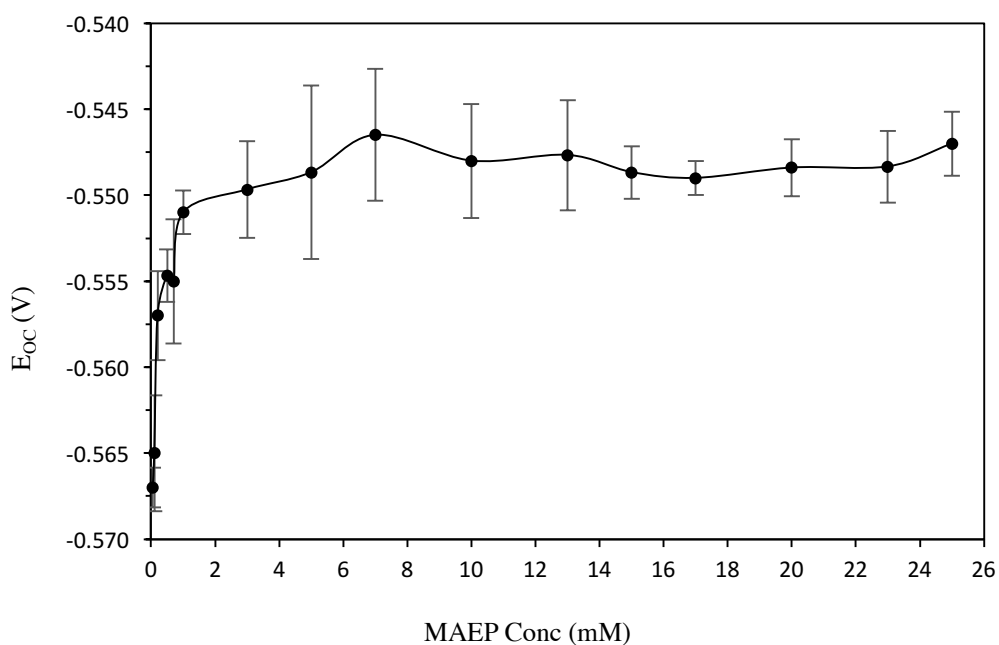


**Figure 5. 5:**  $E_{OC}$  (V) for all the tested MAEP concentrations (mM) recorded after 1 hour of CS immersion in 0.1 M HCl (pH 1.25) at 295 K

### 5.1.2 Effect of MAEP Concentration on Inhibition Efficiency – EIS measurements

To better understand the interaction of the inhibitor with the surface of CS surface, electrochemical impedance spectroscopy (EIS) measurements was made. Fig 5.6 presents selected results in a form of the Nyquist plot. From these plots one can determine the following equivalent electrical circuit (EEC) parameters:  $R_{el}$ -the resistivity of the electrolyte (at high frequencies),  $R_1$ -the charge transfer resistance due to the charge transfer resistance of the corrosion reactions at open circuit potential and its pseudo-capacitance  $CPE_1$  (at low frequencies),  $n_1$  is its exponent ( $n$  falls between 0 and 1. For  $n=1$ , CPE represents an ideal capacitor. For  $n=0$ , CPE would represent a resistor),  $R_2$ -the charge transfer resistance and the pseudo-capacitance  $CPE_2$  due to the presence of the inhibitor layer on the surface (when present), and  $n_2$  is its exponent [80]. Fig 5.6 shows Nyquist plots for a control experiment (MAEP-free) and for systems where MAEP was present at different concentrations. The resistance of the electrolyte is almost constant (common starting points of the curves). As the concentration increases (starting from 0 mM), the diameter of the semi-circles increases implying higher total charge transfer resistance on the surface of the metal.

To get values for the above-outlined EEC parameters, the experimental spectra were modelled using EEC models presented in Fig. 5.7, where model (a) was found to be the best EEC for the MAEP-free system, and (b) for systems where the inhibitor was present. The solid lines in Fig 5.6 as in Table 5.1, fitting of the plots was required as shown in the same figure by continuous curves. The fitting was done using electrical equivalent circuits, EECs, as shown in Fig. 5.7 where model (a) was found to be the best EEC that fits an MAEP-free system, and (b) for systems where the inhibitor was present. The solid lines in Fig. 5.6 present the model data. One can see that the agreement between the experimental (symbols) and model data (lines) is good, confirming that the two EEC models are appropriate for describing the CS/electrolyte interface and corresponding processes occurring at the interface. Table 5.1 presents the resulting EEC parameters.

**Table 5.1:** EIS parameters for CS immersed in selected inhibitor concentrations in 0.1 M HCl (pH 1.25) at 295 K.

MAEP conc. (mM)	0	0.1	0.5	1	5	10	20
$R_{ct}$ ( $\Omega$ )	19	22	19	20	19	21	21
$\pm$ SD	1	7	1	1	3	2	0
$CPE_1 \times 10^6$ ( $\Omega^{-1} s^{n_1}$ )	790	688	1408	905	761	602	412
$\pm$ SD	70	99	790	381	85	320	278
$n_1$	0.83	0.77	0.66	0.73	0.71	0.74	0.78
$\pm$ SD	0.02	0.03	0.04	0.06	0.04	0.06	0.05
$R_1$ ( $\Omega$ )	40	32	15	19	20	28	29
$\pm$ SD	5	8	2	5	9	7	5
$CPE_2 \times 10^6$ ( $\Omega^{-1} s^{n_2}$ )	-	1060	404	393	251	246	225
$\pm$ SD	-	285	233	132	30	45	45
$n_2$	-	0.97	0.87	0.86	0.90	0.88	0.87
$\pm$ SD	-	0.02	0.06	0.02	0.02	0.02	0.01
$R_2$ ( $\Omega$ )	-	29	87	105	138	166	248
$\pm$ SD	-	8	23	45	18	21	43

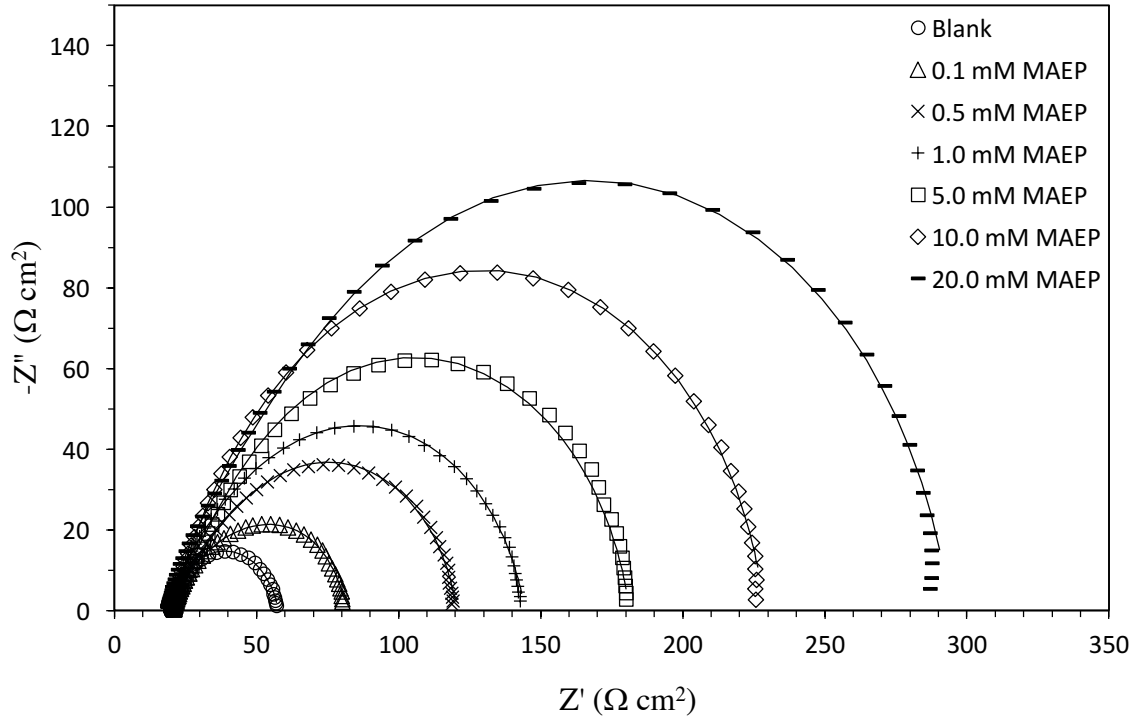


**Figure 5.6:** Nyquist plot of CS taken at different MAEP concentrations in 0.1 M HCl at 295 K. ( $\circ$ ) 0 mM, ( $\Delta$ ) 0.1 mM, ( $\times$ ) 0.5 mM, ( $+$ ) 1 mM, ( $\square$ ) 5 mM, ( $\diamond$ ) 10 mM, ( $-$ ) 20 mM MAEP. The solid curves represent data fitting.

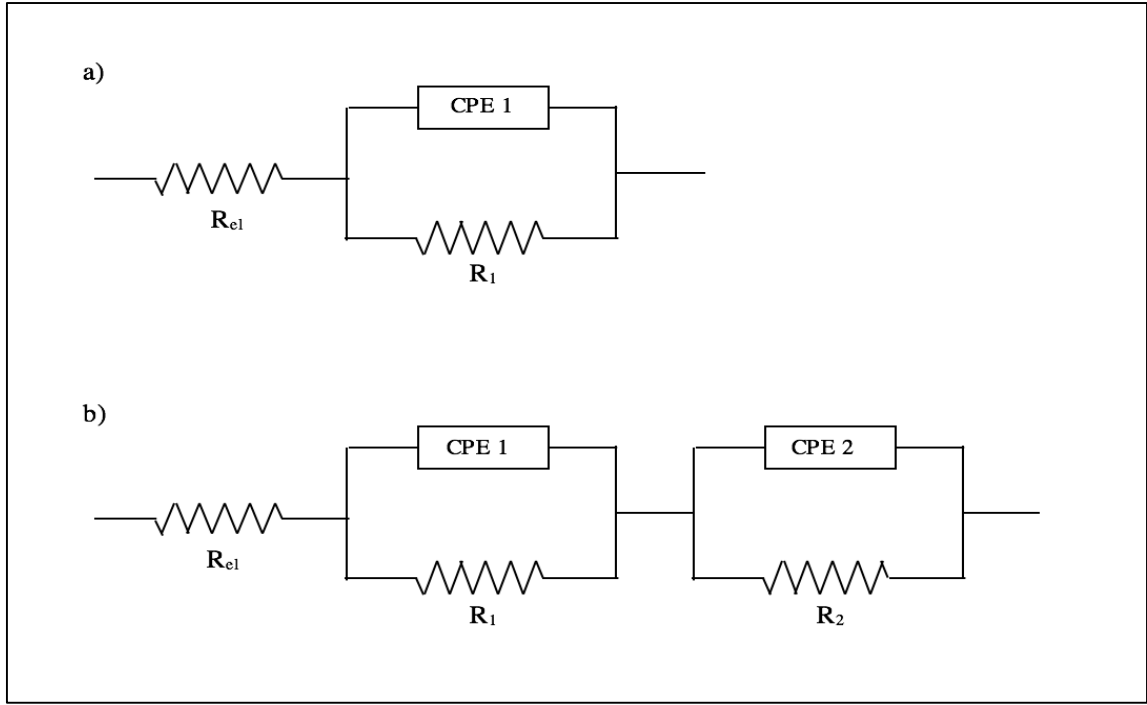


**Figure 5.7:** EEC models used to fit EIS data for (a) CS electrode in blank solution, and (b) on a CS electrode immersed in an electrolyte containing MAEP.  $R_{e1}$ -electrolyte resistance;  $CPE_1$ -double-layer and pseudo-capacitance;  $R_1$ -charge transfer resistance,  $CPE_2$ - SAM layer pseudo-capacitance,  $R_2$ -adsorbed inhibitor layer resistance.

The table shows that  $n_2$  is close to 1 meaning that the constant phase element  $CPE_2$  represents a capacitive behaviour. Capacitance, in general, is directly proportional to the conductive surface area. This implies that as the conductive surface area of CS is being minimized (by the MAEP growing coverage), the capacitance decreases which agrees with the trend in seen the table.

The inhibition efficiency was calculated for each of the MAEP concentrations tested for protecting CS from corrosion in 0.1 M HCl (pH 1.25) at 295 K. This was calculated using Eq. 4.1 where in the presence of the inhibitor  $R_1+R_2$  form  $R_i$  and in the absence of it (i.e. blank solution),  $R_1$  represents  $R_o$ .

$$\eta = \left( 1 - \frac{R_o}{R_i} \right) \times 100\% \quad (4.1)$$

The results are shown in Fig. 5.8. It can be seen that as the concentration increases the efficiency increases too suggesting that larger areas of the CS surface are being covered by the adsorbed inhibitor molecules [14, 80, 94, 128]. The maximum inhibition efficiency was found to reach 90.1%, at 25 mM MAEP.

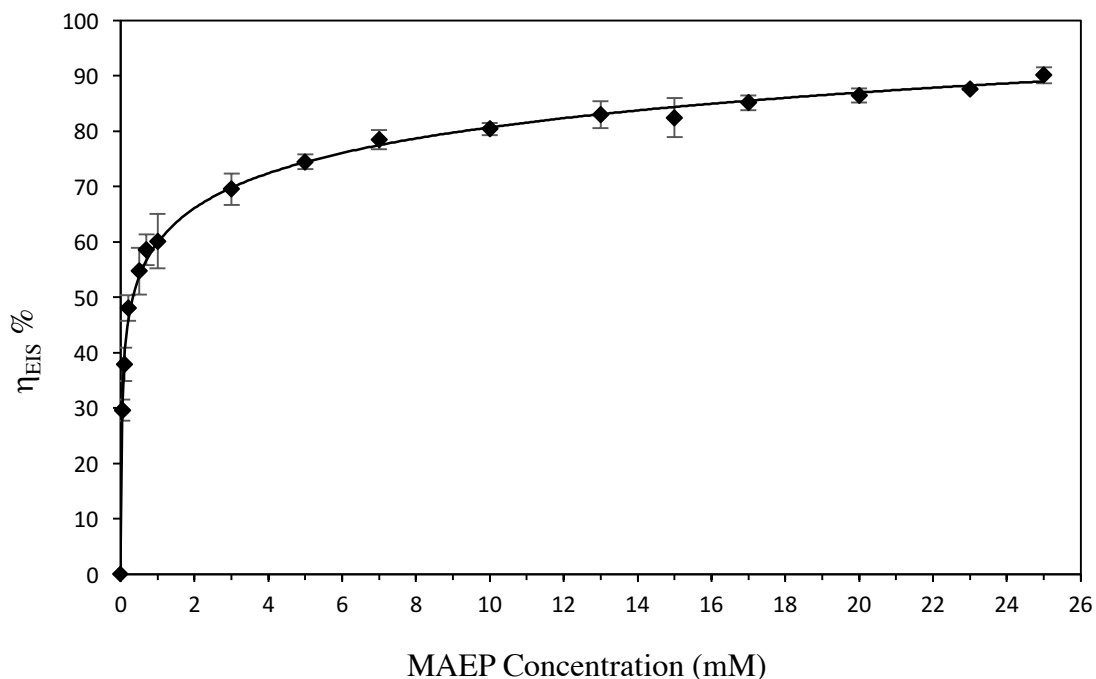


**Figure 5.8:** Inhibition efficiency against blank solution calculated from EIS resistances for all the MAEP tested concentrations in 0.1 M HCl (pH 1.25) at 295 K.

### 5.1.3 Effect of MAEP Concentration on Corrosion Inhibition – PR Measurements

It was seen in the previous section that the inhibition efficiency increased with increasing the inhibitor concentration. In this section, polarization resistance method was used to further this behavior. This technique was presented initially in section 4.5.3. Example of the resulting curves are shown in Fig. 5.9 where it can be seen that the slopes gets more inclined as more MAEP is being added to the system. The inverse of the slopes yields total electrical (and electrochemical) resistance of the system. It should be noted that the curves were corrected by the uncompensated resistance,  $iR$  (which is the resistance between the WE and RE, i.e.  $R_{e1}$ ) obtained from EIS measurements.

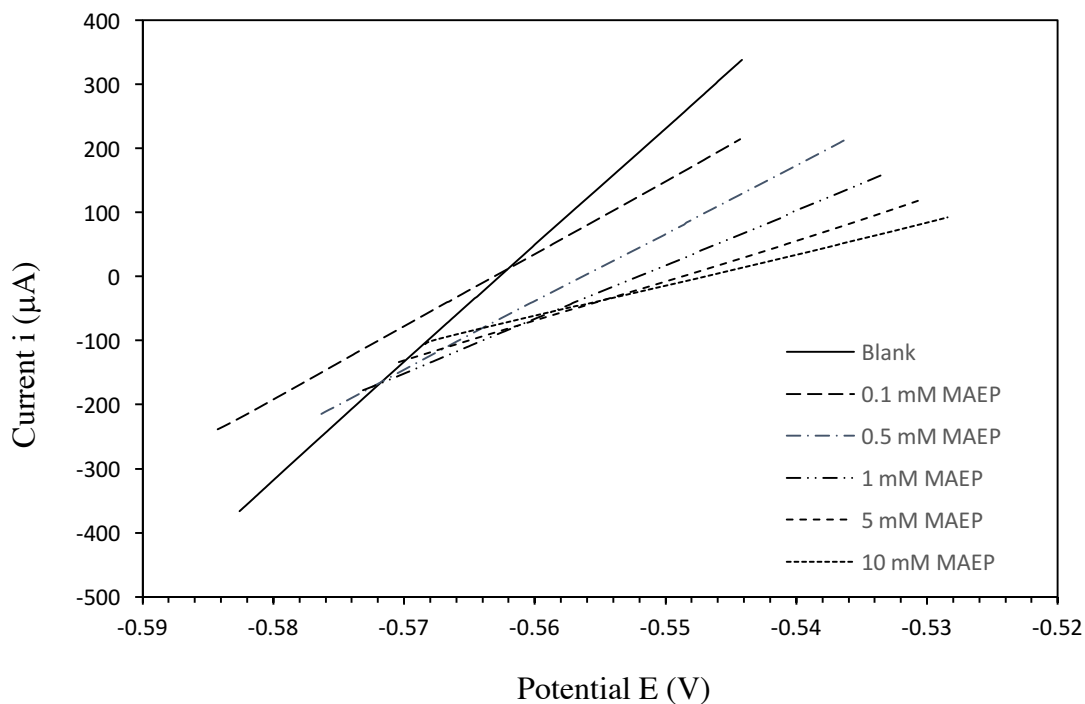


**Figure 5.9:** Current  $i$  ( $\mu\text{A}$ ) vs polarized potential (s) for blank and selected MAEP concentrations in 0.1 M HCl solution (pH 1.25) at 295 K.

The inhibition efficiency was calculated for each of the MAEP concentrations tested for protecting CS from corrosion in 0.1 M HCl (pH 1.25) at 295 K. This was done using Eq. 4.1 where  $R_i$  represents the resistance of charge transfer in the presence of the inhibitor and  $R_o$  for the blank solution.

The results are shown in Fig. 5.10. where it can be seen that they are in very good agreement with those obtained from EIS measurements. This implies that a conclusion similar to the one related to EIS measurements can be drawn. The maximum inhibition efficiency using this method was found to be 90.1%, at 25 mM MAEP.

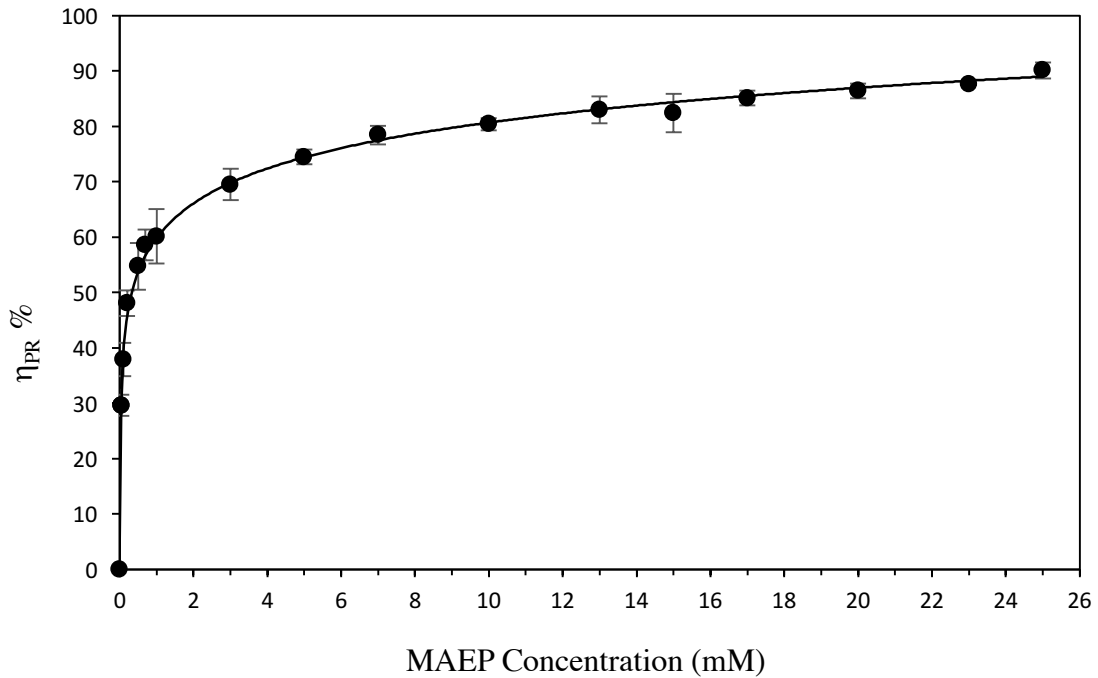


**Figure 5.10:** Inhibition efficiency for inhibitor-free solution calculated from PR resistances for all the MAEP tested concentrations in 0.1 M HCl (pH 1.25) at 295 K.

#### 5.1.4 Effect of MAEP Concentration on Corrosion Inhibition – TP Measurements

Tafel polarization, TP, was carried out to further verify the results presented in the previous two sections, by determining the corrosion inhibition efficiency from both Eqs. 4.1 (employing resistances at  $E_{OC}$ ) and 4.3 (employing current densities  $j_{corr,o}$  and  $j_{corr,i}$  at  $E_{OC}$ ). In addition, corrosion rates in ( $\text{mm year}^{-1}$ ) were calculated to reflect the degree of inhibition using Eqs. 4.4 and 4.5 (refer to section 4.5.3 for more details). The output from TP included the resistance of charge transfer  $R_T$  ( $\Omega$ ) and the current density  $j_{corr}$  ( $\text{A cm}^{-2}$ ) at  $E_{corr}$  (V), and the anodic and the cathodic slopes in ( $\text{V decade}^{-1}$ ),  $\beta_a$  and  $\beta_c$ , respectively.

Similar to PR measurements, it is important to be stated that the TP curves were corrected for the the uncompensated resistance,  $iR$ , so that only the charge transfer resistance is taken into consideration.

A typical Tafel plot is presented in Fig. 5.11. Extrapolating the anodic and cathodic branches to corrosion potential (i.e. OCP) enables estimating certain kinetics parameters. The point of intersection corresponds to  $j_{corr}$  on the current density-axis, while it corresponds to  $E_{corr}$  on the potential-axis. The slopes of the extrapolation lines determine

the Tafel slopes  $\beta_a$  and  $\beta_c$ . Then from equation 4.2,  $R_T$  (i.e.  $\Delta E/\Delta i$ , as  $E \rightarrow E_{\text{corr}}$  and  $i \rightarrow i_{\text{corr}}$ ) can be determined [124, 125].

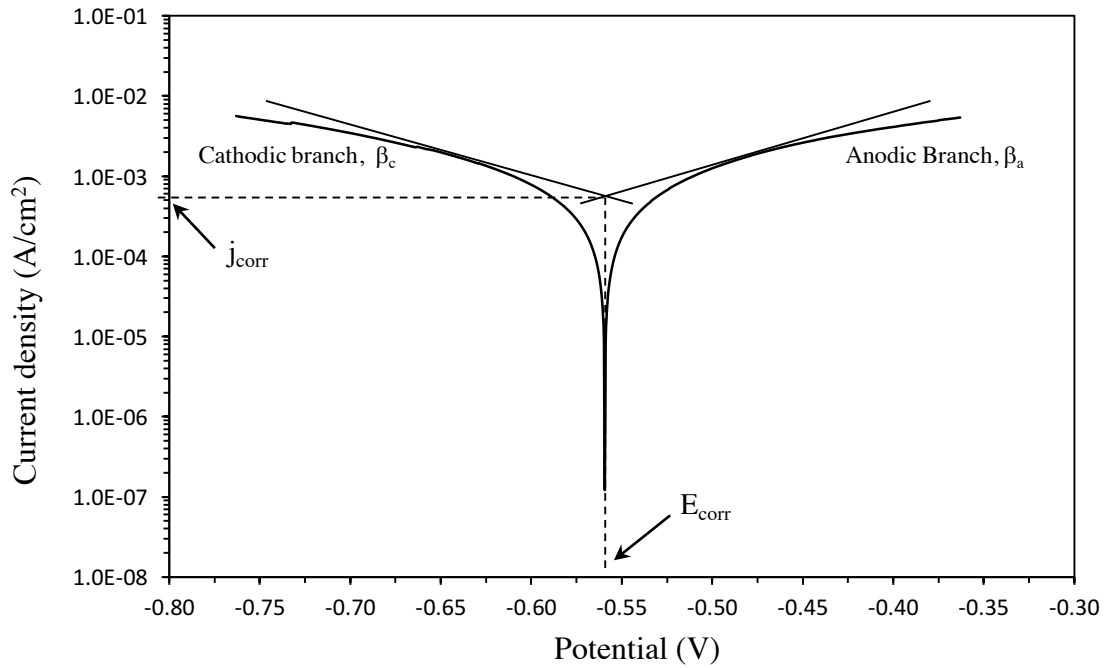


**Figure 5.11:** Tafel Plot for CS in an inhibitor-free solution of 0.1 M HCl (pH 1.25) at 295 K. The method of determining the Tafel parameters graphically.

Fig. 5.12 presents Tafel plots for a blank solution and for some selected MEAP concentrations in 0.1 M HCl (pH 1.25) at 295 K. It can be seen that the current density  $j_{\text{corr}}$  decreases and the corrosion potential  $E_{\text{corr}}$  shifts slightly towards noble (positive) values implying reduction in corrosion rates as the MAEP concentration is increased.

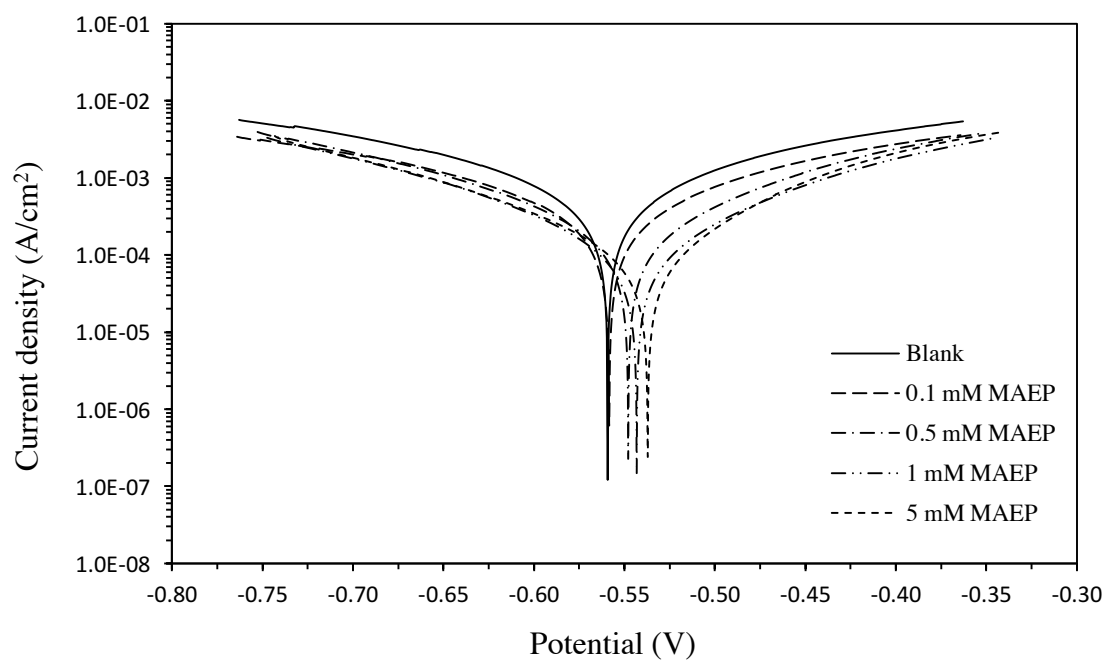


**Figure 5.12:** Tafel plots for CS immersed in 0.1 M HCl (pH 1.25) at 295 K for different MAEP concentrations.

Table 5.2 presents some Tafel parameters, namely,  $j_{\text{corr}}$ ,  $E_{\text{corr}}$ ,  $R_T$ ,  $\beta_a$ ,  $\beta_c$ , and corrosion rates CR, for CS immersed in the electrolyte at different MAEP concentration. The inhibition efficiencies were calculated for each of the MAEP concentrations tested for protecting CS from corrosion in 0.1 M HCl (pH 1.25) at 295 K. They were calculated using Eqs. 4.1 and 4.3 where  $R_i$  is the resistance in the presence of the inhibitor, and  $R_o$  is for the blank solution. The results are shown in Fig. 5.13. where it can be seen that they are in very good agreement with those calculated from EIS and PR results.

**Table 5.2:** Tafel parameters for CS immersed in selected inhibitor concentrations in 0.1 M HCl (pH 1.25) at 295 K.

C MEAP (mM)	0	0.5	1	5	10	20
$j_{\text{corr}}$ ( $\text{A cm}^{-2}$ ) $\times 10^6$	489	185	156	117	94	73
$\pm\text{SD}$	63	55	36	4	18	10
$\beta_c$ ( $\text{V dec}^{-1}$ )	0.083	0.102	0.095	0.105	0.104	0.108
$\pm\text{SD}$	0.006	0.005	0.006	0.005	0.006	0.003
$\beta_a$ ( $\text{V dec}^{-1}$ )	0.089	0.084	0.083	0.078	0.084	0.082
$\pm\text{SD}$	0.010	0.017	0.005	0.005	0.007	0.002
$R_T$ -iR ( $\Omega$ )	39	112	139	167	212	278
$\pm\text{SD}$	6	23	44	4	28	37
$E_{\text{corr}}$ (V)	-0.561	-0.547	-0.545	-0.542	-0.543	-0.543
$\pm\text{SD}$	0.003	0.003	0.002	0.003	0.002	0.002
CR ( $\text{mm year}^{-1}$ )	5.67	2.14	1.81	1.36	1.09	0.84
$\pm\text{SD}$	0.73	0.64	0.42	0.05	0.21	0.12
$\eta_{\text{jcorr}}$ %	-	57	64	76	81	85
$\pm\text{SD}$	-	7	2	1	4	2
$\eta_{\text{RT}}$ %	-	62	67	77	82	86
$\pm\text{SD}$	-	3	4	1	2	2

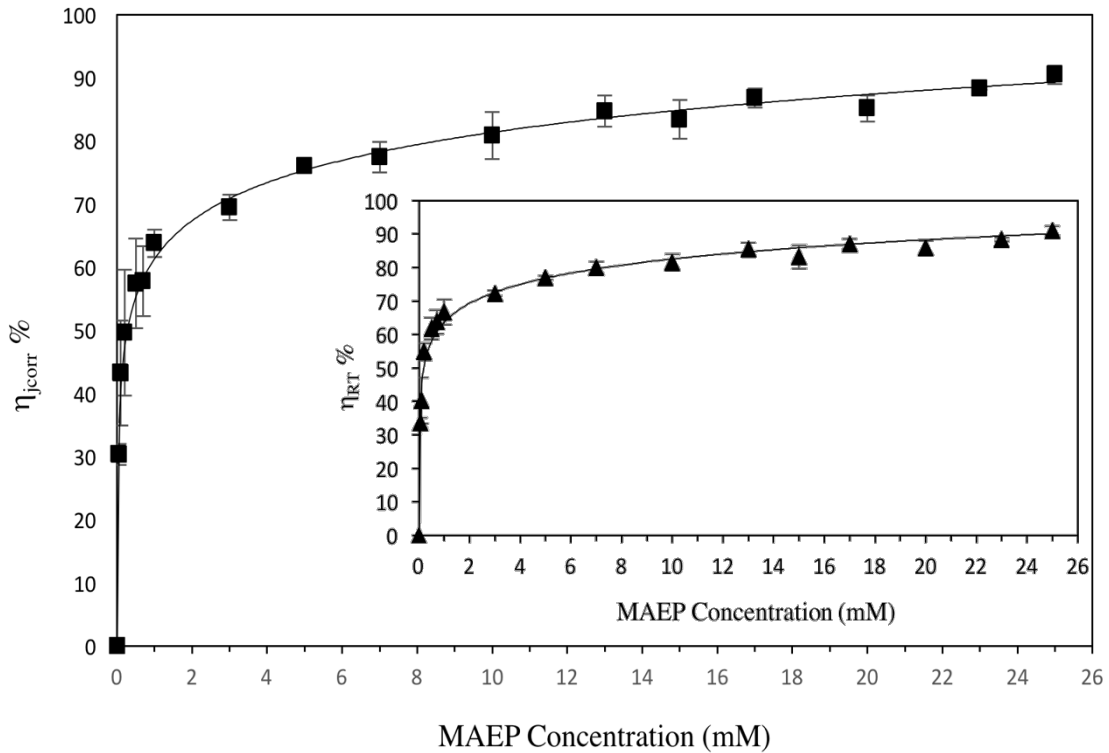


**Figure 5.13:** Inhibition efficiency against blank solution calculated from  $j_{\text{corr}}$  (and  $R_T$  in the inset) for all the MAEP tested concentrations in 0.1 M HCl (pH 1.25) at 295 K.

## 5.2 Adsorption Isotherm for MAEP on a CS Surface

It was seen in the previous sections that the inhibition efficiency rose as the concentration of the inhibitor in the bulk electrolyte increased. Given that the MAEP is a mixed-type inhibitor, one can assume that its inhibition efficiency is proportional to its surface coverage [80]. In other words, the adsorption of the MAEP molecules and the formation of the MAEP protective surface (mono)layer is the origin of corrosion protection observed in the previous sections. Therefore, it is essential the adsorption process be studied since it can shed light on the interaction of the molecule with the metallic surface.

It can be assumed that the relative surface coverage,  $\theta$ , is related to the inhibition efficiency in the following way:  $\theta = \eta / \eta_{\max}$ . Therefore, data that were recorded for any of the previous measurements can be utilized for determining a MAEP adsorption isotherm. Several isotherms were examined but the best agreement between the experimental and model data was obtained when the Langmuir isotherm was used (see Eq 2.20 below and refer to section 2.6 for more details). The inverse of the y-intercept of a plot of  $C/\theta$  vs  $C$  gives the adsorption affinity constant,  $\beta_{\text{ads}}$  ( $\text{L}\cdot\text{mol}^{-1}$ ), which is related to the Gibbs free energy of adsorption ( $\text{J}\cdot\text{mol}^{-1}$ ) by Eq. 2.21.

$$\frac{C}{\theta} = \frac{1}{\beta_{\text{ads}}} + C \quad (2.20)$$

$$\beta_{\text{ads}} = \frac{1}{C_{\text{sol}}} \exp\left(\frac{-\Delta G_{\text{ads}}}{RT}\right) \quad (2.21)$$

where  $C_{\text{sol}}$  is the molar concentration of the solvent (i.e. water in this case) and it equals to  $55.5 \text{ mol}\cdot\text{L}^{-1}$ ,  $R$  is the gas constant in ( $\text{J}\cdot\text{mol}^{-1}\cdot\text{K}^{-1}$ ).

Fig. 5.14 - main plot shows a plot of  $C/\theta$  vs  $C$  created where  $\theta$  was calculated from EIS results presented in Fig. 5.8 (the inset shows the isotherm when  $R_T$  from Tafel results presented in Fig. 5.13 (inset), was used). It can be seen that the trend is linear and the slope is close to one. Taking Eq. (2.20) into account, this confirms that the Langmuir isotherm is a good model that can describe the MAEP adsorption process. Therefore, it is believed that the molecules of the inhibitor build a monolayer on the metal surface [80]. From the main plot in Fig. 5.14,  $\beta_{\text{ads}}$  was calculated to be  $1836.4 \text{ L}\cdot\text{mol}^{-1}$ . Using Eq. 2.21,  $\Delta G_{\text{ads}}$  was calculated to be  $-28.3 \text{ kJ mol}^{-1}$ . The same was repeated for the inhibition data based on  $R_p$ ,  $j_{\text{corr}}$ , and  $R_T$ . The average  $\Delta G_{\text{ads}}$  was calculated and found to equal to  $-28.4 \pm 0.2 \text{ kJ mol}^{-1}$ .

This number indicates that the adsorption of MAEP on the CS surface is a relatively spontaneous process, from the thermodynamic point of view.

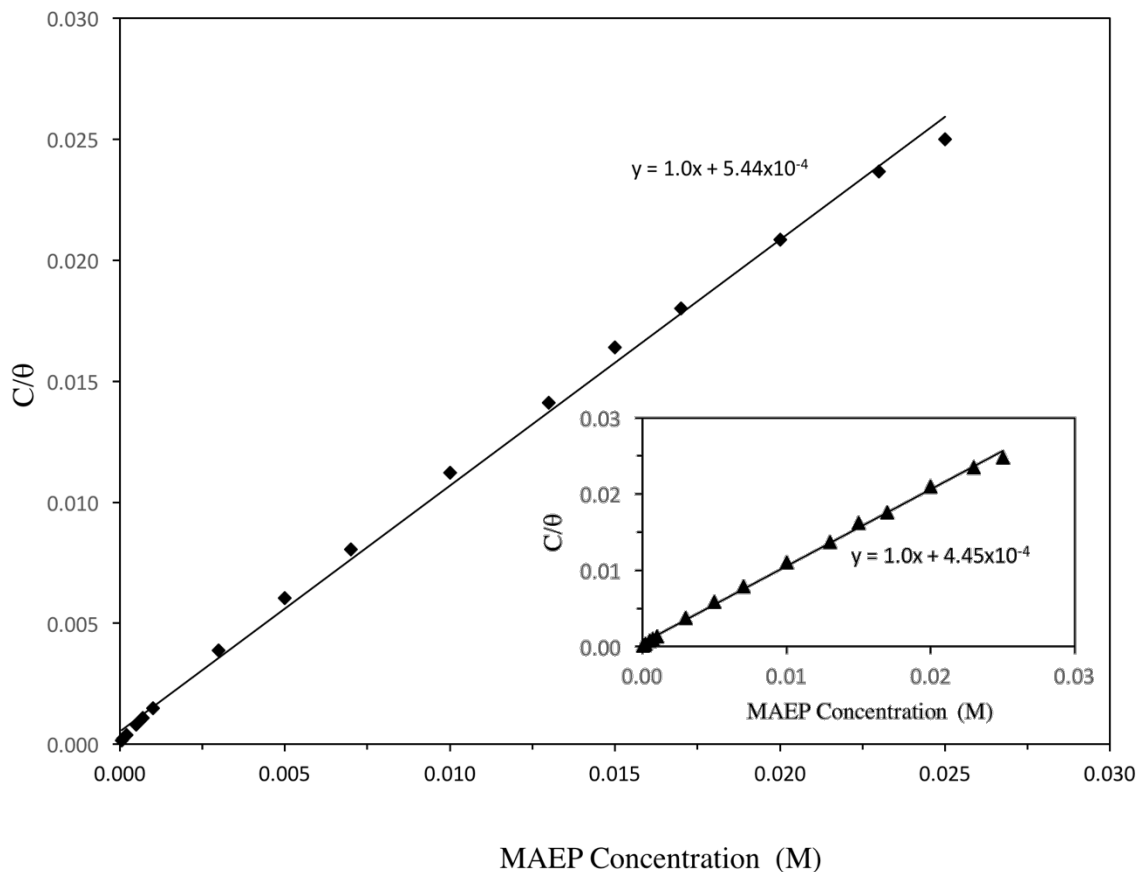


**Figure 5.14:** Linearized form of Langmuir isotherm of MAEP adsorption on CS at 295 K where  $\theta$  was calculated based on EIS results (inset: based on  $R_T$  of Tafel results). The solid line represents the Langmuir model.

### 5.3 Kinetics of Adsorption and Desorption of MAEP

A plot of polarization resistance,  $R_p$ , against time of CS immersed in blank solution, and in 10 mM MAEP in 0.1 M HCl (pH 1.25) solution at 295 K is shown in Fig. 5.15. The figure shows also the variation of the resulting inhibition efficiency as a function of time. It can be seen from the figure that the polarization resistance of CS in the presence of inhibitor increased sharply at very short times and reached its maximum (186  $\Omega$ ) after 10 minutes. Then, it stabilized after 120 minutes at ca. 148  $\Omega$ . On the other hand, the increase in polarization resistance in the absence of inhibitor is minor and gradual, and the final

(steady-state) value is significantly lower (ca.  $35 \Omega$ ) than that in the presence of inhibitor. Further, the trend of inhibition efficiency is similar to that of polarization resistance in the presence of inhibitor. If the extend of inhibitor adsorption (i.e. the area coverage) is directly related to the polarization resistance of the system, then it can be said that the maximum adsorption was reached after ca. 15 minutes of adsorption. The subsequent decrease in the efficiency could be related either to partial MAEP desorption or conformation rearrangement of MAEP molecules on the CS surface to yield a lower protection degree.

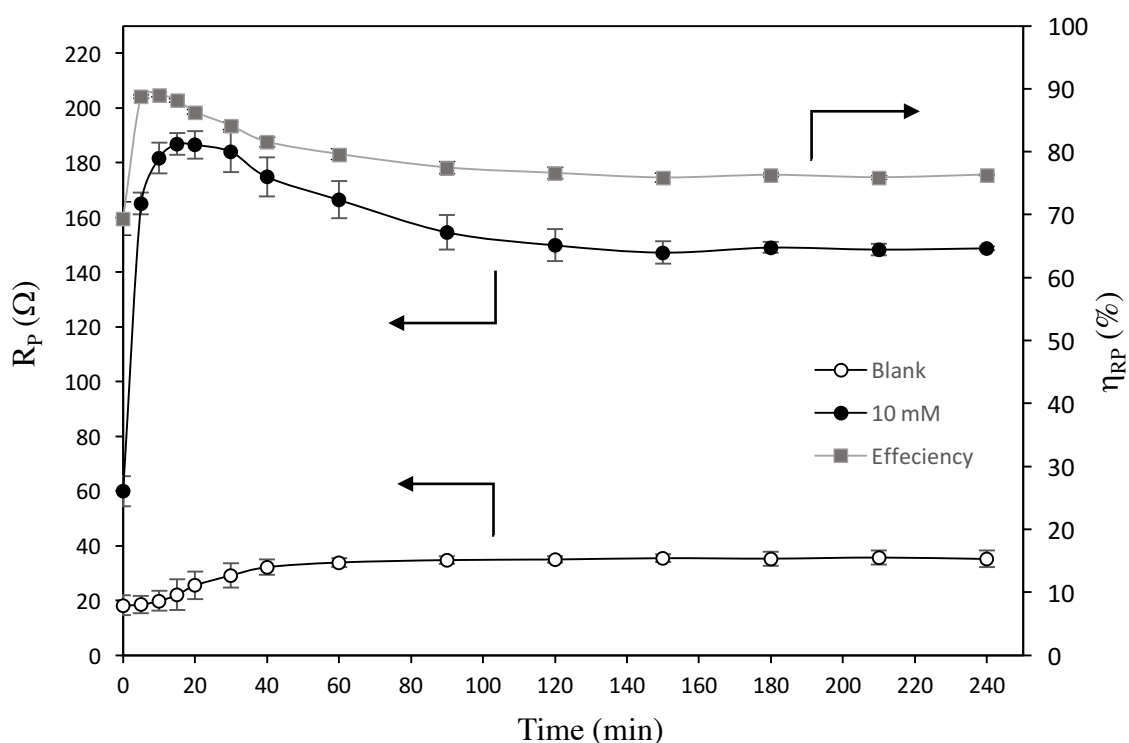


**Figure 5.15:** Polarization resistance,  $R_p$ , against time of CS immersed in blank solution, and in 10 mM MAEP in 0.1 M HCl (pH 1.25) solution at 295 K. Solid line for visual aid only. Results obtained by the polarization resistance method.

To investigate whether adsorbed MAEP molecules are attached to the CS surface by physical or chemical bonds, desorption experiments were performed next. In these experiments, polarization resistance was measured as a function of time in a 10 mM solution of MAEP in 0.1 M HCl (pH 1.25) at 295 K. After 2 hours of immersion, the concentration of MAEP was suddenly decreased to 7 mM by adding an oxygen-free 0.1 M

HCl that did not contain any MAEP, and the polarization resistance was continued to be measured. Again, after additional 2 hours, the MAEP concentration was further decreased to 5 mM. If the MAEP was physically adsorbed on the CS surface, the two dilutions would result in a decrease of polarization resistance to the values obtained in the 7 mM and 5 mM MAEP solutions, as a consequence of MAEP desorption from the CS surface. Fig. 5.16 shows the corresponding results. Namely, Fig. 5.16 shows the polarization resistance as a function of time for CS immersed in 1) blank electrolyte (as a reference), 2) 5mM, 3) 7mM, and 4) 10 mM MAEP in 0.1 M HCl (pH 1.25) at 295 K (control curves), together with the curve that present the dilution experiments. After the first dilution, the polarization resistance decreased slightly, but not to the 7mM-curve. After the 2<sup>nd</sup> dilution, the polarization resistance first decreased slightly, but then recovered. In either case, the resulting polarization resistance was higher than the corresponding resistance recorded in the control electrolyte. Therefore, the results in Fig. 5.16 indicate that MAEP is adsorbed on the surface mostly chemically. A slight drop in the polarization resistance can be related to the desorption of loosely-adsorbed or physisorbed MAEP molecules. The slight recovery in the resistance is speculated to be due reorientation of the adsorbed MAEP molecules on the surface of the metal. There could be also some re-adsorption taking place.

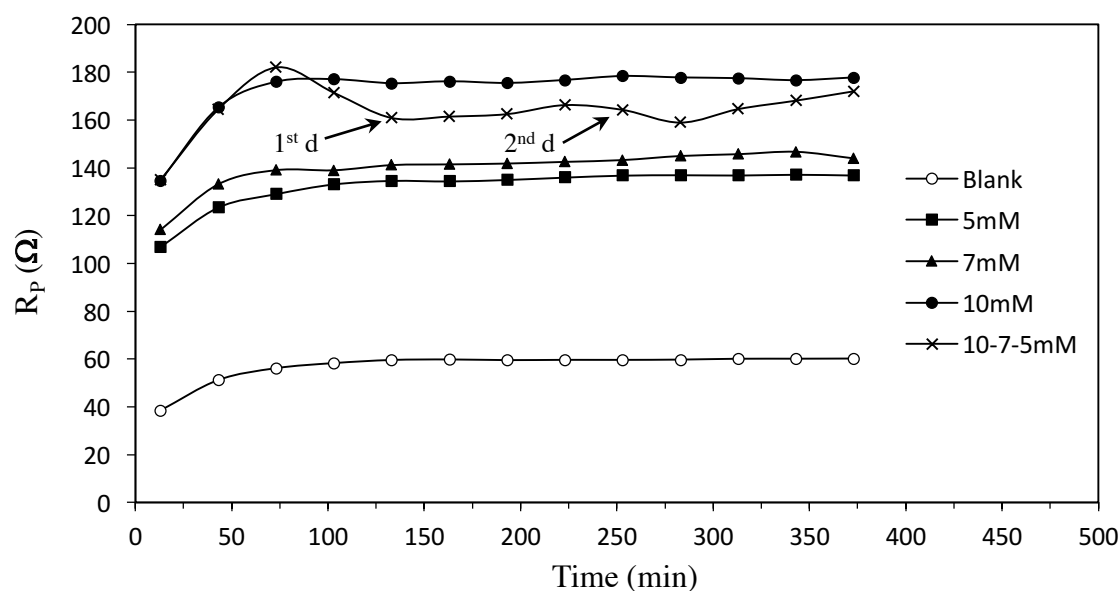


**Figure 5.16:** Polarization resistance,  $R_p$  Vs time for CS immersed in (o) blank electrolyte (■) 5mM, (▲) 7mM, and (●) 10 mM, and (×) 10 mM diluted to 7mM then to 5mM MAEP in 0.1 M HCl (pH 1.25) at 295 K. SD is  $\pm 10 \Omega$  or less. Solid line for visual aid only. Results were obtained by the polarization resistance method.

## 5.4 Effect of Temperature

The effect of temperature on corrosion of CS was studied in 0.1 M HCl (pH 1.25) in the absence and the presence of inhibitor at a concentration of 10 mM. Fig. 5.17 shows the polarization resistance,  $R_p$ , of the system as a function of temperature ranging from 295 to 333 K for both electrolytes. It can be seen that the resistance drops in both cases as the temperature increases, which is expected since corrosion is a process that obeys the Arrhenius law (i.e. it is characterized by an activation energy).

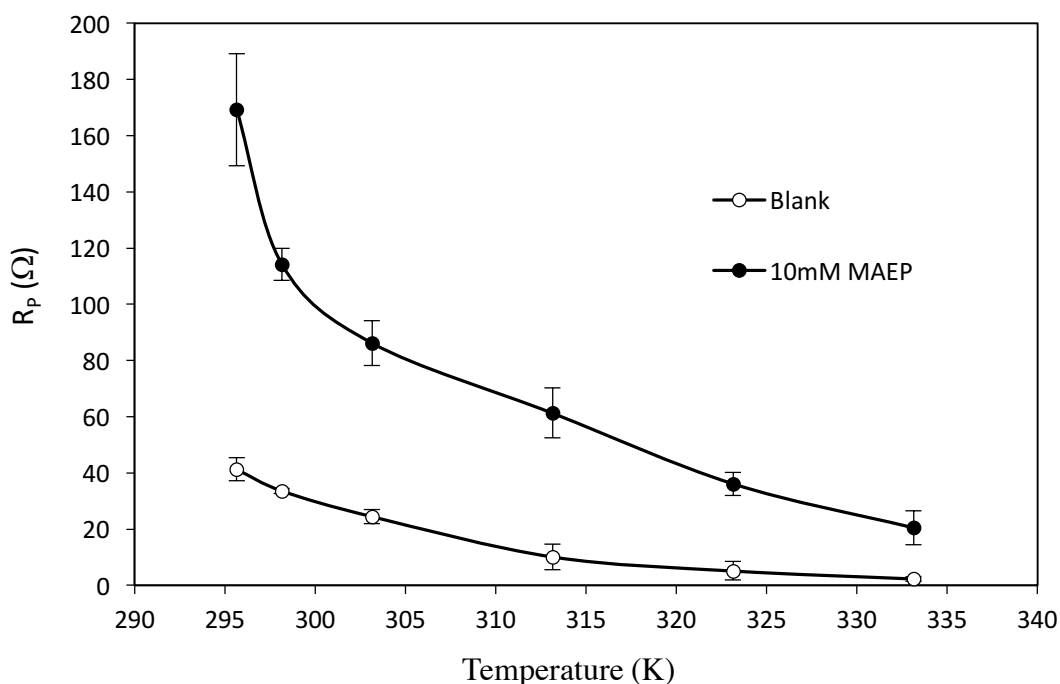


**Figure 5.17:** Temperature dependence of polarization resistance of CS immersed in (○) 0 and in (●) 10mM MAEP in 0.1 M HCl (pH 1.25). Solid line for visual aid only. Resistances were obtained by the polarization resistance method.

The effect of temperature on corrosion of metals is very complex and this is due the rapid etching -in acidic medium- of the metal surface [106] which results in making new active sites very quickly. In addition, as the temperature rises, the ions (and water molecules) in the electrolyte gain thermal energy that is then converted to kinetic energy which causes the electrolytic conductivity to increase. Having higher kinetic energy, corrosive ions would have higher number of collisions with the metal atoms, thus boosting the corrosion reactions. The last two statements are perhaps supported by the drop in the resistance of the electrolyte,  $R_{el}$ , and the rise in the pseudo-capacitance  $CPE_1$ , in Table 5.3

which lists results from EIS measurements for CS in a blank solution at that range of temperatures. In the case of the inhibited solution, similar conclusion can be drawn. Additionally, the drop in  $R_p$  (Fig 5.17, in the case of 10 mM) can also be attributed to some desorption and/or continuous re-orientation of the amino-pyridine molecules that can increase the mass-transfer of the corrosive species to the surface of the metal.

**Table 5.3:** EIS parameters for CS in 0.1 M HCl (pH 1.25) at various temperatures  $\pm 0.5$  K for inhibitor-free electrolyte.

Temperature (K)	295	298	303	313	323	333
$R_{ct}$ ( $\Omega$ )	19.2	18.7	17.3	16.3	14.4	13.9
$\pm SD$	0.6	1.3	0.8	1.2	2.9	1.4
$CPE_1 \times 10^6$ ( $\Omega^{-1} s^{n_1}$ )	696	703	934	2000	3112	4495
$\pm SD$	125	94	280	680	1301	2323
$n_1$	0.82	0.81	0.79	0.77	0.76	0.76
$\pm SD$	0.02	0.02	0.02	0.03	0.03	0.01
$R_1$ ( $\Omega$ )	42.2	34.8	25.4	11.7	5.8	2.5
$\pm SD$	4.7	1.4	2.0	5.0	3.6	1.0

The inhibition efficiency, calculated from the data in Fig. 5.17, is shown in Fig. 5.18. It is not clear why a minimum is observed at 25°C. With an increase in temperature, the inhibition efficiency increases slightly, which is contrary to expectations. Namely, with an increase in temperature, one would expect to observe an increase in desorption of MAEP from the CS surface, and thus a decrease in inhibition efficiency. The fact that an opposite trend is observed might be related (possibly) to temperature-related conformational changes of MAEP on the CS surface.

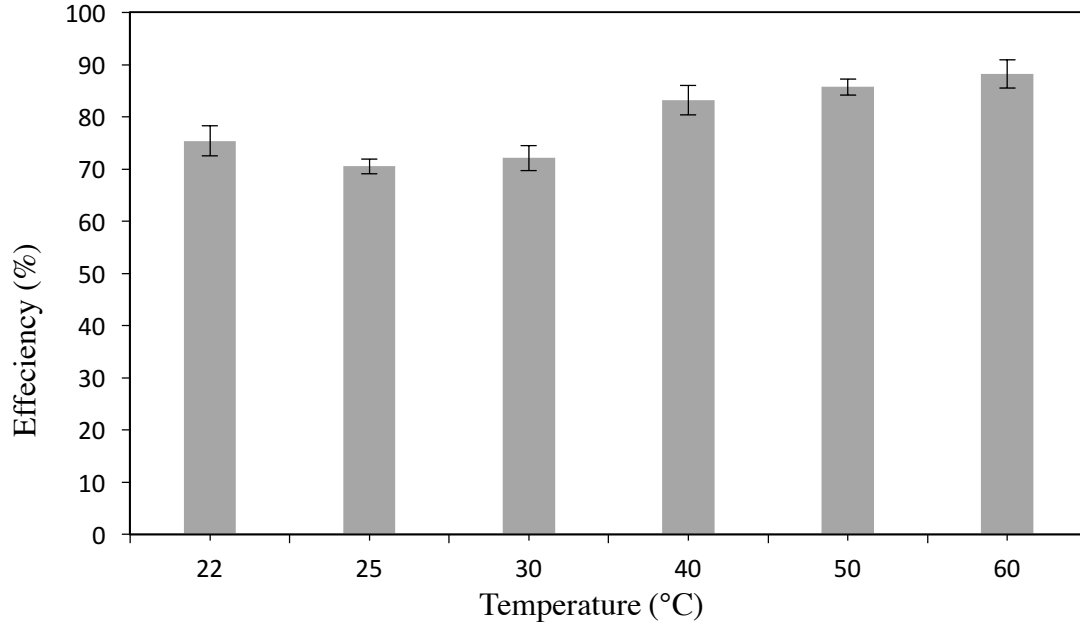


**Figure 5.18:** Inhibition efficiency of CS in 10 mM MAEP in 0.1 M HCl (pH 1.25) at various temperatures. The efficiencies were calculated based on  $R_p$ .

Temperature dependent measurements can also be used to estimate an apparent activation energy of corrosion in the presence/absence of inhibitor, and thus (possibly) on the inhibitor adsorption influence on the corrosion reactions mechanisms. Generally, changes in corrosion mechanisms when the inhibitor is present can be correlated to the apparent activation energy (refer to section 2.7). In addition, the number of collisions per unit time of the corrosive species with the iron atoms (i.e. the frequency factor in an Arrhenius-type equation, Eq. 2.21) is important to be known to have a clearer idea as to how the inhibitor works. Fig. 5.19 shows the variation of inverse of polarization resistance with inverse of temperature ( $\ln(R_p^{-1})$  vs  $1/T$ ) for both the inhibited (with 10 mM MAEP) and the uninhibited CS surface. Employing Eq. 2.23, the corresponding values of activation energy ( $E_a$ ,  $\text{kJ mol}^{-1}$ ) and pre-exponential factor ( $A$ ,  $\text{A}\cdot\text{cm}^{-2}$ ) were determined, Table 5.4.

$$\ln R_p^{-1} = \ln A - \frac{E_a}{RT} \quad (2.23)$$

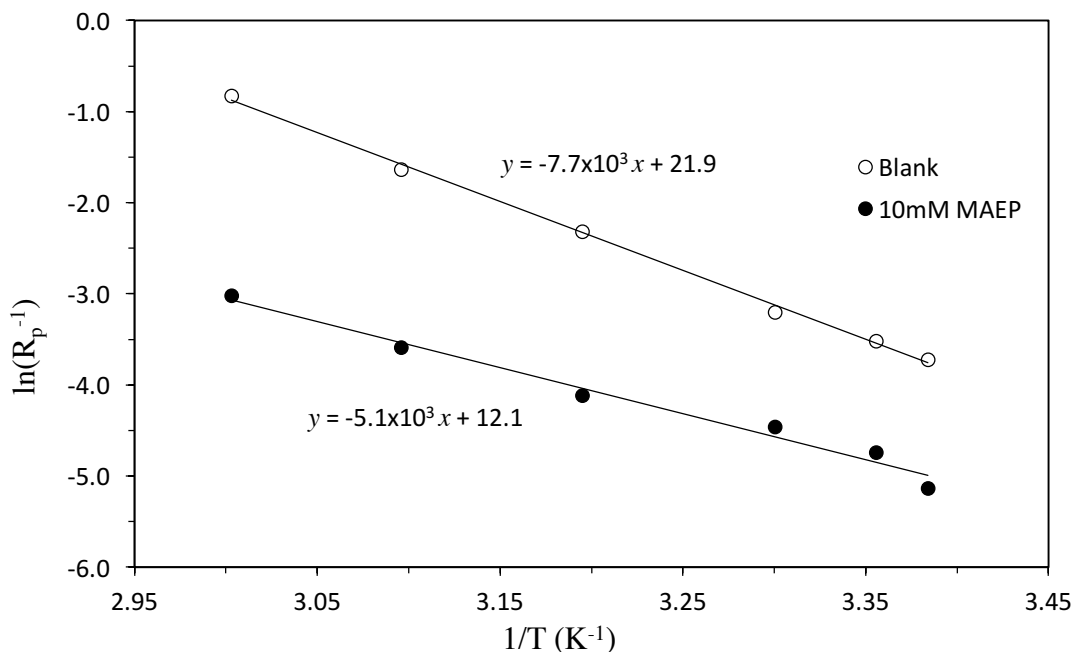


**Figure 5.19:** Arrhenius plots for CS immersed in (○) 0, and in (●) 10mM MAEP in 0.1 M HCl (pH 1.25) at various temperatures. Results were obtained from the polarization resistance method.

**Table 5.3:** Activation energies and frequency factors for uninhibited and inhibited corrosion reactions of CS in blank solution and in 10 mM MAEP (pH 1.25). Results were obtained by averaging the results of the three methods (EIS, PR, and Tafel polarization).

MAEP Conc. (mM)	0 (Blank)	10
$E_a$ (kJ mol <sup>-1</sup> )	60.7	40.5
±SD	1.2	0.9
$A$ (A cm <sup>-2</sup> )x10 <sup>-6</sup>	2278	0.14
±SD	714	0.04

The results in the table show that in the presence of MAEP in the solution, the activation energy decreased by ca. 20 kJ mol<sup>-1</sup>. This conceivably made the corrosion reactions faster when the inhibitor is present. However, the other beneficial factor should be also considered: the frequency factor has dropped by four orders of magnitude which is possibly due to the fact that the CS surface is covered by the inhibitor, thus, minimizing the number of collision of electrolyte corrosive species with the CS surface, resulting in an overall (measured) decrease in corrosion rate [101].

## 5.5 Effect of pH

The effect of pH on corrosion of CS in the presence/absence of MAEP in the electrolyte was studied next at 295 K. Polarization resistance, EIS, and Tafel were carried out for all the experiments and their results showed good consistency. Fig. 5.20 shows Tafel plots for CS in 0.1 M HCl solution at different pH values of 1.25, 2.0, 3.0, and  $4.0 \pm 0.01$  at 295 K, and Fig. 5.21 is for the ones in the presence of the inhibitor at 10 mM. The pH in both experiments was adjusted using 0.5 NaOH (except for pH 1.25 which represents an average value (SD  $\pm 0.05$ ) of 0.1 M HCl for different batches without NaOH addition). In the un-inhibited electrolytes, it can be seen that  $E_{\text{corr}}$  shifts to more negative values and  $j_{\text{corr}}$  to smaller values with a pH increase, which reflects lower corrosion reaction rates at higher pH values. It is also observed that the cathodic Tafel slopes increase as the pH increases, indicating a change in the reaction mechanism of the cathodic hydrogen evolution reaction.

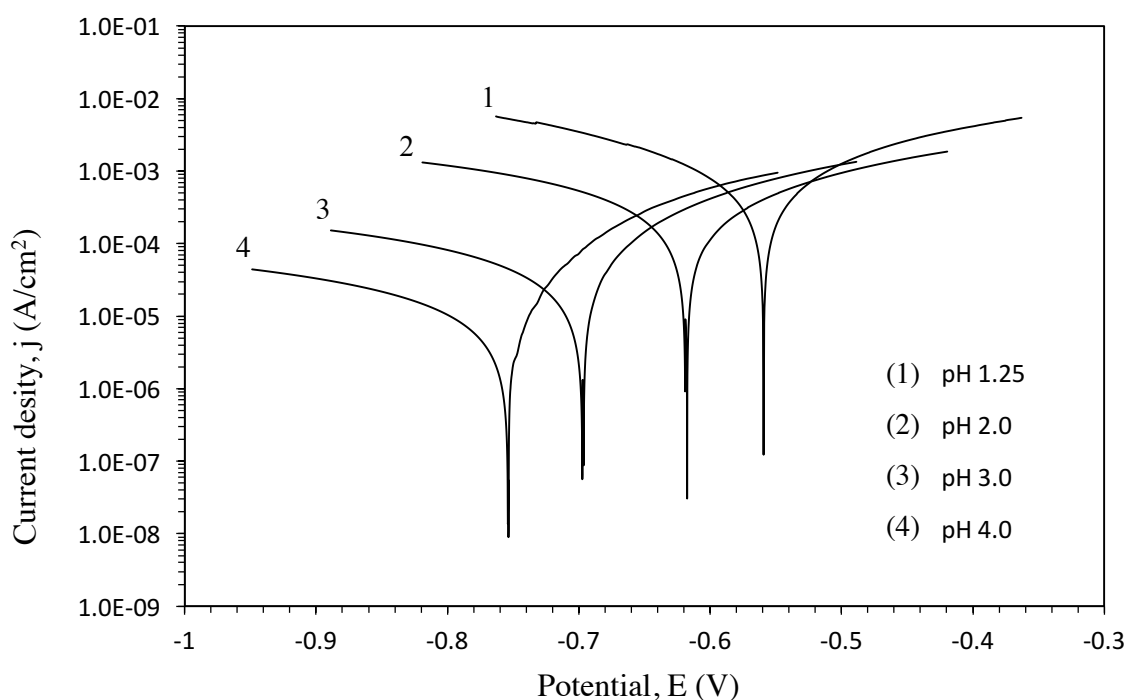


**Figure 5.20:** Tafel plots for CS in 0.1 M HCl solution at different pH values of 1.25, 2.0, 3.0, and  $4.0 \pm 0.01$  at 295 K.

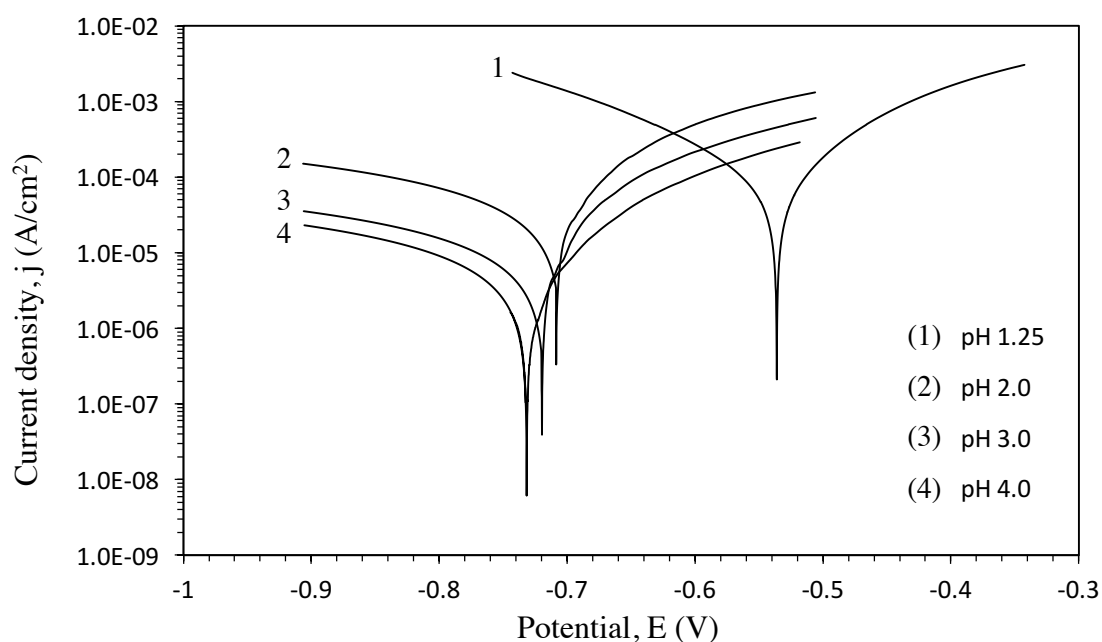


**Figure 5.21:** Tafel plots for CS in 10 mM MAEP in 0.1 M HCl solution at different pH values of 1.25, 2.0, 3.0, and  $4.0 \pm 0.01$  at 295 K.

Similar tendencies were found in the inhibited solutions, Fig. 5.21. It is not clear as to why corrosion reactions rate decreased with a pH increase, but one explanation could be related to a decreased kinetics of the cathodic hydrogen reduction reaction due to a decrease in concentration of  $H^+$  at higher pH.

Fig. 5.22 shows the corresponding variation in inhibition efficiency with pH. It was found that as the pH increases, the inhibition efficiency remains at a relatively high level (ca 80% to 70%). However, increasing the pH above 3 resulted in a sudden recession in the efficiency that reached approximately 40%. The reduction in the inhibitor performance at higher pH is not yet understood. However, a possible explanation could be related the adsorptive-type interactions that could be affected by the isoelectric point of the molecule and the metal.

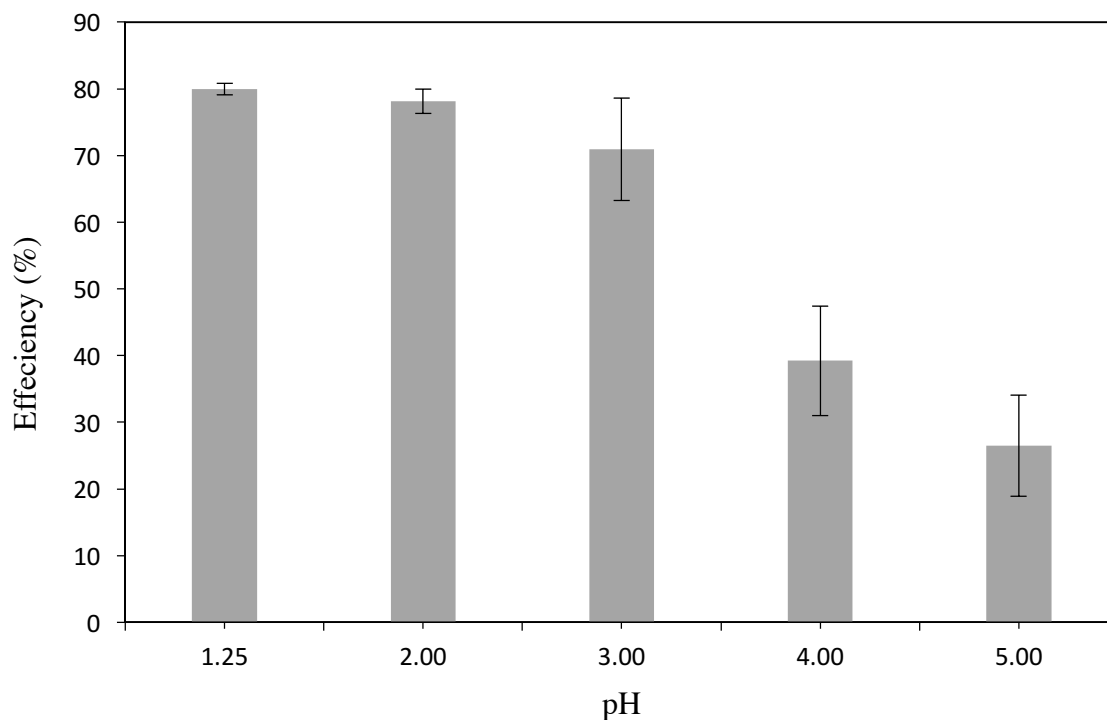


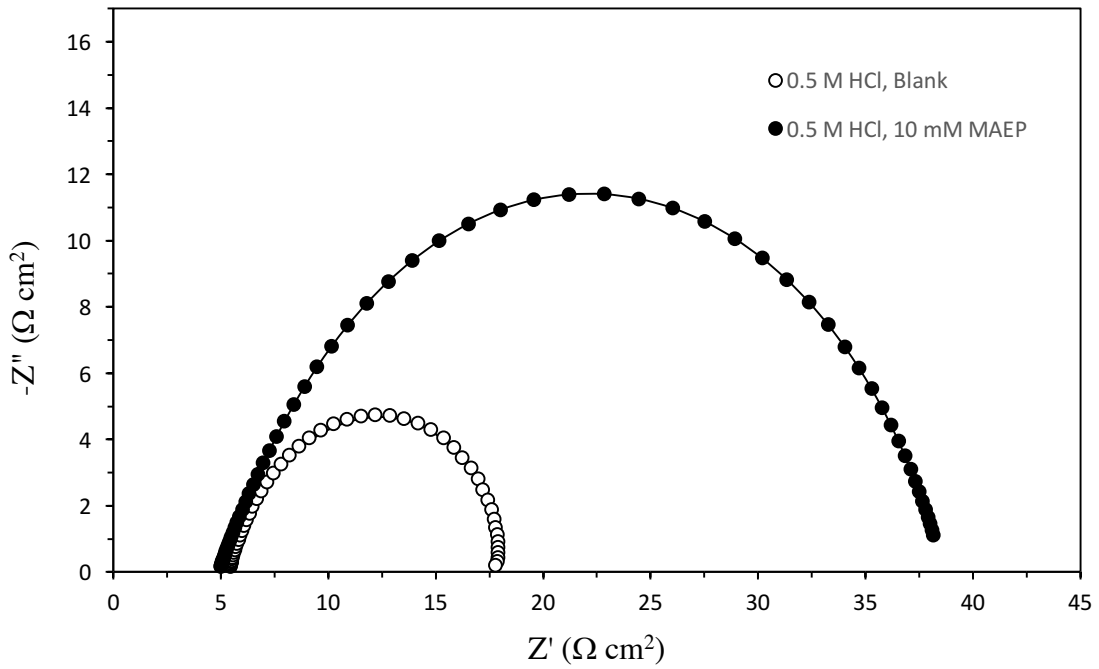
**Figure 5.22:** Corrosion inhibition efficiency for CS in 10 mM MAEP in 0.1 HCl at 295 K of different pH values (calculated from  $R_p$ ).

## 5.6 Effect of Hydrochloric Acid Concentration

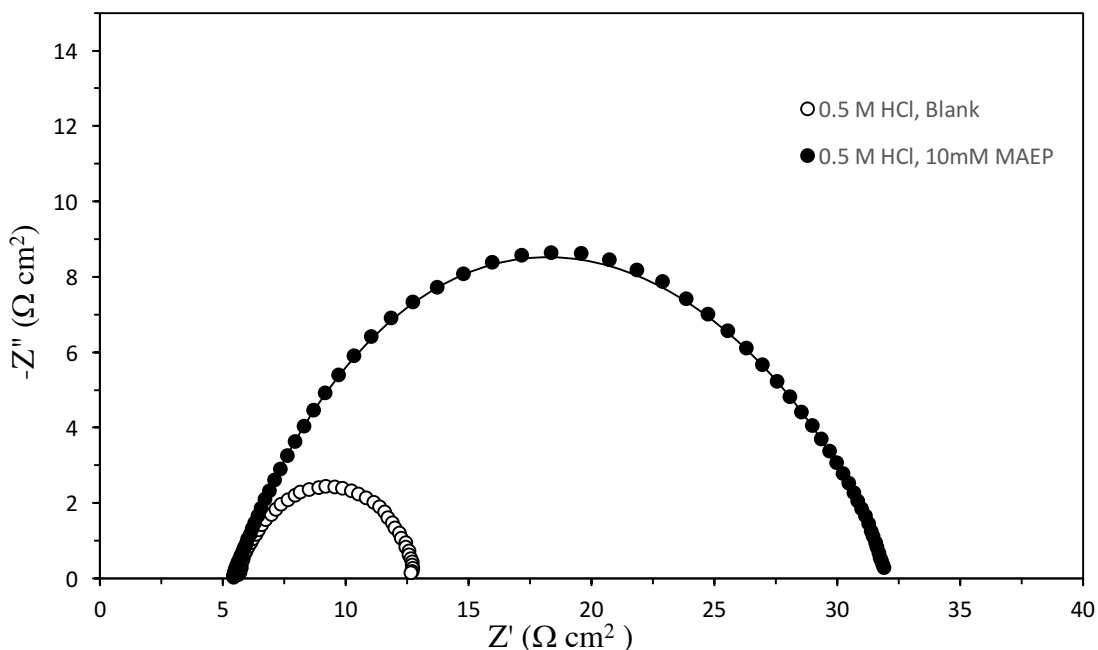
The effect of increasing the acidity of the electrolyte (hence, decreasing its pH below 1.25) on the corresponding corrosion efficiency of MAEP was studied across multiple HCl concentrations (i.e. 0.1, 0.5, 1.0, 1.5 and 2.0 M). Fig. 5.23 and Fig. 5.24 show examples of EIS spectra taken for CS immersed in 0.5 M HCl (and its inhibited counterpart with 10 mM MAEP), and in 1.5 M HCl (and its inhibited one at the same MAEP concentration), respectively. It can be seen that the inhibitor performs well even in harsher media, indicated by an increased diameter of the EIS semi-circle in the presence of inhibitor. Also, the same EEC was used to model the data, indicating that the increase in HCl concentration does not influence the structure of the CS/MAEP interface.

Fig. 5.25 shows the variation of polarization resistance with HCl concentration. As expected, the resistance decrease with an increase in HCl concentration, indicating an increase in corrosion rate. However, despite this, Fig. 5.26 shows that the corresponding MAEP inhibition efficiency remains constant, demonstrating a good performance of the

inhibitor even at very high HCl concentrations. This probably can be attributed to the type of adsorption (i.e. predominant chemisorption) where even at high HCl concentrations, the inhibitor molecules were able to ‘stay’ on the surface and maintain a high concentration difference of the corrosive species between the bulk and on the surface.



**Figure 5.23:** Nyquist plots ( $-Z''$  vs  $Z'$ ) for CS immersed in (○) the absence and (●) presence of inhibitor at 10 mM in 0.5 M HCl at 295 K. Symbols are experimental data and solid lines represent the simulated (modeled) spectra using the models in Fig. 5.7.



**Figure 5.24:** Nyquist plots ( $-Z''$  vs  $Z'$ ) for CS immersed in (○) the absence and (●) presence of inhibitor at 10 mM in 1.5 M HCl at 295 K. Symbols are experimental data and solid lines represent the simulated (modeled) spectra using the models in Fig. 5.7.

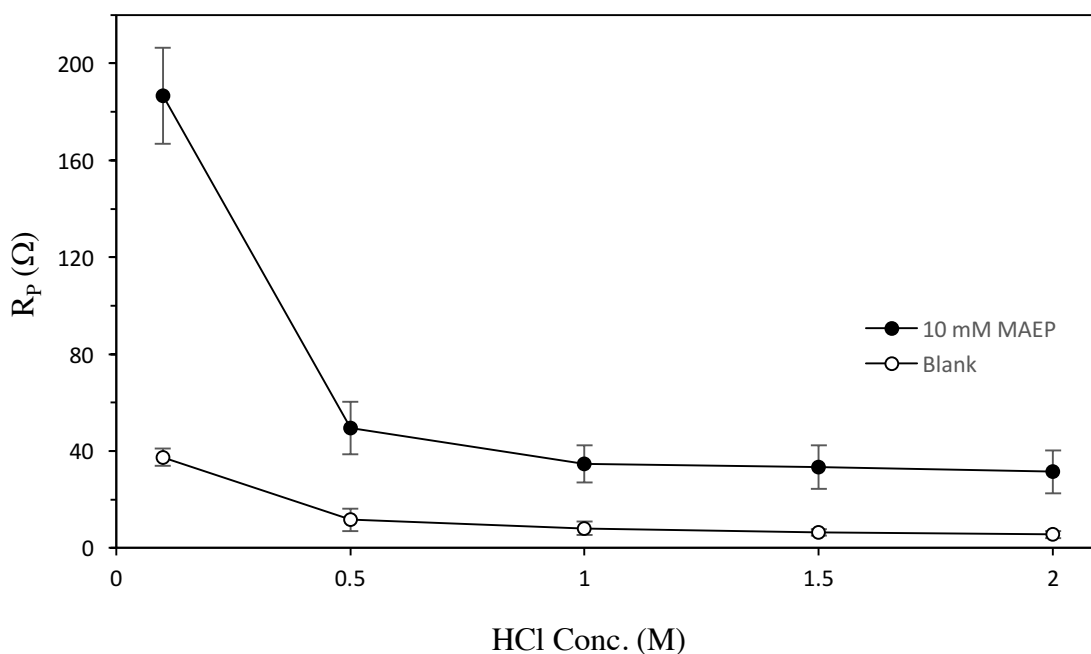


**Figure 5.25:** Polarization resistances  $R_p$  of CS in (○) the absence and (●) the presence of the inhibitor at 10 mM in various HCl concentrations at 295 K. Solid lines for visual aid only. Results were obtained from the polarization resistance method.

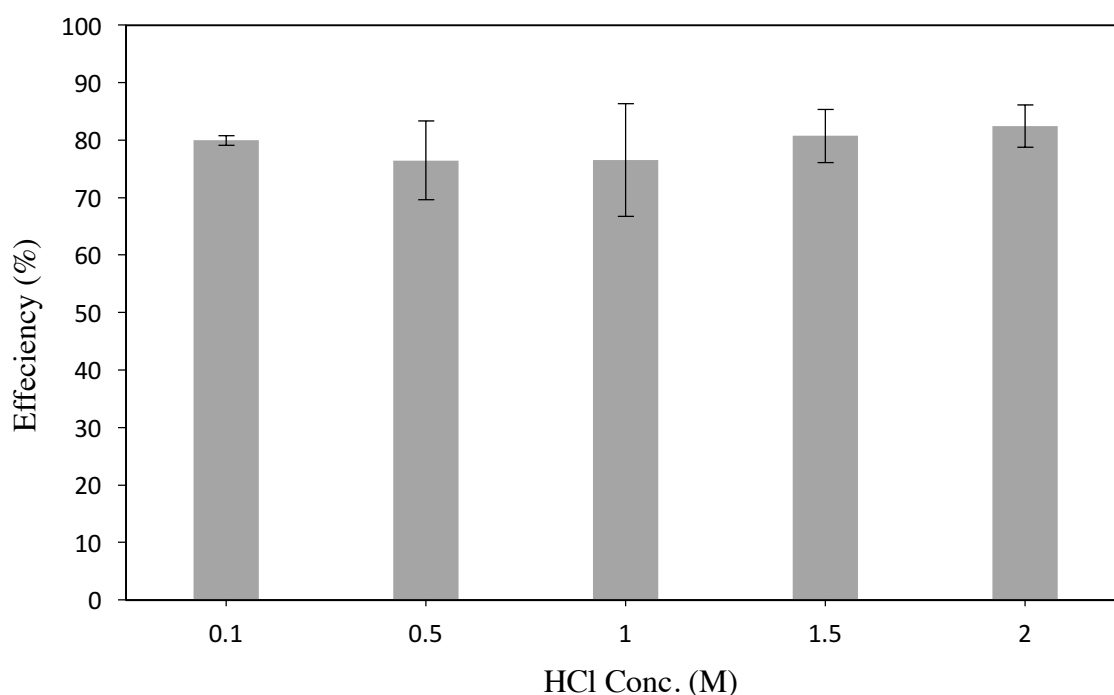
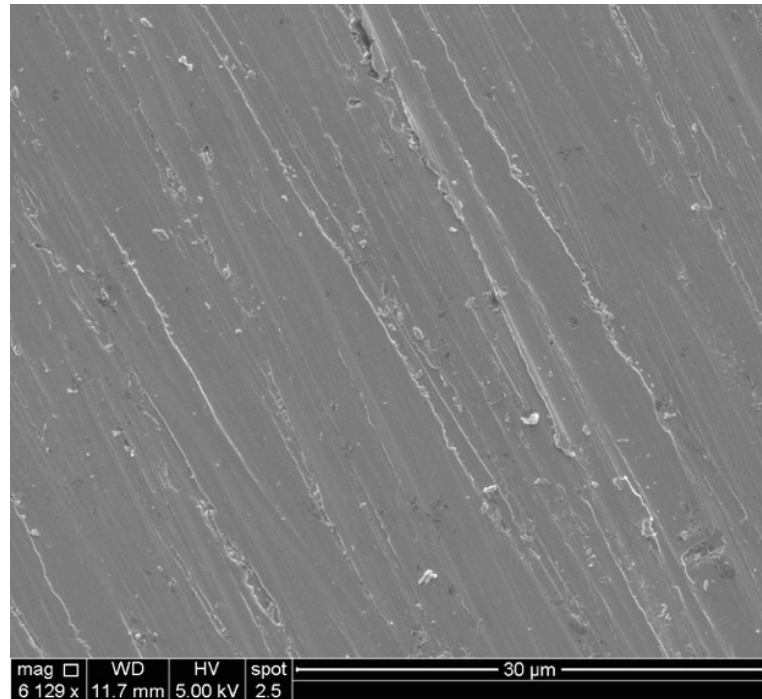


**Figure 5.26:** The inhibition efficiency of the inhibitor at 10 mM for different HCl concentrations at 295 K. Results were obtained based on the polarization method.

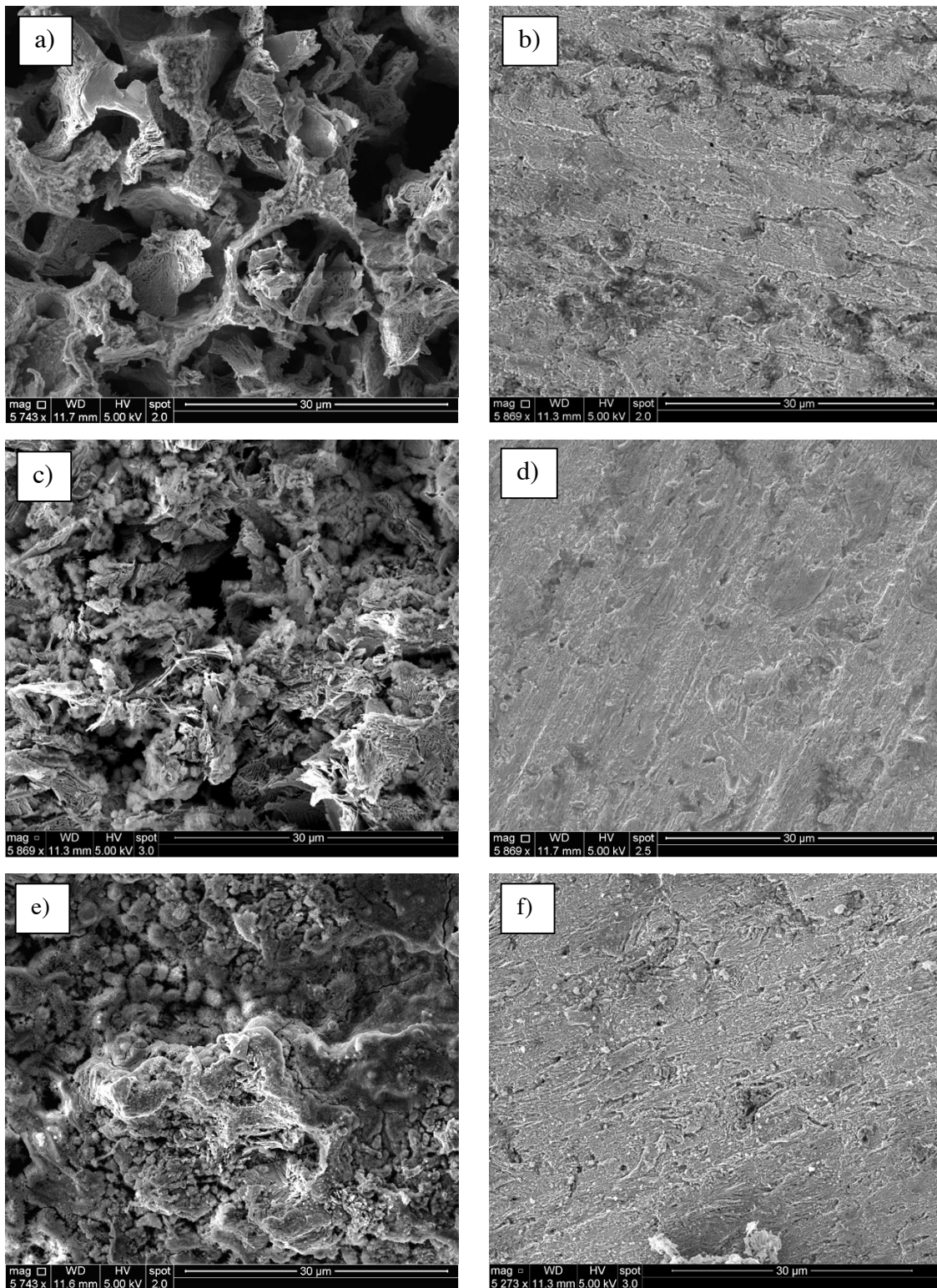
### 5.7 Effect of Long-Term Immersion of CS in Electrolyte

The effect of long-term immersion of CS in 0.1 M HCl was investigated in the absence and in the presence of the inhibitor at 10 mM and at 295 K. The investigation included imaging the metal samples topography (using SEM) after the elapse of different time intervals. In addition, the iron content in both solutions was analyzed (by ICP-OES) at different corrosion times. Fig 5.27 shows an image of a freshly-polished CS sample (with 600-grit paper). It can be utilized as a reference for comparison to those in Fig. 5.28 where a) is for a sample immersed in a blank solution for 1 day, b) is the same but in the presence of the inhibitor, c) is for a sample immersed in a blank solution for 7 days, d) is the same but in the presence of the inhibitor, e) is for a sample immersed in a blank solution for 30 days, and f) is the same but in the presence of the inhibitor. For the samples in the blank solutions (i.e. a, c, and e), it can be seen that the level of damage to the surface of the sample kept increasing as the time of immersion increased. The damage is obvious even after the first day. However, for the solutions where the inhibitor was present (i.e. b, d, and f), it can

be seen that a high level of corrosion protection was demonstrated even after spending 30 days in the acidic solution (judging on the basis of surface appearance, only).



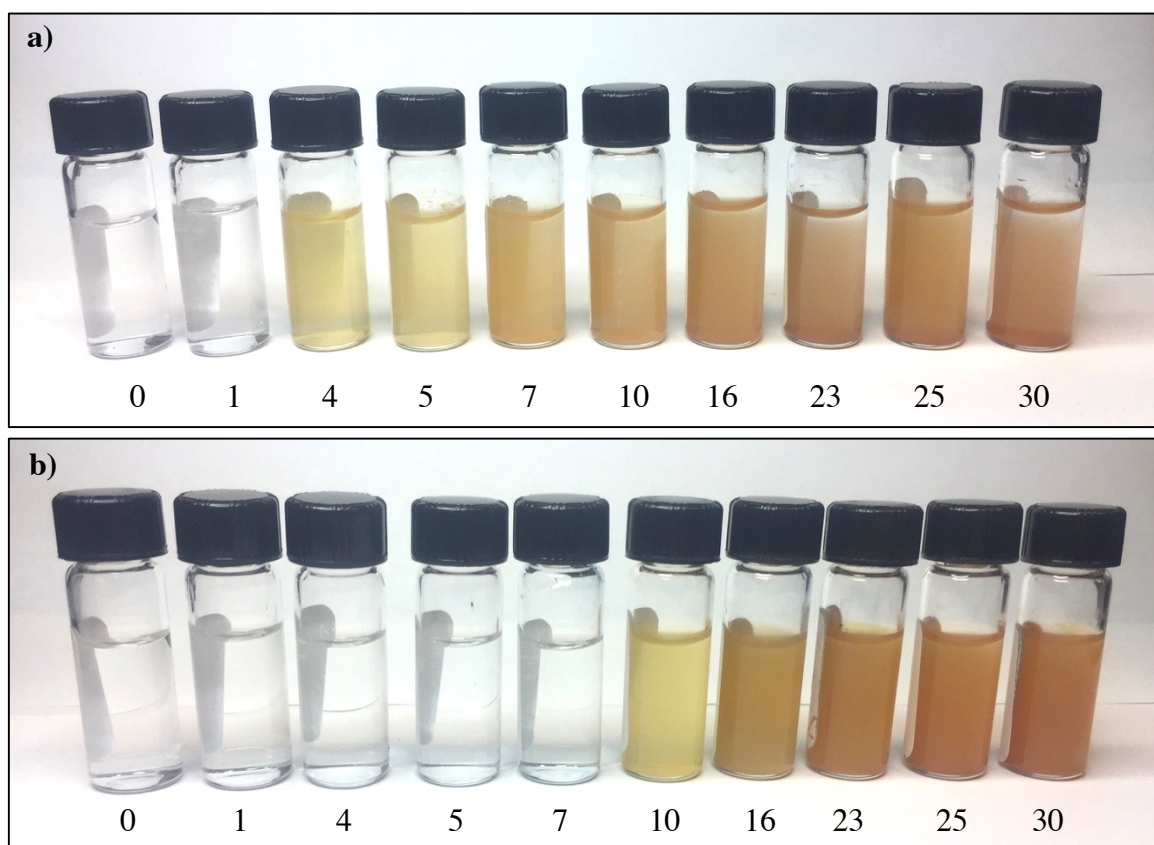
**Figure 5.27:** Scanning Electron Microscopy (SEM) image for CS freshly-polished with 600-grit paper. The corresponding length bar is 30 µm.



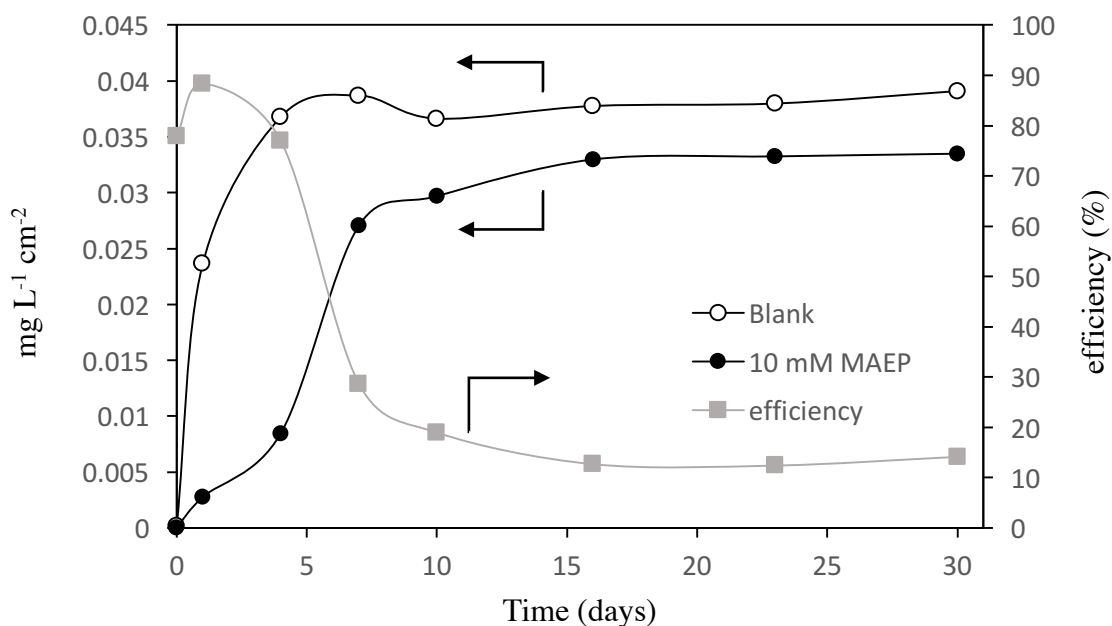
**Figure 5.28:** Scanning Electron Microscopy (SEM) images for CS immersed in solutions in the absence of the inhibitor for a) 1 day, c) 7 days, and e) 30 days; and in the presence of the inhibitor at 10 mM for b) 1 day, d) 7 days, and f) 30 days where all at a temperature of 295 K during the immersion. The corresponding length bar is 30 μm.

Fig 5.29 shows samples of the solution taken from the beakers where CS samples were dipped: a) in the blank solution, and b) in the presence of 10 mM MAEP. The sampling was done after the passage of 0, 1, 4, 5, 7, 10, 16, 23, 25, and 30 days. It can be seen that in the absence of inhibitor, the color of the solution changed after the 1<sup>st</sup> day, while it appeared before the 10<sup>th</sup> day when the inhibitor was present.

However, a more detailed analysis of dissolved (corroded) iron content was done by ICP-OES, Fig 5.30. It can be seen that the iron (rusts) concentration started to appear very soon in even after the passing 1 day and stabilized at day 3 onward (i.e. equilibrium was reached) in the case of the blank solution. However, it took 7 days for the iron concentration to be considerable in the inhibited solution. The corrosion reactions took more than 15 days to reach equilibrium. This shows the level of protection of the amino-pyridine derivative against corrosion.



**Figure 5.29:** Sample of solutions sampled from the electrolytes where the CS samples (of total geometric area equal to ca. 9.34 cm<sup>2</sup>) were immersed for a period of time shown in numbers (0 to 30 in days).



**Figure 5.30:** Iron concentration ( $\text{mg L}^{-1}$  per  $\text{cm}^2$  CS exposed to electrolyte) in the liquid samples as a function of time. Results obtained by ICP-OES only for one run.

## 5.8 Effect of Crude Oil

The MAEP inhibition efficiency was investigated in the presence of Wyoming crude oil (light and sweet) as a second phase at low oil/aqueous HCl volume ratios (0.0, 2.5, 5.0, and 10.0 % ( $\pm 0.1$ )). As the aqueous phase, 0.1 HCl (pH 1.25) was used and the measurements were done at 295 K. The corresponding results are presented in Fig. 5.31. It was found that the MAEP inhibition efficiency decreased drastically as the oil/electrolyte ratio increased. At 10 vol% of oil in the two-phase system, the MAEP's corrosion inhibition efficiency was only 10%. The origin for the observed behavior can be deduced from Fig. 5.32. Namely, as the volume ration of the oil phase increases, the polarization resistance in the absence of inhibitor in the electrolyte also increases. This indicates that the oil phase is partially replacing the aqueous phase at the CS/liquid interface, yielding an increase in corrosion protection relative to the control (only aqueous phase). Then, comparing the results in Figs. 5.31 and 5.32, one can conclude that in the presence of oil phase, the adsorption of MAEP at the CS surface decreases, and thus its corrosion efficiency.

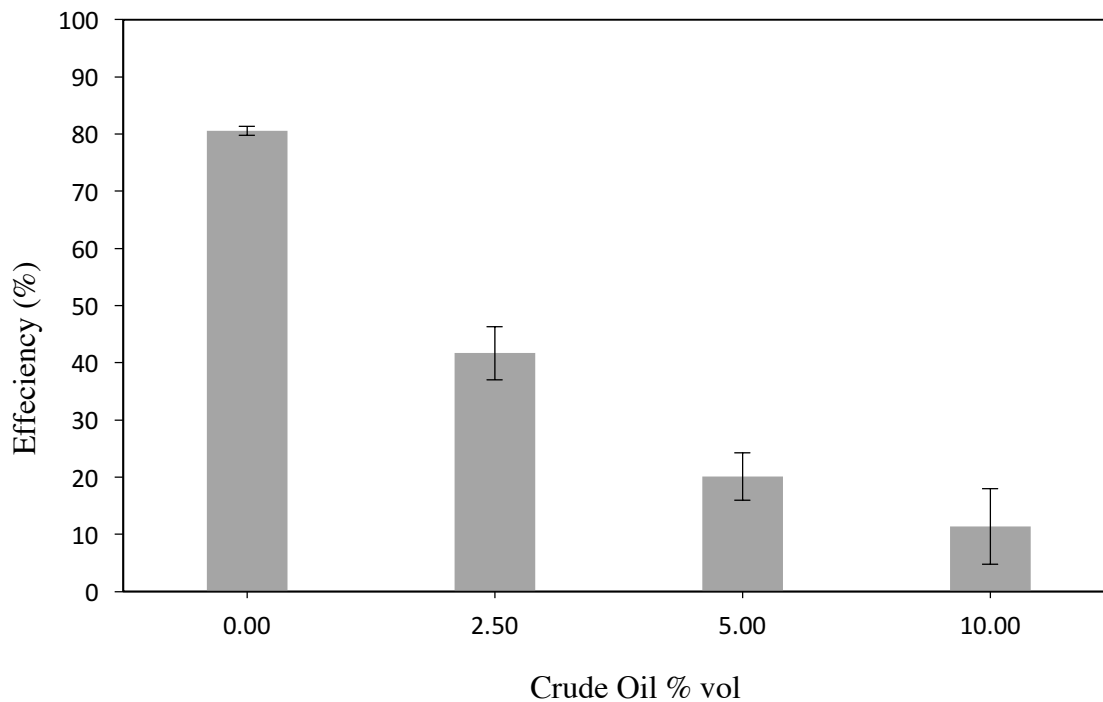


**Figure 5.31:** Inhibition Efficiency of MAEP in 0.1 M HCl in the presence of Wyoming crude oil at different volume ratios ( $\pm 0.1$ ) at 295 K

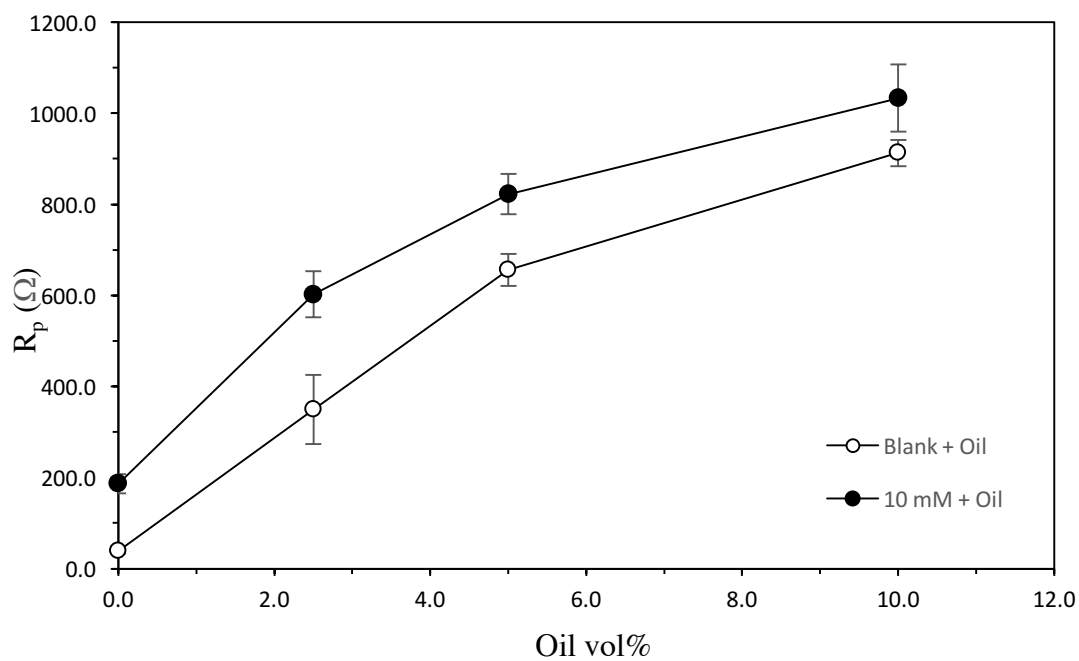


**Figure 5.32:** Polarization Resistance of CS in ( $\circ$ ) 0.1 M HCl and oil, and in ( $\bullet$ ) 0.1 M HCl, 10 mM MAEP and oil.

## **CHAPTER 6: CONCLUSIONS**

## 6. Conclusions

### 6.1 Summary and Conclusions

The main conclusions of this work can be as follows:

- i. Three electrochemical techniques were used in this work (i.e. EIS, polarization resistance, and Tafel polarization) to evaluate the inhibition efficiency of MAEP on CS in HCl aqueous solution. The results of these techniques demonstrated a very good agreement in inhibition efficiencies.
- ii. The results show that as the concentration of inhibitor increases, the corrosion inhibition increases and reaches 92% at 25 mM MAEP in 0.1 M HCl at room temperature.
- iii. The corrosion inhibition mechanism of CS by MAEP is by adsorption of MAEP where the molecule forms a (mono)layer that minimizes the interaction between the corrosive species in the electrolyte and the surface of the metal.
- iv. It was found that the adsorption of inhibitor follows the Langmuir isotherm. The Gibbs free energy of adsorption suggests that the adsorption process is spontaneous.
- v. The measurements on the kinetics of MAEP adsorption show that the adsorption (thus, the inhibition) is very fast. It takes less than a minute to reach a corrosion inhibition efficiency of ca. 70%, and 5 minutes to reach ca. 90%. This is followed by a drop in efficiency to stabilized at 80%. The drop was explained by desorption and re-orientation of MAEP molecules.
- vi. Dilution experiments performed to investigate tendency of MAEP desorption demonstrated that the MAEP adsorption is of a mixed-type (chemi-/physisorption). However, it was determined that MAEP predominantly chemisorb on the CS surface.
- vii. The temperature-dependant measurements showed that as the temperature increased, the MAEP corrosion inhibition efficiency first dropped slightly and then again increased. The initial drop can be explained by the desorption of loosely adsorbed (physisorbed) MAEP molecules. On the other hand, the subsequent increase can be attributed to temperature-induced MAEP surface

conformational changes to offer better barrier properties towards diffusion of corrosive species to the CS surface at higher temperatures.

- viii. The Arrhenius plots suggest that the apparent activation energy of the corrosion reactions dropped by ca. 20 kJ/mol in the presence of MAEP in the electrolyte, while the pre-exponential factor decreased by four orders of magnitude.
- ix. The corrosion inhibition efficiency decreased as the pH of solution increased, especially above pH of 3. This is assumed to be related to the relative change in the charge of the MAEP and CS surface as a results of a difference in their respective isoelectric points.
- x. It was found that as the MAEP inhibition efficiency is not dependant on the HCl concentration in the electrolyte within the concentration range studied in this work.
- xi. The SEM images showed that in the absence of inhibitor, the surface of the CS sample was damaged even after one day of exposure to the corrosive medium. On the other hand, when the inhibitor was added into the electrolyte, it protected the surface of the sample even after 30 days of immersion.
- xii. ICP-OES results demonstrated that the amount of dissolved iron in the presence of inhibitor is significantly lower at short sample-exposure times (up to 5 days), but the inhibition efficiency decreases between the 5<sup>th</sup> and the 7<sup>th</sup> day of exposure.
- xiii. The presence of Wyoming crude oil in the aqueous HCl electrolyte was shown to yield corrosion-protection benefits to CS, even in the absence of inhibitor in the fluid phase. However, the addition of MAEP further decreased the corrosion rate at low volumetric oil/aqueous solution rations. At higher ratios, the presence of MAEP was not found to influence the corrosion rate.

## 6.2 Original Contribution

Carbon steel is extensively used in the oil and gas industry as a material of construction for equipment and piping facilities. However, this metal is prone to corrosion especially when it is exposed to acidic media. Although there are several ways to mitigate corrosion, the use of corrosion inhibitor to control internal general corrosion is a viable option. Today, most of corrosion inhibitors that are used in the oil and gas industry are

toxic and not environmentally friendly. For this reason, this research work aimed at exploring a possibility of using 2-(2-methylaminoethyl)pyridine as a green corrosion inhibitor for carbon steel in acidic media for applications in the oil and gas industry.

The major contribution of this work are:

1. The results in this thesis represent the first attempt on the use of MAEP as green corrosion inhibitor for carbon steel across conditions that may simulate applications in the oil industry like in well-acidizing and acid-pickling processes.
2. Fundamental aspects of the interaction between MAEP and the surface of CS such as adsorption thermodynamics and kinetics aspects were studied.

### **6.3 Future Opportunities**

From this work, it was found that MAEP performs very well as a corrosion inhibitor at various conditions. However, more work is required to be done to further investigate the phenomenon of the interaction of MAEP with CS and other materials under other experimental conditions. The following is a set of suggestions:

1. To investigate the possibility to use MAEP on different metals like aluminum and stainless steel since they are also widely used in the oil and gas industry.
2. It is also recommended that the molecule is tested in other electrolytes like sea water since sea water is used widely in refining facilities on coastal areas.
3. To investigate the possibility of using the inhibitor in the flowing conditions (simulating heat exchangers flow environments) in both laminar and turbulent regimes.
4. To study the effect of using MAEP in the presence of sour and grades of sweet crude oil.

## REFERENCES

## References

- [1] L. M. Rodríguez-Valdez, W. Villamizar, M. Casales, J. G. González-Rodríguez, A. Martínez-Villafañe, L. Martinez, *et al.*, "Computational simulations of the molecular structure and corrosion properties of amidoethyl, aminoethyl and hydroxyethyl imidazolines inhibitors," *Corrosion Science*, vol. 48, pp. 4053-4064, 2006.
- [2] "Research and Markets Adds Report: Corrosion Resistant Steels and Alloys in the Oil & Gas Industry," *Professional Services Close-Up*, 2013.
- [3] M. B. Kermani and A. Morshed, "Carbon dioxide corrosion in oil and gas production-a compendium," *Corrosion*, vol. 59, p. 659, 2003.
- [4] M. K. a. D. Harr, "The impact of corrosion on oil and gas industry," presented at the SPE Annual Technical Conference and Exhibition, Bahrain, 1995.
- [5] E. Lunarska, Y. Ososkov, and Y. Jagodzinsky, "Correlation between critical hydrogen concentration and hydrogen damage of pipeline steel," *International Journal of Hydrogen Energy*, vol. 22, pp. 279-284, 1997.
- [6] G. H. Koch, M. P. Brongers, N. G. Thompson, Y. P. Virmani, and J. H. Payer, "Corrosion cost and preventive strategies in the United States," 2002.
- [7] U. S. R.W. Revie, *Corrosion and Corrosion Control: An Introduction to Corrosion Science and Engineering*. New Jersey: John Wiley and Sons, 2008.
- [8] Z. Ahmad, *Principles of Corrosion Engineering and Corrosion Control*. Oxford, UK: Butterworth-Heinemann, 2006.
- [9] P. A. Schweitzer, *Fundamentals of metallic corrosion: atmospheric and media corrosion of metals*: CRC press, 2006.
- [10] M. Fahlman, S. Jasty, and A. J. Epstein, "Corrosion protection of iron/steel by emeraldine base polyaniline: an X-ray photoelectron spectroscopy study," *Synthetic Metals*, vol. 85, pp. 1323-1326, 1997.
- [11] P. A. Schweitzer, *Corrosion of Linings & Coatings: Cathodic and Inhibitor Protection and Corrosion Monitoring*: CRC press, 2006.
- [12] H. Ju, Z.-P. Kai, and Y. Li, "Aminic nitrogen-bearing polydentate Schiff base compounds as corrosion inhibitors for iron in acidic media: A quantum chemical calculation," *Corrosion Science*, vol. 50, pp. 865-871, 2008.
- [13] V. Sastri and J. Perumareddi, "Molecular orbital theoretical studies of some organic corrosion inhibitors," *Corrosion*, vol. 53, pp. 617-622, 1997.
- [14] F. Bentiss, M. Traisnel, and M. Lagrenee, "The substituted 1, 3, 4-oxadiazoles: a new class of corrosion inhibitors of mild steel in acidic media," *Corrosion science*, vol. 42, pp. 127-146, 2000.
- [15] M. Lagrenee, B. Mernari, M. Bouanis, M. Traisnel, and F. Bentiss, "Study of the mechanism and inhibiting efficiency of 3, 5-bis (4-methylthiophenyl)-4H-1, 2, 4-

- triazole on mild steel corrosion in acidic media," *Corrosion Science*, vol. 44, pp. 573-588, 2002.
- [16] M. Şahin, S. Bilgiç, and H. Yılmaz, "The inhibition effects of some cyclic nitrogen compounds on the corrosion of the steel in NaCl mediums," *Applied Surface Science*, vol. 195, pp. 1-7, 2002.
- [17] M. Behpour, S. M. Ghoreishi, N. Soltani, M. Salavati-Niasari, M. Hamadani, and A. Gandomi, "Electrochemical and theoretical investigation on the corrosion inhibition of mild steel by thiosalicylaldehyde derivatives in hydrochloric acid solution," *Corrosion Science*, vol. 50, pp. 2172-2181, 2008.
- [18] J. M. Costa and J. M. Lluch, "The use of quantum mechanics calculations for the study of corrosion inhibitors," *Corrosion Science*, vol. 24, pp. 929-933, 1984.
- [19] A. Yurt, A. Balaban, S. U. Kandemir, G. Bereket, and B. Erk, "Investigation on some Schiff bases as HCl corrosion inhibitors for carbon steel," *Materials Chemistry and Physics*, vol. 85, pp. 420-426, 2004.
- [20] V. S. Sastri, "Environmentally Friendly Corrosion Inhibitors," in *Green Corrosion Inhibitors*, ed: John Wiley & Sons, Inc., 2011, pp. 257-303.
- [21] M. Antonijevic and M. Petrovic, "Copper corrosion inhibitors. A review," *Int. J. Electrochem. Sci*, vol. 3, pp. 1-28, 2008.
- [22] A. K. Coker, *Ludwig's applied process design for chemical and petrochemical plants*: Gulf Professional Publ., 2015.
- [23] P. Sarin, V. L. Snoeyink, J. Bebee, W. M. Kriven, and J. A. Clement, "Physico-chemical characteristics of corrosion scales in old iron pipes," *Water Research*, vol. 35, pp. 2961-2969, 2001.
- [24] L. T. Popoola, A. S. Grema, G. K. Latinwo, B. Gutti, and A. S. Balogun, "Corrosion problems during oil and gas production and its mitigation," *International Journal of Industrial Chemistry*, vol. 4, p. 35, 2013.
- [25] R. M. Powell, R. W. Puls, S. K. Hightower, and D. A. Sabatini, "Coupled iron corrosion and chromate reduction: mechanisms for subsurface remediation," *Environmental science & technology*, vol. 29, pp. 1913-1922, 1995.
- [26] F. W. Dean and S. W. Powell, "Hydrogen flux and high temperature acid corrosion," *Corrosion*, 2006.
- [27] O. Yépez, "Influence of different sulfur compounds on corrosion due to naphthenic acid," *Fuel*, vol. 84, pp. 97-104, 2005.
- [28] A. Turnbull, E. Slavcheva, and B. Shone, "Factors controlling naphthenic acid corrosion," *Corrosion*, vol. 54, pp. 922-930, 1998.
- [29] L.-F. Li, P. Caenen, M. Daerden, D. Vaes, G. Meers, C. Dhondt, *et al.*, "Mechanism of single and multiple step pickling of 304 stainless steel in acid electrolytes," *Corrosion Science*, vol. 47, pp. 1307-1324, 2005.
- [30] M. Regel-Rosocka, "A review on methods of regeneration of spent pickling solutions from steel processing," *Journal of Hazardous Materials*, vol. 177, pp. 57-69, 2010.

- [31] B. Nimmo and G. Hinds, "Beginners guide to corrosion," *NPL's corrosion Gr*, 2003.
- [32] J. K. Heuer and J. F. Stubbins, "An XPS characterization of FeCO<sub>3</sub> films from CO<sub>2</sub> corrosion," *Corrosion Science*, vol. 41, pp. 1231-1243, 1999.
- [33] S. Oh, D. C. Cook, and H. E. Townsend, "Characterization of Iron Oxides Commonly Formed as Corrosion Products on Steel," *Hyperfine Interactions*, vol. 112, pp. 59-66, 1998.
- [34] S. Hœrlé, F. Mazaudier, P. Dillmann, and G. Santarini, "Advances in understanding atmospheric corrosion of iron. II. Mechanistic modelling of wet-dry cycles," *Corrosion Science*, vol. 46, pp. 1431-1465, 2004.
- [35] H. Jafari, K. Akbarzade, and I. Danaee, "Corrosion inhibition of carbon steel immersed in a 1 M HCl solution using benzothiazole derivatives," *Arabian Journal of Chemistry*.
- [36] J. D. R. T. By David E.J. Talbot, *Corrosion Science and Technology*, Second Edition ed.: CRC Press, 2007.
- [37] V. M. Balsaraf, *Applied Chemistry II*. New Delhi, India: I. K. International Pvt Ltd, 2009.
- [38] A. K. Satapathy, G. Gunasekaran, S. C. Sahoo, K. Amit, and P. V. Rodrigues, "Corrosion inhibition by Justicia gendarussa plant extract in hydrochloric acid solution," *Corrosion Science*, vol. 51, pp. 2848-2856, 2009.
- [39] O. Olivares, N. V. Likhanova, B. Gómez, J. Navarrete, M. E. Llanos-Serrano, E. Arce, *et al.*, "Electrochemical and XPS studies of decylamides of  $\alpha$ -amino acids adsorption on carbon steel in acidic environment," *Applied Surface Science*, vol. 252, pp. 2894-2909, 2006.
- [40] C. Guedes Soares, Y. Garbatov, A. Zayed, and G. Wang, "Corrosion wastage model for ship crude oil tanks," *Corrosion Science*, vol. 50, pp. 3095-3106, 2008.
- [41] K. D. Efirid and R. J. Jasinski, "Effect of the Crude Oil on Corrosion of Steel in Crude Oil/Brine Production," *Corrosion*, vol. 45, pp. 165-171, 1989.
- [42] T. K. Nick Cunningham, Josh Owens. (2009) A Detailed Guide on the Many Different Types of Crude Oil. *OilPrice.com*. Available: <http://oilprice.com/Energy/Crude-Oil/A-Detailed-Guide-On-The-Many-Different-Types-Of-Crude-Oil.html>
- [43] A. P. Watkinson, "Deposition from Crude Oils in Heat Exchangers," *Heat Transfer Engineering*, vol. 28, pp. 177-184, 2007.
- [44] S. Portier, L. André, and F.-D. Vuataz, "Review on chemical stimulation techniques in oil industry and applications to geothermal systems," *Engine, work package*, vol. 4, p. 32, 2007.
- [45] M. A. Migahed and I. F. Nassar, "Corrosion inhibition of Tubing steel during acidization of oil and gas wells," *Electrochimica Acta*, vol. 53, pp. 2877-2882, 2008.

- [46] D. Brondel, F. Montrouge, R. Edwards, A. Hayman, D. Hill, S. Mehta, *et al.*, "Corrosion in the Oil Industry," *Journal of Petroleum Technology*, vol. 39, pp. 756-762, 1987.
- [47] A. P. Institute, "Acidizing: Treatment in Oil and Gas Operators," 2014.
- [48] SPE, "Acidizing preparations," *Society of Petroleum Engineers*, 2015.
- [49] U. S. D. O. Energy, "Elk Hills Naval Petroleum Reserve No.1: Environmental Impact Statement," pp. 3.2-10, 1992.
- [50] W. Kladnig, "New development of acid regeneration in steel pickling plants," *Journal of iron and steel research, international*, vol. 15, pp. 1-6, 2008.
- [51] Vecom, "Pre-commission Cleaninf of a Polypropylene Plant", 2007.
- [52] K. F. Khaled and N. Hackerman, "Ortho-substituted anilines to inhibit copper corrosion in aerated 0.5 M hydrochloric acid," *Electrochimica Acta*, vol. 49, pp. 485-495, 2004.
- [53] M. P. O'Donoghue and V. M. S. Datta, "In-Situ Coating of Corroded Pipelines in the Canadian Oil Patch," *Journal of Protective Coatings & Linings*, vol. 28, pp. 11-12,14-15, 2011
- [54] K. Zakowski, M. Narozny, M. Szocinski, and K. Darowicki, "Influence of water salinity on corrosion risk—the case of the southern Baltic Sea coast," *Environmental Monitoring and Assessment*, vol. 186, pp. 4871-4879, 2014.
- [55] M. Yari, "The 6 Corrosive Components That Can Be Found in Crude Oil," in *Corrosionpedia*, <http://www.corrosionpedia.com/>, 2015
- [56] A. J. Szyprowski, "Methods of investigation on hydrogen sulfide corrosion of steel and its inhibitors," *Corrosion*, vol. 59, p. 68, 2003
- [57] R. V. Rao, "A material selection model using graph theory and matrix approach," *Materials Science and Engineering: A*, vol. 431, pp. 248-255, 2006.
- [58] G. L. Huyett, *Engeneering Handbook*, Second Edition. Kansas, USA: G. L. Huyett, 2014.
- [59] M. Ueda, H. Takabe, and P. I. Nice, "The development and implementation of a new alloyed steel for oil and gas production wells," *Corrosion*, 2000.
- [60] C. A. Palacios and J. R. Shadley, "CO<sub>2</sub> Corrosion of N-80 Steel at 71°C in a Two-Phase Flow System," *Corrosion*, vol. 49, pp. 686-693, 1993.
- [61] E. Gulbrandsen, S. Nesic, A. Stangeland, T. Burchardt, B. Sundfaer, S. Hesjevik, *et al.*, "Effect of Pre-Corrosion on the Performance of Inhibitors for CO<sub>2</sub> Corrosion of Carbon Steel," in *Corrosion-National Association of Corrosion Engineers Annual Conference*, 1998.
- [62] M. Finšgar and J. Jackson, "Application of corrosion inhibitors for steels in acidic media for the oil and gas industry: A review," *Corrosion Science*, vol. 86, pp. 17-41, 2014.
- [63] D. Gielen and Y. Moriguchi, "CO<sub>2</sub> in the iron and steel industry: an analysis of Japanese emission reduction potentials," *Energy Policy*, vol. 30, pp. 849-863, 2002.

- [64] A. Dugstad, L. Lunde, and S. Nesic, "Control of internal corrosion in multi-phase oil and gas pipelines," in *Proceedings of the conference Prevention of Pipeline Corrosion*, Gulf Publishing Co, 1994.
- [65] B. Hedges, H. J. Chen, T. H. Bieri, and K. Sprague, "A Review of Monitoring and Inspection Techniques for CO<sub>2</sub> and H<sub>2</sub>S Corrosion in Oil & Gas Production Facilities: Location Location Location," *Corrosion*, 2006.
- [66] H. J. De Bruyn, "Current corrosion monitoring trends in the petrochemical industry," *International Journal of Pressure Vessels and Piping*, vol. 66, pp. 293-303, 1996.
- [67] A. Talo, P. Passiniemi, O. Forsén, and S. Yläsaari, "Polyaniline/epoxy coatings with good anti-corrosion properties," *Synthetic Metals*, vol. 85, pp. 1333-1334, 1997.
- [68] W. K. Lu, R. L. Elsenbaumer, and B. Wessling, "Corrosion protection of mild steel by coatings containing polyaniline," *Synthetic Metals*, vol. 71, pp. 2163-2166, 1995.
- [69] A. Mirmohseni and A. Oladegaragoze, "Anti-corrosive properties of polyaniline coating on iron," *Synthetic Metals*, vol. 114, pp. 105-108, 2000.
- [70] B. Navinšek, P. Panjan, and I. Milošev, "PVD coatings as an environmentally clean alternative to electroplating and electroless processes," *Surface and Coatings Technology*, vol. 116–119, pp. 476-487, 1999.
- [71] D.-K. Kim, S. Muralidharan, T.-H. Ha, J.-H. Bae, Y.-C. Ha, H.-G. Lee, *et al.*, "Electrochemical studies on the alternating current corrosion of mild steel under cathodic protection condition in marine environments," *Electrochimica Acta*, vol. 51, pp. 5259-5267, 2006.
- [72] K. C. Emregül, E. Düzgün, and O. Atakol, "The application of some polydentate Schiff base compounds containing aminic nitrogens as corrosion inhibitors for mild steel in acidic media," *Corrosion Science*, vol. 48, pp. 3243-3260, 2006.
- [73] P. B. Raja and M. G. Sethuraman, "Natural products as corrosion inhibitor for metals in corrosive media — A review," *Materials Letters*, vol. 62, pp. 113-116, 2008.
- [74] A. Kalendová, D. Veselý, and J. Stejskal, "Organic coatings containing polyaniline and inorganic pigments as corrosion inhibitors," *Progress in Organic Coatings*, vol. 62, pp. 105-116, 2008.
- [75] A. Wachter, T. Skei, and N. Stillman, "Dicyclohexylammonium Nitrite, A Volatile Inhibitor for Corrosion Preventive Packaging," *Corrosion*, vol. 7, pp. 284-294, 1951.
- [76] D. M. Bastidas, E. Cano, and E. Mora, "Volatile corrosion inhibitors: a review," *Anti-Corrosion Methods and Materials*, vol. 52, pp. 71-77, 2005.
- [77] B. Shaw, "ASM handbook volume 13a: corrosion: fundamentals, testing and protection," ed: Edited by D. Stephen, ASM International, Materials Park, Ohio, USA, 2003.

- [78] P. R. Roberge, "Handbook of Corrosion Engineering McGraw-Hill," *New York, NY*, 2000.
- [79] L. M. Vračar and D. M. Dražić, "Adsorption and corrosion inhibitive properties of some organic molecules on iron electrode in sulfuric acid," *Corrosion Science*, vol. 44, pp. 1669-1680, 2002.
- [80] S. Ghareba and S. Omanovic, "Interaction of 12-aminododecanoic acid with a carbon steel surface: Towards the development of 'green' corrosion inhibitors," *Corrosion Science*, vol. 52, pp. 2104-2113, 2010.
- [81] P. B. Raja, A. K. Qureshi, A. Abdul Rahim, H. Osman, and K. Awang, "Neolamarckia cadamba alkaloids as eco-friendly corrosion inhibitors for mild steel in 1.0 M HCl media," *Corrosion Science*, vol. 69, pp. 292-301, 2013.
- [82] D. Kesavan, M. Gopiraman, and N. Sulochana, "Green inhibitors for corrosion of metals: A review," *Chem. Sci. Rev. Lett*, vol. 1, p. 1, 2012.
- [83] K. Khaled, "New synthesized guanidine derivative as a green corrosion inhibitor for mild steel in acidic solutions," *Int. J. Electrochem. Sci*, vol. 3, pp. 462-475, 2008.
- [84] G. Moretti, F. Guidi, and G. Grion, "Tryptamine as a green iron corrosion inhibitor in 0.5 M deaerated sulphuric acid," *Corrosion Science*, vol. 46, pp. 387-403, 2004.
- [85] A. S. Fouda and A. S. Ellithy, "Inhibition effect of 4-phenylthiazole derivatives on corrosion of 304L stainless steel in HCl solution," *Corrosion Science*, vol. 51, pp. 868-875, 2009.
- [86] S. Ramesh and S. Rajeswari, "Corrosion inhibition of mild steel in neutral aqueous solution by new triazole derivatives," *Electrochimica Acta*, vol. 49, pp. 811-820, 2004.
- [87] Z. Tao, S. Zhang, W. Li, and B. Hou, "Corrosion inhibition of mild steel in acidic solution by some oxo-triazole derivatives," *Corrosion Science*, vol. 51, pp. 2588-2595, 2009.
- [88] B. Wang, M. Du, J. Zhang, and C. J. Gao, "Electrochemical and surface analysis studies on corrosion inhibition of Q235 steel by imidazoline derivative against CO<sub>2</sub> corrosion," *Corrosion Science*, vol. 53, pp. 353-361, 2011.
- [89] J.-j. Fu, S.-n. Li, Y. Wang, X.-d. Liu, and L.-d. Lu, "Computational and electrochemical studies on the inhibition of corrosion of mild steel by l-Cysteine and its derivatives," *Journal of Materials Science*, vol. 46, pp. 3550-3559, 2011.
- [90] K. F. Khaled, "Monte Carlo simulations of corrosion inhibition of mild steel in 0.5 M sulphuric acid by some green corrosion inhibitors," *Journal of Solid State Electrochemistry*, vol. 13, pp. 1743-1756, 2009.
- [91] G. Gece, "Drugs: A review of promising novel corrosion inhibitors," *Corrosion Science*, vol. 53, pp. 3873-3898, 2011.
- [92] R. Solmaz, G. Kardaş, B. Yazıcı, and M. Erbil, "Adsorption and corrosion inhibitive properties of 2-amino-5-mercapto-1,3,4-thiadiazole on mild steel in hydrochloric acid media," *Colloids and Surfaces A: Physicochemical and Engineering Aspects*, vol. 312, pp. 7-17, 2008.

- [93] A. El-Awady, B. Abd-El-Nabey, and S. Aziz, "Kinetic-thermodynamic and adsorption isotherms analyses for the inhibition of the acid corrosion of steel by cyclic and open-chain amines," *Journal of the Electrochemical Society*, vol. 139, pp. 2149-2154, 1992.
- [94] J. Aljourani, K. Raciissi, and M. A. Golozar, "Benzimidazole and its derivatives as corrosion inhibitors for mild steel in 1M HCl solution," *Corrosion Science*, vol. 51, pp. 1836-1843, 2009.
- [95] M. Nuñez, *Prevention of Metal Corrosion: New Research*. New York, USA: Nova Science Publishers, Inc., 2007.
- [96] H. Luo, Y. C. Guan, and K. N. Han, "Inhibition of mild steel corrosion by sodium dodecyl benzene sulfonate and sodium oleate in acidic solutions," *Corrosion*, vol. 54, p. 619, 1998
- [97] E. McCafferty, *Introduction to corrosion science*: Springer Science & Business Media, 2010.
- [98] A. K. Singh and M. A. Quraishi, "Effect of Cefazolin on the corrosion of mild steel in HCl solution," *Corrosion Science*, vol. 52, pp. 152-160, 2010.
- [99] H. N. Tran, S.-J. You, and H.-P. Chao, "Thermodynamic parameters of cadmium adsorption onto orange peel calculated from various methods: A comparison study," *Journal of Environmental Chemical Engineering*, vol. 4, pp. 2671-2682, 2016.
- [100] L. Herrag, B. Hammouti, S. Elkadiri, A. Aouniti, C. Jama, H. Vezin, *et al.*, "Adsorption properties and inhibition of mild steel corrosion in hydrochloric solution by some newly synthesized diamine derivatives: Experimental and theoretical investigations," *Corrosion Science*, vol. 52, pp. 3042-3051, 2010.
- [101] L. Tang, G. Mu, and G. Liu, "The effect of neutral red on the corrosion inhibition of cold rolled steel in 1.0 M hydrochloric acid," *Corrosion Science*, vol. 45, pp. 2251-2262, 2003.
- [102] A. Y. Musa, A. A. H. Kadhum, A. B. Mohamad, M. S. Takriff, A. R. Daud, and S. K. Kamarudin, "On the inhibition of mild steel corrosion by 4-amino-5-phenyl-4H-1, 2, 4-triazole-3-thiol," *Corrosion Science*, vol. 52, pp. 526-533, 2010.
- [103] E. A. Noor and A. H. Al-Moubaraki, "Thermodynamic study of metal corrosion and inhibitor adsorption processes in mild steel/1-methyl-4[4'(-X)-styryl pyridinium iodides/hydrochloric acid systems," *Materials Chemistry and Physics*, vol. 110, pp. 145-154, 2008.
- [104] F. Mohsenifar, H. Jafari, and K. Sayin, "Investigation of Thermodynamic Parameters for Steel Corrosion in Acidic Solution in the Presence of N,N'-Bis(phloroacetophenone)-1,2 propanediamine," *Journal of Bio- and Tribo-Corrosion*, vol. 2, pp. 1-13, 2016.
- [105] R. Solmaz, G. Kardaş, M. Çulha, B. Yazıcı, and M. Erbil, "Investigation of adsorption and inhibitive effect of 2-mercaptothiazoline on corrosion of mild steel in hydrochloric acid media," *Electrochimica Acta*, vol. 53, pp. 5941-5952, 2008.

- [106] F. Bentiss, M. Lebrini, and M. Lagrenée, "Thermodynamic characterization of metal dissolution and inhibitor adsorption processes in mild steel/2,5-bis(n-thienyl)-1,3,4-thiadiazoles/hydrochloric acid system," *Corrosion Science*, vol. 47, pp. 2915-2931, 2005.
- [107] S. K. Shukla and E. E. Ebenso, "Corrosion inhibition, adsorption behavior and thermodynamic properties of streptomycin on mild steel in hydrochloric acid medium," *Int. J. Electrochem. Sci*, vol. 6, pp. 3277-329, 2011.
- [108] F. Bentiss, M. Lagrenee, M. Traisnel, and J. C. Hornez, "The corrosion inhibition of mild steel in acidic media by a new triazole derivative," *Corrosion Science*, vol. 41, pp. 789-803, 1999.
- [109] M. Finšgar and I. Milošev, "Inhibition of copper corrosion by 1,2,3-benzotriazole: A review," *Corrosion Science*, vol. 52, pp. 2737-2749, 2010.
- [110] A. S. Yaro, A. A. Khadom, and S. M. Lahmod, "Kinetics of the corrosion inhibition reaction of steel alloys in acidic media by potassium iodide," *Reaction Kinetics, Mechanisms and Catalysis*, vol. 109, pp. 417-432, 2013.
- [111] H. A. Al-Megren and A. A. Al-Suhybani, "Polarization resistance studies on Corrosion inhibition of 304 austenitic and 430 ferritic stainless steels in H<sub>2</sub>SO<sub>4</sub> solutions," *Materialwissenschaft und Werkstofftechnik*, vol. 24, pp. 26-31, 1993.
- [112] S. Martinez and I. Štern, "Inhibitory mechanism of low-carbon steel corrosion by mimosa tannin in sulphuric acid solutions," *Journal of Applied Electrochemistry*, vol. 31, pp. 973-978, 2001.
- [113] F. S. de Souza and A. Spinelli, "Caffeic acid as a green corrosion inhibitor for mild steel," *Corrosion Science*, vol. 51, pp. 642-649, 2009.
- [114] O. Prepared by the Working Party on Corrosion in, M. B. Gas - Edited by: Kermani, and L. M. Smith, "CO<sub>2</sub> Corrosion Control in Oil and Gas Production - Design Considerations: (EFC 23)," Maney Publishing.
- [115] H. Fang, "Investigation of Localized Corrosion of Carbon Steel in Hydrogen Sulfide Environments," 3503948 Ph.D., Ohio University, Ann Arbor, 2012.
- [116] M. A. Kappes, "Evaluation of thiosulfate as a substitute for hydrogen sulfide in sour corrosion fatigue studies," 3493520 Ph.D., The Ohio State University, Ann Arbor, 2011.
- [117] G. Gao, C. H. Liang, and H. Wang, "Synthesis of tertiary amines and their inhibitive performance on carbon steel corrosion," *Corrosion science*, vol. 49, pp. 1833-1846, 2007.
- [118] S. L. Granese, B. M. Rosales, C. Oviedo, and J. O. Zerbino, "The inhibition action of heterocyclic nitrogen organic compounds on Fe and steel in HCl media," *Corrosion Science*, vol. 33, pp. 1439-1453, 1992.
- [119] SigmaAldrichCorporation, "2-(2-Methylaminoethyl)pyridine, Safety Data Sheet," A. R. Sigma-Aldrich Corporation, St. Louis, Missouri, USA, 2014.
- [120] S. A. Ali, A. A. Soliman, A. H. Marei, and D. H. Nassar, "Synthesis and characterization of new chromium, molybdenum and tungsten complexes of 2-[2-

- (methylaminoethyl)] pyridine," *Spectrochimica Acta Part A: Molecular and Biomolecular Spectroscopy*, vol. 94, pp. 164-168, 2012.
- [121] C. Li, S. Richter, and S. Nešićl, "How Do Inhibitors Mitigate Corrosion in Oil-Water Two-Phase Flow Beyond Lowering the Corrosion Rate?," *Corrosion*, vol. 70, pp. 958-966, 2014.
- [122] Y. Wei, K. F. Hsueh, and G.-W. Jang, "Monitoring the chemical polymerization of aniline by open-circuit-potential measurements," *Polymer*, vol. 35, pp. 3572-3575, 1994.
- [123] S. Ghareba and S. Omanovic, "12-Aminododecanoic acid as a corrosion inhibitor for carbon steel," *Electrochimica acta*, vol. 56, pp. 3890-3898, 2011.
- [124] E. McCafferty, "Validation of corrosion rates measured by the Tafel extrapolation method," *Corrosion Science*, vol. 47, pp. 3202-3215, 2005.
- [125] P. A. Research, "Application Note CORR-1: Basics of Corrosion Measurements," 2010.
- [126] G. Badea, A. Caraban, M. Sebesan, S. Dzitac, P. Cret, and A. Setel, "Polarisation Measurements Used for Corrosion Rates Determination," *Journal of Sustainable Energy*, vol. 1, pp. 140-144, 2010.
- [127] M. Migahed, H. Mohamed, and A. Al-Sabagh, "Corrosion inhibition of H-11 type carbon steel in 1 M hydrochloric acid solution by N-propyl amino lauryl amide and its ethoxylated derivatives," *Materials chemistry and physics*, vol. 80, pp. 169-175, 2003.
- [128] M. Tourabi, K. Nohair, M. Traisnel, C. Jama, and F. Bentiss, "Electrochemical and XPS studies of the corrosion inhibition of carbon steel in hydrochloric acid pickling solutions by 3, 5-bis (2-thienylmethyl)-4-amino-1, 2, 4-triazole," *Corrosion Science*, vol. 75, pp. 123-133, 2013.